LBL--24418

DE88 005327

NMR WITH GENERALIZED DYNAMICS OF SPIN AND SPATIAL COORDINATES

by

Chang Jae Lee

Lawrence Berkeley Laboratory
University of California
Berkeley, California 94720

DISCLAIMER

This work was supported by the Director, Office of Energy Research, Office of Basic Energy Sciences, Materials Sciences Division of the U.S. Department of Energy under Contract Number DE-AC03-76SF00098.

NMR WITH GENERALIZED DYNAMICS OF SPIN AND SPATIAL COORDINATES

Chang Jae Lee

Abstract

This work is concerned with theoretical and experimental aspects of the generalized dynamics of nuclear spin and spatial coordinates under magnetic-field pulses and mechanical motions. Specific goals include: a description of the interaction of spins with a quantized radiation field; the design of multiple-pulse sequences for the averaging of all linear and bilinear spin operators; schemes for heteronuclear decoupling of spins in multi-level systems; methods for the removal of anisotropic spin interactions in orientationally disordered solids.

The main text begins with an introduction to the concept of "fictitious" interactions. A systematic method for construction of the fictitious spin-1/2 operators is given. The interaction of spins with a quantized-field is described using this formalism.

The concept of the fictitious interactions under the irradiation of multiple pulses is utilized to design sequences for selectively averaging linear and bilinear operators. Relations between the low-field sequences and high-field iterative schemes are clarified. These relations and the transformation properties of the spin operators are exploited to develop schemes for heteronuclear decoupling of multi-

level systems. The resulting schemes are evaluated for heteronuclear decoupling of a dilute spin-1/2 from a spin-1 in liquid crystal samples and from a homonuclear spin-1/2 pair in liquids.

A relation between the spin and the spatial variables is discussed. The transformation properties of the spin operators are applied to spatial coordinates and utilized to develop methods for removing the orientational dependence responsible for line broadening in a powder sample. Elimination of the second order quadrupole effects, as well as the first order anisotropies is discussed. It is shown that various sources of line broadening can effectively be eliminated by spinning and/or hopping the sample about judiciously chosen axes along with appropriate radio-frequency pulse sequences.

ACKNOWLEDGEMENTS

I can never bring you to realize the importance of sleeves, the suggestiveness of thumbnails, or the great issues that may hang from a bootlace.

——— *Sherlock Holmes to Watson.*

A philosopher said," I can see far because I am on a shoulder of a giant." It gives me a great pleasure to thank all the giants in this Berkeley lab of Professor Alex Pines. Nonetheless, the responsibility that I cannot see far into nature's subtleties lies squarely upon my shoulders. Alex has always been helpful, directly and indirectly. I am lucky to be one of those who have worked for him and witnessed his indefatigable enthusiasm about science. I also benefited by learning from him approaches to solving challenging problems.

Dan Weitekamp taught me some of the most essential tools to carry out research and got me started. A. J. Shaka has been a constant source of knowledge and working with him has been a fun and rewarding. I thank Dave Shykind for always having been "there" whenever I needed an immediate answer, and pleasant with his at times irreverent jokes. It has been fun working with Boqin Sun for the last few months, who did the simulation for the powder spectra in Chapter VI. Dan Caplan did painstaking proof-reading for the thesis. But, any blame for typographical errors should be directed to me. Also, I thank all other group members, who have been pleasant company.

Finally, I thank my parents who have endured the pain of sending

their only child away. Although they are halfway around the world, their thoughts and wishes have always been with me. Thus

With Love and Appreciation

This Work is Dedicated

To My Parents

TABLE OF CONTENTS

CHAPTER I. **Fundamental Phenomena and Tools**.....1

I.1. Introduction.....1

I.2. The Nuclear Spin and the Hamiltonian.....4

I.3. Remarks.....12

CHAPTER II. **Full Quantum Mechanical Treatment of the Spin-Radiation Interaction**.....14

II.1. Introduction.....14

II.2. The Second Quantization Treatment of a Spin-1/2 (Fermion) Interacting with a Quantized-Field.....16

II.3. Spin-1 Operators in the Second Quantization Method.....25

II.4. Average Hamiltonian Treatment of the Spin-Quantized Radiation Interaction.....25

II.5. Remarks.....42

CHAPTER III. **Orchestration of Multiple-Pulses in 15-Dimensional Spin Space in Solids**.....47

III.1. Introduction.....47

III.2. The Spin Hamiltonian.....48

III.3. Transformation Properties of the Spin Operators.....52

III.4. The 12-pulse Sequences.....72

CHAPTER IV. **Iterative Schemes in NMR**.....78

IV.1. Introduction.....78

IV.2. Offset-Incorporated Pulses.....79

IV.3. Iterative Schemes for Linear Operators.....82

IV.4. Connection to the Average Hamiltonian Theory.....83

IV.5. Schemes for Removing Linear and Bilinear Operators....91

CHAPTER V. Broadband Heteronuclear Decoupling in the Presence of Homonuclear Interactions.....105

V.1. General Theory of Heteronuclear Decoupling.....105

V.2. Applications to Heteronuclear Decoupling for a I = 1 and S = 1/2 System in Liquid Crystal Samples.....106

V.3. Heteronuclear Decoupling in Liquids for Scalar-Coupled Spins.....115

V.4. The Offset Dependence of the Scalar Interaction.....149

V.5. Experimental Details.....156

CHAPTER VI. The Modulation of the Spatial Coordinates of the Sample.....175

VI.1. Introduction.....175

VI.2. The Hamiltonian.....179

VI.3. The Removal of the First Order Anisotropies.....181

VI.4. The Design of the Dead Time for Evolution.....191

VI.5. The Second-Order Quadrupole Effect.....196

VI.6. Remarks.....211

Appendices.....217

CHAPTER I. Fundamental Phenomena and Tools

I.1. Introduction

What is remarkable about nuclear magnetism is that it continues to be a fertile source of fundamental physical phenomena and at the same time it has found an enormous number of applications in fields such as physics, chemistry, biology, and medicine to name a few. A reason for the versatility of NMR may be due to the fact that nuclear spin dynamics can be described with relative ease, although accurately with standard quantum mechanics: the difference between energy levels is quite small even at high magnetic fields, so the high temperature approximation is usually possible except for some extraordinary circumstances; in addition, a semiclassical description for the spin-radiation interaction is adequate under most experimental conditions. The simplicity along with accurate predictions has made a great variety of sophisticated experiments possible. In short, NMR is a field which enjoys a happy marriage between the fundamentals and applications.

Accordingly, in this Dissertation an attempt has been made to incorporate the duality: the fundamentals and applications. However, because $\Delta E \cdot \Delta t \geq \hbar \rightarrow 0$, the focus will be paid only on limited aspects of this vast field: in the following sections of this chapter some basics on the nuclear spin itself and the spin Hamiltonian are discussed. Then in Chapter II, a simple model for the interaction of a spin with an electromagnetic field is described on a consistent full-quantum mechanical footing. The rationale behind the inclusion of the

chapter is not merely to provide a balanced exposition on the spin dynamics with the fundamentals and applications to abide by the principle of duality mentioned above, but also to be pragmatic: Although the basic nature of this chapter may be considered to be on the fundamental side, it is hoped that it will find some applications in cases which require microscopic treatment. NMR, being a branch of general spectroscopy, can be described on a universal dynamical footing applicable to all branches of spectroscopy. Thus the full quantum mechanical analysis of nuclear spin-electromagnetic radiation interaction may find applications in, for example, optical spectroscopy, or vice versa. Also it is hoped that some benefits will result as by-products from the treatment itself.

Later chapters deal with more complicated systems: there are many spins in the system, interacting with each other and suject to much more complicated external perturbations. Most relevant to this Dissertation is the removal of unwanted term(s) from the Hamiltonian while keeping the desired term(s) as intact as possible, by modulating the spatial and/or the spin parts of the Hamiltonian with mechanical motions, or radiofrequency pulses or with a combination of the two.

Chapter III deals with the design of multiple pulse sequences for solids under general interactions: the sequences developed for high field Hamiltonians have to deal with only the truncated part of the Hamiltonian. Hence, it is necessary to devise a generalized scheme for sequences to be used for averaging the Hamiltonian at low static magnetic fields, because the Hamiltonian contains full untruncated interactions. The sequences for these low (and zero) fields may also

have important applications for high field experiments, where pulse imperfections produce terms that appear in the low field Hamiltonian which were absent in the original high field Hamiltonian. Also the transformation properties of these various terms may be useful for designing some experiments, and this will be discussed in a later chapter. Other possible applications include homo and heteronuclear spin decoupling by applying multiple pulses.

Chapter IV discusses iterative schemes frequently used in NMR in connection with the multiple-pulse sequences developed in Chapter III. However, in this chapter the pulses will no longer be considered ideal: the radiofrequency field srength is of the same order as the internal error terms, and furthermore they may have amplitude imbalance and phase shift errors as well. So a goal of this chapter is to show the relationship between the schemes for the low field multiple pulse sequence design and the iterative schemes especially developed for modern decoupling experiments for a single-spin case. The similarities as well as the differences between the two methods will be analyzed, and the result of the analysis will be utilized to extend the decoupling schemes to treat the two-spin case, where bilinear spin operator terms as well as linear terms have to be dealt with.

The first discussion given in Chapter V is on the criteria of the heteronuclear decoupling for multi-level systems. The decoupling schemes developed in Chapter IV along with other schemes will be evaluated by applying the criterion for liquid crystal samples. Then it will be discussed in detail how to design composite pulses and put them together in a sequence for the heteronuclear spin decoupling in liquids

in the presence of homonuclear interactions. Various comparisons will be made on these schemes using both simulation and experiment.

In the chapters thus far the modulation schemes are aimed at affecting the nuclear spin coordinates. In Chapter VI, external perturbations will be applied on the spatial degrees of the freedom of the Hamiltonian. The major goal is to achieve highly resolved resonance lines in powder samples. Although the pulsed NMR techniques are quite versatile and powerful in many instances, they cannot be used for extracting the isotropic chemical shifts; because in the presence of high magnetic fields the spin part of the chemical shift Hamiltonian is proportional to I_z. Consequently, the radiofrequency pulses can not distinguish the isotropic part from the anisotropic part. Therefore carefully designed mechanical motions affecting the spatial part of the Hamiltonian are used to deal with the problem. A theoretical background for dealing with the various anisotropies which cause the broadening of the resonance lines will be given and some experimental possibilities will be discussed.

Finally some useful relationships and data too lenthy to include in the main text are compiled in Appendices.

I.2. The Nuclear Spin and the Hamiltonian

I.2.A. The Nuclear Spin

A very fundamental property of a nucleus is its intrinsic spin angular momentum. The concept of the intrinsic spin angular momentum

(or simply the "spin") of the electron was proposed by Uhlenbeck and Goudsmit[1] to explain the appearance of two closely spaced lines of the D line in a sodium spectrum. The electron may be regarded as a charged sphere spinning around one of its axis. Then by analogy to classical electromagnetism the intrinsic angular momentum may arise from such motion. Thus the name "spin" was given to the intrinsic angular momentum. But the simple classical model turned out to be untenable. Dynamical variables may be (first-)quantized by replacing the corresponding classical mechanical quantities by appropriate operators. In the classical limit $\hbar \to 0$ the spin reduces to zero. So the spin has no classical analog of the classical mechanics, and thus there is no explicit operator form for it. Dirac later showed in his relativistic quantum mechanical treatment that the spin arises naturally.[2] However, the theory of Dirac does not hold for other elementary particles, and the value of the spin of each particle has been experimentally determined. The elementary particles of concern in this Dissertation are nuclei.

I.2.B. The General Form of the Spin Hamiltonian

Since the spin Hamiltonian has been detailed many times in standard texts,[3,4] monographs,[5] and theses, no exhaustive discussion on it will be given here. Only some points which will be utilized extensively in later chapters are given.

The spin Hamiltonian of interest to this work consists of the Zeeman ($\mathcal{H}_Z$), radiofrequency ($\mathcal{H}_{rf}$), chemical shift ($\mathcal{H}_{CS}$), dipole ($\mathcal{H}_D$),

quadrupole ($\mathcal{H}_Q$), and indirect coupling ($\mathcal{H}_J$) interaction terms. $\mathcal{H}_Z$ and $\mathcal{H}_{rf}$ may be regarded as external Hamiltonians and the rest as the internal Hamiltonians. The decomposition, however, is not unique. For example, when transformed to the rotating frame, certain parts of $\mathcal{H}_Z$, more specifically, the resonance offset ($\mathcal{H}_{off}$) term is considered as an internal Hamiltonian. Conversely, when the second averaging[6] condition is met, the resonance offset term may be regarded as a new "Zeeman" term and hence may be considered to be an external part of the spin Hamiltonian. Therefore, the terms "internal" or "external" should be used in accordance with the particular situation under consideration.

In the laboratory frame (LAB) each individual (internal) interaction term in $\mathcal{H}_Z$, $\mathcal{H}_{CS}$, $\mathcal{H}_D$, $\mathcal{H}_Q$ and $\mathcal{H}_J$ may in general be written as

$$\mathcal{H}^{\lambda} = \vec{I}\cdot\overleftrightarrow{R}^{\lambda}\cdot\vec{A}^{\lambda}, \quad \lambda = Z, CS, D, Q, J. \tag{1.1}$$

Here

$$\overleftrightarrow{R} = \begin{cases} -\gamma\, 1 & : Z \\ \gamma\overleftrightarrow{\sigma} & : CS \\ -\gamma\gamma'\hbar\,\overleftrightarrow{D} & : D \\ \dfrac{eQ}{6I(2I-1)}\overleftrightarrow{V} & : Q \\ \overleftrightarrow{J} & : J \end{cases} \tag{1.2}$$

γ and γ' are the magnetogyric ratios, $\overleftrightarrow{\sigma}$ the shielding tensor, $\overleftrightarrow{D}$ the dipole coupling tensor, $\overleftrightarrow{V}$ the electric field gradient tensor.

$$\vec{A}^{\lambda} = \overleftrightarrow{B}_0 \quad : Z,\ CS$$
$$I' \quad : D,\ J \qquad (1.3)$$
$$I \quad : Q.$$

Alternatively, the Hamiltonian can also be written as

$$\mathcal{H} = \overleftrightarrow{R} \cdot \overleftrightarrow{T}, \qquad (1.4)$$

where $\overleftrightarrow{T}$ is constructed from the direct product of $\vec{I}$ and $\vec{A}$:

$$T_{\alpha\beta} = I_{\alpha} A_{\beta}. \qquad (1.5)$$

$\overleftrightarrow{R}$ and $\overleftrightarrow{T}$ represent the spatial and the spin part of the Hamiltonian respectively except for the cases of $\lambda = Z$ and CS. These tensors can be either Cartesian or spherical. Thus

$$\mathcal{H} = \sum_{\alpha,\beta} R_{\alpha\beta} T_{\beta\alpha} \qquad (\alpha,\beta = x,y,z) \qquad (1.6)$$

or

$$\mathcal{H} = \sum_{\ell=0}^{2} \sum_{m=-\ell}^{\ell} (-1)^{m} R_{\ell-m} T_{\ell m}. \qquad (1.7)$$

The Cartesian tensor form provides some useful physical insights which will be discussed in section I.2.C. The spherical tensor form is useful when rotations or other unitary transformations are involved. It is the form which has been used extensively by Haeberlen and Waugh[7] for the

description of the spin-lattice relaxation in periodically perturbed systems.

I.2.C. The Analogy between the Spin and Spatial Parts of the Hamiltonian

The Hamiltonian in Eq.(1.6) expressed in terms of Cartesian tensors will now be used to point out an analogy between the spatial and the spin parts. The analogy is general. However, it is most striking for quadrupole and dipole interactions. $\mathcal{H}_Q$ and $\mathcal{H}_D$ have quite similar structures and the quadrupole interaction is more general in the sense that it has the asymmetry parameter(η). So $\mathcal{H}_Q$ will be considered here as a representative case without the loss of generality.

It can be shown (the proof is given in Appendix 1) that a second rank Cartesian tensor $A_{\alpha\beta}$ may be regarded as a direct product of two vectors

$$A_{\alpha\beta} = p_\alpha q_\beta \qquad (\alpha,\beta = x,y, \text{ or } z) \tag{1.8}$$

where p_α and q_β are components of vectors $\vec{p}$ and $\vec{q}$. Hence $R_{\alpha\beta}$ can be written as a product of components of two vectors $i_\alpha i_\beta'$, quite analogous to the fact that $T_{\alpha\beta}$ is expressed as a product of two angular momentum operators $I_\alpha I_\beta'$. Therefore, there is a one-to-one correspondence between spin and spatial parts of the Hamiltonian.

The general analogy can be made more explicit for the simple case

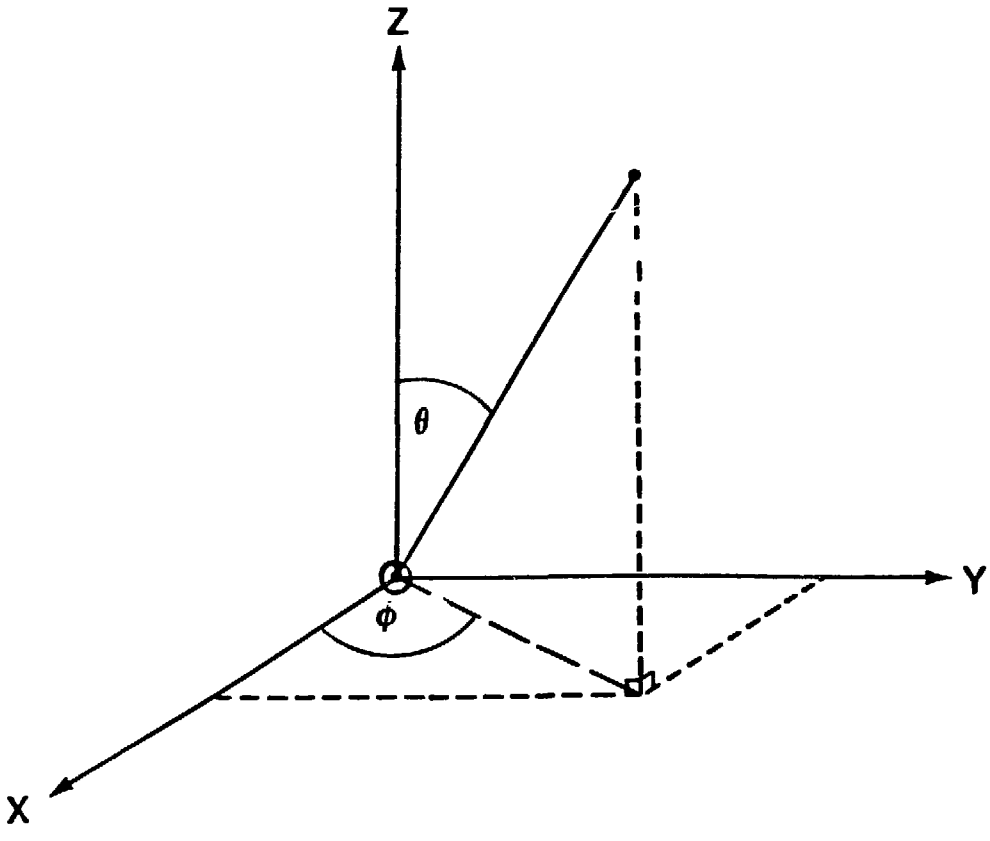

Figure 1.1 Laboratory coordinate system and polar angles θ and ϕ of the axis of the symmetry of a axially symmetric quadrupole.

of η=0 (this includes dipole interactions). In this case because of axial symmetry only the principal axis of symmetry is important and the Hamiltonian may be expressed in terms of the two polar angles θ and ϕ shown in Fig.1.1. Thus (apart from a constant factor)

$$\mathcal{H}_Q \sim \left\{\frac{1}{2}(3\cos^2\theta-1)(3I_z^2-I^2) + \frac{3}{2}\sin\theta\cos\theta(I_zI_+ + I_+I_z)e^{-i\phi}\right.$$
$$\left. + \frac{3}{2}\sin\theta\cos\theta(I_zI_- + I_-I_z)e^{i\phi} + \frac{3}{4}\sin^2\theta(I_+^2e^{-2i\phi} + I_-^2e^{2i\phi})\right\}. \qquad (1.9)$$

The two vectors $\vec{I}$ and $\vec{I}'$ making up the tensor $\overleftrightarrow{R}$ are now identical to each other and are parallel to the symmetry axis of the quadrupole. The unit vector along this direction has the following components

$$\begin{aligned} x &= \sin\theta\cos\phi \\ y &= \sin\theta\sin\phi \\ z &= \cos\theta \end{aligned} \qquad (1.10)$$

Then $\mathcal{H}_Q$ may be written as

$$\mathcal{H}_Q \sim -\frac{1}{2}(3z^2-1)(3I_z^2-I^2) - 3zx(I_zI_x+I_xI_z) - 3yz(I_yI_z+I_zI_y)$$
$$-3xy(I_xI_y+I_yI_x) - \frac{3}{2}(x^2-y^2)(I_x^2-I_y^2). \qquad (1.11)$$

Thus we can now clearly see the close analogy between spin and spatial parts, and it will be fully exploited in designing the experiments to be discussed in Chapter VI.

I.2.D. Some Useful Properties of the Spherical Tensors

An irreducible tensor operator $\overset{\leftrightarrow}{A}_\ell$ of rank ℓ has $(2\ell+1)$ components, which under a coordinate rotation R, satisfy

$$R\, A_{\ell m}\, R^{\dagger} = \sum_{m'} A_{\ell m'} D^{(\ell)}_{m'm}(R) \qquad (1.12)$$

$$\ell = 0, 1, 2, \ldots$$

$$m = \ell, \ell-1, \ldots, -\ell$$

where $D^{(\ell)}_{mm'}$ are Wigner rotation matrices.

Some useful commutation relationships between $A_{\ell m}$ and the angular momentum operators are:

$$\left[I_0, A_{\ell m} \right] = m\, A_{\ell m} \qquad (1.13)$$

$$\left[I_{\pm 1}, A_{\lambda m} \right] = \mp \left[1/2 \left\{ \ell(\ell+1) - m(m+1) \right\} \right]^{1/2} A_{\ell m \pm 1} \qquad (1.14)$$

For $\ell = 1$ and $A_{1m} = I_m$ Eqs.(1.13) and(1.14) reduce to

$$\left[I_0, I_{1\pm 1} \right] = \pm I_{1\pm 1} \qquad (1.15)$$

$$\left[I_{+1}, I_{-1} \right] = - I_0. \qquad (1.16)$$

Principle axis system (PAS)

The relationship between the spatial part $\overleftrightarrow{R}$ of the Hamiltonian in the LAB and $\overleftrightarrow{\rho}$ in the PAS can be expressed using Eq.(1.12)

$$R_{\ell\text{-}m} = \sum_{m'} \rho_{\ell\text{-}m'} \mathcal{D}^{(\ell)}_{\text{-}m\text{-}m'}(\Omega'), \tag{1.17}$$

where Ω' is the solid angle relating the two frames. $\rho_{2m} = 0$ $(m \neq \pm 2)$ for $\lambda = D,Q$. $\rho^{CS}_{00} = -\sqrt{3}\gamma\sigma_{iso}$ and $m = 1$ term corresponds to the antisymmetry component, which has no effect on the first order spectra and thus is usually ignored.

I.3. Remarks

It should be remembered that these internal Hamiltonian terms are scalar quantities as evidenced by Eq.(1.1) or Eq.(1.4). Thus they have the isotropic symmetry, and this is the property which the zero-field NMR methods capitalize on. In zero field the Hamiltonian is orientation independent, so a single-crystal-like spectrum is obtained from a powder sample. Once an external field is applied, the spin components orthogonal to the applied field undergo rapid motion, and the isotropic symmetry under rotation is broken. (However, the symmetry broken this way is different from the "broken symmetry" occurring in the condensed phases such as ferromagnets. In such cases there exist intrinsic alignments of spins even if there is no external field present. If the external field is present, even spins in a normal phase (paramagnet) line up parallel to the field and this is not an intrinsic property of the spin system.)

Line broadening is removed by isotropic motion of the molecules in liquids provided by the nature. However, in solids the motion must be provided by the experimenter either by pulses to affect the spin part, by mechanical motions to affect the spatial part, or a combination of the two.

References

1. G. E. Uhlenbeck and S. Goudsmit, Naturwiss. 13, 953 (1925); Nature, 117, 264 (1926).
2. P. A. M. Dirac, Proc. Roy. Soc. (London) A 117, 610 (1928); A 118, 351 (1928).
3. A. Abragam, The Principles of Nuclear Magnetism, (Clarendon, Oxford, 1961).
4. M. Mehring, High Resolution NMR in Solids, (Springer- Verlag, Berlin, 1983).
5. U. Haeberlen, High Resolution NMR in Solids: Selective Averaging, (Academic, New York, 1976).

6(a). U. Haeberlen, J. D. Ellet, Jr. and J. S. Waugh, J. Chem. Phys. 55, 53 (1971).

6(b). A. Pines and J. S. Waugh, J. Mag. Res., 8, 354 (1972).

7. U. Haeberlen and J. S. Waugh, Phys. Rev. 185, 420 (1969).

CHAPTER II. Full Quantum Mechanical Treatment of the Spin-Radiation Interaction.

II.1. Introduction.

Chapter I focused on the nuclear spin and general form of the internal Hamiltonian. This chapter will concentrate on the dynamics of the interaction of spins with electromagnetic radiation. The second quantization method[1,2] is highly useful for those systems in which the number of particles in a given state changes, and the production and disappearance of particles of a given species occurs. Thus for describing the spin-radiation interaction the second quantization method is frequently employed. One feature that arises in the method of second quantization is the concept of "fictitious" particles.[3] The concept is found in many branches of physics dealing with many-particle systems. The idea behind the concept is to transform the "coupled" or complicated real system to some "uncoupled" (or at least less strongly coupled) "fictitious" system, so that they may become amenable to calculation. Some familiar examples include: the separation of an otherwise unsolvable two-body system into a non-interacting center of mass system and a reduced mass system, the transformation of a coupled harmonic oscillator into uncoupled normal coordinates, the Hartree-Fock method for calculating electronic energy, and phonons for describing vibrations in crystal lattice. The replacement of a time-dependent Hamiltonian with a fictitious time-independent "average" Hamiltonian has been a powerful tool for multiple-pulse techniques in NMR.[4,5] The concept of fictitious

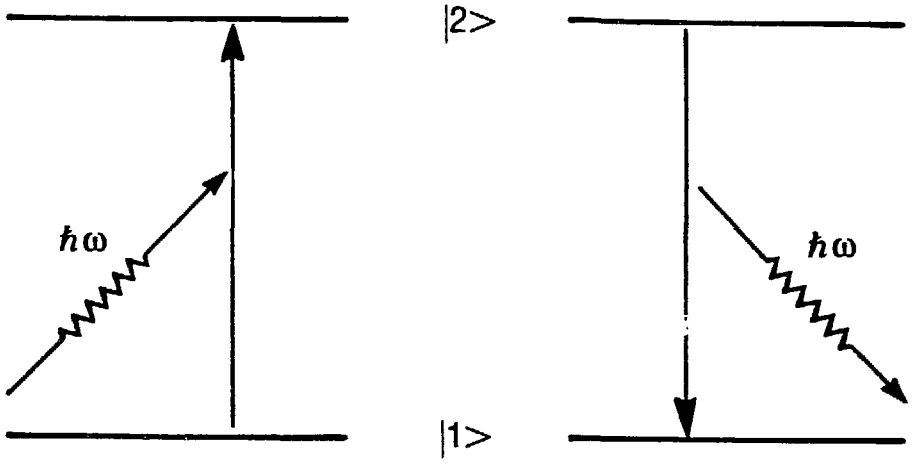

Fig .2.1 Two processes of a spin-1/2 and electromagneic field interaction. The spin is excited or de-excited by absorbing or emitting a photon respectively.

spin-1/2 has been used with eminent success in dealing with multiple-quantum transitions.[6,7,8]

In this section a few simple model cases of interaction of a spin with radiation will be given, following closely the discussion given by Pines.[9]

II.2. The Second Quantization Treatment of a Spin-1/2 (Fermion) Interacting with a Quantized-Field.

A. The Hamiltonian

Consider first a two-level system generated by placing a spin-1/2 in a large static magnetic field. Next the spin is made to interact with a field oscillating with a single mode such that only the two processes depicted in Fig. 2.1 occur, that is non-linear couplings are ignored. The energy level $|2\rangle$ is assumed to be higher than $|1\rangle$ with a difference in frequency given by $\omega_1 - \omega_2 = \omega_0$. Finally introduce creation and annihilation operators $C_j^\dagger$ and C_j (j=1,2) for the spin, and $a^\dagger$ and a for the radiation respectively. Then the total Hamiltonian may be written as

$$\begin{aligned} \mathcal{H} &= \mathcal{H}_S + \mathcal{H}_R + \mathcal{H}_{SR} \\ &= \hbar(\omega_1 C_1^\dagger C_1 + \omega_2 C_2^\dagger C_2) + \hbar\omega a^\dagger a + \frac{\hbar\lambda}{2}(aC_2^\dagger C_1 + a^\dagger C_1^\dagger C_2), \end{aligned} \tag{2.1}$$

where λ is a spin-radiation coupling constant and the zero point energy is ignored.

Table 2.1 Complete set of orthogonal basis functions in the occupation number formalism.

N	$\lvert n_1, n_2, \ldots\ldots, n_M \rangle$
0	$\lvert 0,0,0,\cdots\rangle = \lvert \emptyset\rangle$
1	$\lvert 1,0,0,\cdots\rangle, \lvert 0,1,0,\cdots\rangle, \lvert 0,0,1\cdots\rangle, \cdots\cdots$
2	$\lvert 1,1,0\cdots\rangle, \lvert 1,0,1,\cdots\rangle, \lvert 0,1,1\cdots\rangle, \cdots\cdots$
⋮	

B. Is a Single Particle too many?

A question arises, however, whether $\mathcal{H}_{SR}$ given in Eq.(2.1) is equal to

$$\mathcal{H}_{SR} = \frac{\hbar\lambda}{2}\left(aC_1C_2^\dagger + a^\dagger C_1^\dagger C_2\right). \tag{2.2}$$

In other words, whether operators satisfy commutation rules

$$[\, C_1 \,,\, C_2^\dagger \,] = 0 \tag{2.3}$$

and

$$[\, C_1^\dagger \,,\, C_2 \,] = 0. \tag{2.4}$$

It is perfectly clear that when there is a system consisting of many identical particles, the following commutation or anticommutation rules must apply:

$$\begin{aligned} &\{\, C_j \,,\, C_k \,\} = \{\, C_j^\dagger \,,\, C_k^\dagger \,\} = 0 \\ &\{\, C_j \,,\, C_k^\dagger \,\} = \delta_{jk} \,, \end{aligned} \qquad \text{(fermions)} \tag{2.5}$$

and

$$\begin{aligned} &[\, a_j \,,\, a_k \,] = [\, a_j^\dagger \,,\, a_k^\dagger \,] = 0 \\ &[\, a_j \,,\, a_k^\dagger \,] = \delta_{jk}. \end{aligned} \qquad \text{(bosons)} \tag{2.6}$$

However, what if there is only one particle in the system to begin with? Is there any commutation rule at all for this case? To answer the question, the complete set of basis functions in the occupation number formalism is given in Table 2.1. The number of states M depends on the system. For example $M \longrightarrow \infty$ for a hydrogen atom or a harmonic

oscillator, but there are only two energy levels for a spin-1/2. The number N varies depending on the processes occurring in the system. For example,

$$C_1C_2C_3C_2^\dagger C_1^\dagger |\, 0,0,1,0,\cdots\rangle \qquad (N = 1)$$

$$= C_1C_2C_3C_2^\dagger |\, 1,0,1,0,\cdots\rangle \qquad (N = 2)$$

$$= C_1C_2C_3 |\, 1,1,1,\cdots\rangle \qquad (N = 3)$$

$$= C_1C_2 |\, 1,1,\cdots\rangle \qquad (N = 2)$$

$$= C_1 |\, 1,0,0,\cdots\rangle \qquad (N = 1)$$

$$= |\, 0,0,0,\cdots\rangle \qquad (N = 0)$$

where the signs involved in the process are temporarily ignored. It can be clearly seen that the number of particles varies from zero to three. Now return to the problem of a spin-1/2, a two-level system. The complete set of basis functions in the occupation number space and the number of particles associated with each function is given in Table 2.2. It can easily be seen from the table that the number of particles (in this case fermions) varies as $0 \leq N \leq 2$. It is clear that these are not the real particles but <u>fictitious</u> particles. Furthermore in the second quantization formalism even though we started with one real fermion, there can be a variable number of fictitious particles during the process, depending on the number of states and the type of interactions involved. In the above case of interaction where the total number of particles is conserved, the variation of the number of fictitious particles may be likened to injecting test particles to facilitate the

Table 2.2 Complete basis set for the two-level system of a spin-1/2.

No. of particles	basis
0	$\|0\rangle$: the vacuum state
1	$\|1,0\rangle$, $\|0,1\rangle$
2	$\|1,1\rangle$

calculation and removing them at the end of the calculation. In some sense, the above method is reminescent of the method of Lagrangian multipliers. To be more specific, consider the variational equation as an example:[10]

$$\delta\left\{ \mathcal{E}[\rho] - \mu N \right\} = 0, \tag{2.7}$$

where $\mathcal{E}[\rho]$ denotes an energy functional of electron density, and

$$N[\rho] = \int \rho(\vec{r})\, d^3\vec{r} \tag{2.8}$$

is the total number of electrons in the system. Here, the electron density is varied even though the total number of particles is a constant. Back to the case of the spin-1/2 interacting with the radiation, the conservation of the number of particle should be relaxed <u>during</u> the calculation. Otherwise, operators $C_1^\dagger C_2$ and $C_2^\dagger C_1$ appearing in Eq.(2.2) would be meaningless: If $N = 1$ is rigidly required throughout the calculation, then

$$C_2^\dagger C_1 |\, 1,0\rangle \; - C_2^\dagger |\, 0,1\rangle = 0. \tag{2.9}$$

The first equality holds because of the conservation of particle number and the second equality is due to the fact that no more than one particle (fermion) may occupy a state. Similarly,

$$C_1^\dagger C_2 |\, 0,1\rangle - C_1^\dagger |\, 1,0\rangle = 0. \tag{2.10}$$

However, if the condition is relaxed during the calculation,

$$c_1^\dagger c_2 |\, 0,1\rangle \;=\; c_1^\dagger |\, 0,0\rangle \;=\; |\, 1,0\rangle$$

$$N = 1 \longrightarrow N = 0 \longrightarrow N = 1$$

$$c_2^\dagger c_1 |\, 1,0\rangle = c_2^\dagger |\, 0,0\rangle = |\, 0,1\rangle$$

$$N = 1 \longrightarrow N = 0 \longrightarrow N = 1$$

$$c_2 c_1^\dagger |\, 0,1\rangle = c_2 |\, 1,1\rangle = |\, 1,0\rangle$$

$$N = 1 \longrightarrow N = 2 \longrightarrow N = 1$$

$$c_1 c_2^\dagger |\, 1,0\rangle = c_1 |\, 1,1\rangle = |\, 0,1\rangle$$

$$N = 1 \longrightarrow N = 2 \longrightarrow N = 1$$

So, one can see that the operators cause the transitions between states $|\, 1\rangle$ and $|\, 2\rangle$. It is also confirmed that the number of fictitious particles changes as $0 \le N \le 2$ during the process, and that it is conserved at the end of the calculation.

The spin-1/2 just discussed is not an isolated example where there are a number of fictitious particles even if there is only one real particle. Another example easily found is a harmonic oscillator in the mode k with the energy given by

$$E(n_k) = (n_k + \tfrac{1}{2})\hbar\omega_k, \quad n_k = 1,2,.... \tag{2.11}$$

Eq.(2.11) can either be interpreted as the energy level associated with quantum number n_k of a real harmonic oscillator or as the energy of a system of n_k fictitious particles in the k-th state, all excited by $\hbar\omega_k/2$, thus given the name "elementary excitations".[11] The fictitious

particles satisfy either the anticommutation rules or the commutation rules depending on whether the real particles are fermions or bosons.

C. Connection to the Spin Angular Momentum Operators

The Hamiltonian in Eq.(2.1) will now be transcribed into a more familiar form by transforming it back to the coordinate representation from the occupation number representation. To do this it first should be noted that the matrix element should be identical in both representations:

$$O_{ij} = \langle\phi_i|\, O \,|\phi_j\rangle = \langle\cdots 1_i \cdots|\, O^{occ} \,|\cdots 1_j \cdots\rangle. \tag{2.12}$$

Here O is an one-particle operator. Since there is only one spin-1/2 in the system, operators representing many-particle interactions need not be considered. $\{\phi_k\}$ are one-particle wave functions. O^{occ} is the corresponding operator in the occupation number representation. Then it can be shown that

$$O^{occ} = \sum_{m,n} O_{mn} c_m^\dagger c_n, \tag{2.13}$$

where O_{mn} represents the matrix element of the operator in the coordinate representation. As an application, consider the following operator given in the occupation number representation

$$O^{occ} = \frac{1}{2}\,(c_1^\dagger c_2 + c_2^\dagger c_1). \tag{2.14}$$

With Eq.(2.13) the corresponding matrix O can be found as

$$\begin{array}{c|cc} O & \phi_1 & \phi_2 \\ \hline \phi_1 & 0 & 1/2 \\ \phi_2 & 1/2 & 0 \end{array}$$

which is identical to the matrix representation of I_x for a spin-1/2. With the same procedure the following set of identities for spin-1/2 operators is found

$$\begin{aligned} I_x &= \tfrac{1}{2}\,(c_1^\dagger c_2 + c_2^\dagger c_1) \\ I_y &= -\tfrac{i}{2}(c_1^\dagger c_2 - c_2^\dagger c_1) \\ I_z &= \tfrac{1}{2}\,(c_1^\dagger c_1 - c_2^\dagger c_2). \end{aligned} \tag{2.15}$$

Note that because of the anticommutation rules for fermions

$$O^{occ} = \tfrac{1}{2}\,(\,c_1^\dagger c_2 + c_1 c_2^\dagger) = \tfrac{1}{2}\,(\,c_1^\dagger c_2 - c_2^\dagger c_1\,) = iI_y. \tag{2.16}$$

With the above operators it is possible to recast the Hamiltonian given by Eq.(2.1) as

$$H = \hbar\omega_0 I_z + \hbar\omega a^\dagger a + \frac{\hbar\lambda}{2}(aI_+ + a^\dagger I_-), \tag{2.17}$$

where $I_\pm = I_x \pm iI_y$. Eq.(2.17) then is the full quantum mechanical Hamiltonian for the spin-radiation interaction, and one can recognize it to be identical to the Jaynes-Cummings model[12] (JCM) in which rotating

wave approximation is made. The JCM has been one of the most examined models in quantum optics.[13,14,15]

II.3. Spin-1 Operators in the Second Quantization Method

Spin-1 operators can also be expressed in terms of particle creation and annihilation operators applying the method discussed above. It suffices here to state that in this case because the spin-1 is a boson, C and $C^\dagger$ operators satisfy boson commutation rules and to give a representative example:

$$O^{occ} = \frac{1}{\sqrt{2}} (c_1^\dagger c_2 + c_1 c_2^\dagger + c_2^\dagger c_3 + c_2 c_3^\dagger). \tag{2.18}$$

The corresponding matrix representation for O is then

$$\underset{\approx}{O} = \begin{bmatrix} 0 & 1/\sqrt{2} & 0 \\ 1/\sqrt{2} & 0 & 1/\sqrt{2} \\ 0 & 1/\sqrt{2} & 0 \end{bmatrix} = \frac{1}{\sqrt{2}} \begin{bmatrix} 0 & 1 & 0 \\ 1 & 0 & 0 \\ 0 & 0 & 0 \end{bmatrix} + \frac{1}{\sqrt{2}} \begin{bmatrix} 0 & 0 & 0 \\ 0 & 0 & 1 \\ 0 & 1 & 0 \end{bmatrix}$$

$$= \sqrt{2}(I_x^{1-2} + I_x^{2-3}) = I_x, \qquad \text{(spin-1)} \tag{2.19}$$

where the definition of fictitious spin-1/2 operators[6,7] has been used. For concreteness, a set of basis operators for the spin-1 expressed in terms of C and $C^\dagger$ operators is listed in Table 2.3.

II.4. Average Hamiltonian Treatment of the Spin-Quantized Radiation Interaction.

Table 2.3 Basis operators for a spin-1

$$I_x = 2^{-1/2}(c_1^\dagger c_2 + c_2^\dagger c_1 + c_2^\dagger c_3 + c_3^\dagger c_2)$$

$$I_y = i\,2^{-1/2}(-c_1^\dagger c_2 + c_2^\dagger c_1 - c_2^\dagger c_3 + c_3^\dagger c_2)$$

$$I_z = \quad c_1^\dagger c_1 - c_3^\dagger c_3$$

$$Q_x = i\,2^{-1/2}(-c_1^\dagger c_2 + c_2^\dagger c_1 + c_2^\dagger c_3 - c_3^\dagger c_2)$$

$$Q_y = 2^{-1/2}(c_1^\dagger c_2 + c_2^\dagger c_1 - c_2^\dagger c_3 - c_3^\dagger c_2)$$

$$Q_z = 3^{-1}(c_1^\dagger c_1 - 2c_2^\dagger c_2 + c_3^\dagger c_3)$$

$$Q_{+2} = c_1^\dagger c_3$$

$$Q_{-2} = c_3^\dagger c_1 .$$

A. The Time-Independent Fictitious Hamiltonian

The Schrödinger equation for the simple model Hamiltonian given by Eq.(2.17) can be solved exactly and the solution is provided by Jaynes and Cummings.[12]

$$E_{n\pm} = \hbar\omega(n+1/2) \pm \hbar\sqrt{(\Delta\omega)^2 + \lambda^2(n+1)} \tag{2.20}$$

with

$$\Delta\omega = \omega - \omega_0 \tag{2.21}$$

$$\phi_{n+} = \left(\lambda\sqrt{n+1}\ \sin\theta_n + \Delta\omega\ \cos\theta_n\right)| n+1,-> + \left(\lambda\sqrt{n+1}\ \cos\theta_n - \Delta\omega\ \sin\theta_n\right)| n,+> \tag{2.22}$$

and

$$\phi_{n-} = \left(\lambda\sqrt{n+1}\ \cos\theta_n - \Delta\omega\ \sin\theta_n\right)| n+1,-> - \left(\lambda\sqrt{n+1}\ \sin\theta_n + \Delta\omega\ \cos\theta_n\right)| n,+>, \tag{2.23}$$

where $| n,+>$ is the state with n quanta in the field with the spin "up" and $| n+1,->$ is the state with n+1 quanta with the spin "down". Thus

$$a^\dagger a\ | n> = n\ | n> \tag{2.24}$$

and

$$I_z| \pm> = \pm 1/2| \pm>. \tag{2.25}$$

θ_n satisfies

$$\tan\theta_n = \frac{\sqrt{n+1}}{\Delta\omega + \epsilon_n} \tag{2.26}$$

and ϵ_n is given by

$$\epsilon_n = \sqrt{(\Delta\omega)^2 + \lambda^2(n+1)} \ . \tag{2.27}$$

Eigenfunctions $\phi_{n\pm}$ are mixtures of eigenfunctions of the unperturbed Hamiltonian

$$\mathcal{H}_0 = - \hbar\omega\left(I_z + a^\dagger a\right) \tag{2.28}$$

and the perturbation due to the interaction of the spin and the radiation causes the transition between the two states $|\, n+1,- \rangle$ and $|\, n,+ \rangle$.

Although there exists the exact solution for this simple model Hamiltonian, in general one is forced to resort to approximate solutions. With the anticipation of extending the treatment to general cases an approximate solution based on the Average Hamiltonian Theory (AHT) will be presented. AHT, a variant of the time-dependent perturbation theory, has been quite successful for dealing with many dynamical phenomena encountered in NMR[16] and recently in quantum optics as well.[17] The basic idea of AHT is to replace a time-dependent Hamiltonian by a fictitious time-independent "average" Hamiltonian.

We first transform the system into a rotating frame defined by

$$U_0 = \exp\left(-i\omega t(I_z + a^\dagger a)\right). \tag{2.29}$$

Then the Hamiltonian given by Eq.(2.17) becomes

$$\mathcal{H} = -\hbar\Delta\omega I_z + \frac{\hbar\lambda}{2}(aI_+ + a^\dagger I_-), \tag{2.30}$$

where $\Delta\omega = \omega - \omega_0$. Now suppose $\|\mathcal{H}_{SR}\| \gg \|\mathcal{H}_{off}\|$, where $\mathcal{H}_{off}$ is the offset Hamiltonian and the "size" of a Hamiltonian is defined by[16,18]

$$\|\mathcal{H}\| = \mathrm{Tr}\left[\mathcal{H}^2\right]^{1/2}. \tag{2.31}$$

Then the offset Hamiltonian transformed into a second interaction frame may be written as

$$\tilde{\mathcal{H}}_{off}(t) = U_{rf}^\dagger(t)\ -\hbar\Delta\omega I_z\ U_{rf}(t), \tag{2.32}$$

where

$$U_{rf}(t) = \exp\left[-\frac{i}{\hbar}t\mathcal{H}_{SR}\right] = \exp\left[-it\frac{\lambda}{2}(aI_+ + a^\dagger I_-)\right]. \tag{2.33}$$

Our goal is then to find the time-independent Average Hamiltonian $\bar{\mathcal{H}}$ such that

$$U_{rf}\ \exp(-\frac{i}{\hbar}\bar{\mathcal{H}}t) = U_{rf}\ \mathcal{T}\ \exp\left(-\frac{i}{\hbar}\int_0^t \tilde{\mathcal{H}}(t')dt'\right), \tag{2.34}$$

where $\mathcal{T}$ is the Dyson time-ordering operator.[19] $\bar{\mathcal{H}}$ is usually expanded as a power series, in which the first two terms are given by

$$\bar{\mathcal{H}}^{(0)} = \frac{1}{\tau}\int_0^\tau \tilde{\mathcal{H}}(t)dt$$

$$\bar{\mathcal{H}}^{(1)} = -\frac{i}{2\tau}\int_0^\tau dt_1 \int_0^{t_1} dt_2 [\tilde{\mathcal{H}}(t_1), \tilde{\mathcal{H}}(t_2)]. \tag{2.35}$$

However, explicit calculation of $\tilde{\mathcal{H}}_{off}$ with U_{rf} given by Eq.(2.33) shows that it does not yield functions having closed forms, so the average Hamiltonian terms become difficult to calculate.It therefore is necessary to find a picture in which the exponential of Eq.(2.33) becomes a single term, to which the next section is devoted.

B. The Fictitious-Spin Operators

With a slight rearrangement one gets

$$(aI_+ + a^\dagger I_-) = (a+a^\dagger)I_x + i(a-a^\dagger)I_y \tag{2.36}$$

and may be tempted to find some function $\phi(a,a^\dagger)$ such that

$$(a+a^\dagger)I_x + i(a-a^\dagger)I_y = D(I_x \cos\phi + I_y \sin\phi) \tag{2.37}$$

where D is a constant. The quantity in the parenthesis on the right-hand side is

$$e^{-i\phi I_z} I_x e^{i\phi I_z} = I_x \cos\phi + I_y \sin\phi, \tag{2.38}$$

and the constant D may be obtained from

$$\langle n| (a+a^\dagger)^2 + \left\{i(a-a^\dagger)\right\}^2 | n\rangle = 4\langle n | (\hat{n} + \tfrac{1}{2}) | n\rangle = D^2. \tag{2.39}$$

Then $\phi(a,a^\dagger)$ has the following form

$$\phi(a,a^\dagger) = \cos^{-1} \frac{(a + a^\dagger)}{2\sqrt{n + \frac{1}{2}}} \tag{2.40}$$

or

$$\phi(a,a^\dagger) = \sin^{-1} \frac{i(a - a^\dagger)}{2\sqrt{n + \frac{1}{2}}}. \tag{2.41}$$

Thus in a frame transformed by $\exp(-i\phi I_z)$ the exponent in Eq.(2.33) becomes a single term:

$$aI_+ + a^\dagger I_- \longrightarrow 2\sqrt{n + \frac{1}{2}}\ I_x', \tag{2.42}$$

where the prime denotes the new frame.

However one can easily verify that a and $a^\dagger$ resulting from Eqs.(2.40) and (2.41) are

$$a = \sqrt{n+1/2}\ e^{i\phi}$$

$$a^\dagger = \sqrt{n+1/2}\ e^{-i\phi} \tag{2.43}$$

and they satisfy

$$aa^\dagger - a^\dagger a = n+1/2, \tag{2.44}$$

instead of satisfying the usual boson commutation relations. In the next section the reason for this inconsistency will be discussed and a correct transformation will be given.

C. The Phase of the Quantized Radiation

The definition of the phase of the quantized radiation is not unique. The requirements the quantum phase of the radiation must satisfy are:

1) The quantum phase and the number of photons in the radiation field must satisfy the uncertainty rule

2) It must correspond to the classical phase in the classical limit.

A definition of a and $a^\dagger$ operators including the quantum phase is given by[1,20]

$$a = \sqrt{n+1}\; e^{i\phi}$$

$$a^\dagger = \sqrt{n}\; e^{-i\phi} = e^{-i\phi}\sqrt{n+1}\;. \tag{2.45}$$

The exponential operators satisfy

$$e^{i\phi}\, e^{-i\phi} = \left(\sqrt{n+1}\right)^{-1} a a^\dagger \left(\sqrt{n+1}\right)^{-1} = 1 \tag{2.46}$$

and

$$e^{-i\phi}\, e^{i\phi} = a^\dagger \frac{1}{n+1}\, a. \tag{2.47}$$

The righthand side of Eq.(2.47) can be simplified as follows: If Eq.(2.46) is true,

$$e^{-i\phi}\, e^{i\phi}\; e^{-i\phi}\, e^{i\phi} \;=\; e^{-i\phi}\, e^{i\phi}. \tag{2.48}$$

With a slight rearrangement the above equation becomes

$$e^{-i\phi}\, e^{i\phi}\left(e^{-i\phi}\, e^{i\phi} - 1\right) = 0. \tag{2.49}$$

Since the operators on the left-hand side of the parenthesis cannot be zero, the quantity within the parenthesis must be zero, in contrast to a claim in the literature.[21] As a matter of fact, for any photon state $\sum_n c_n |n\rangle$,

$$a^{\dagger}\frac{1}{n+1}\, a \sum_n c_n |n\rangle = \sum_n c_n |n\rangle. \tag{2.50}$$

It follow that $\exp(\pm i\phi)$ is rigorously an exponential function.

After some algebra it can be shown that the following uncertainty rule between the phase and the number of photons in the field holds:

$$\Delta n\, \Delta\phi \geq \hbar, \tag{2.51}$$

as is given in standard texts on quantum mechanics.[22]

The reason for the inconsistency of the definitions given by Eq.(2.43) can now be explained. To show this first rearrange Eq.(45), the correct quantum mechanical definition of a and $a^{\dagger}$:

$$a + a^{\dagger} = \left(\sqrt{n+1} + \sqrt{n}\right)\cos\phi + i\left(\sqrt{n} - \sqrt{n+1}\right)\sin\phi \tag{2.52}$$

and

$$i\left(a - a^{\dagger}\right) = \left(\sqrt{n+1} + \sqrt{n}\right)\sin\phi + i\left(\sqrt{n+1} - \sqrt{n}\right)\cos\phi$$

$$-\left(\sqrt{n+1} + \sqrt{n}\right)\cos\left(\phi - \frac{\pi}{2}\right) + i\left(\sqrt{n} - \sqrt{n+1}\right)\sin\left(\phi - \frac{\pi}{2}\right). \tag{2.53}$$

The above equations show that the two quantities are orthogonal to each other. However, it is not possible to assign a definite phase and the

number of photons simultaneously because of the uncertainty principle. By contrast, the definitions for a and $a^{\dagger}$ operators given by Eq.(2.43) demands a definite knowlege of the phase and the photon number. As a result, the number of photons in the field ($\sqrt{(n+1/2)}$) is incorrect. The correct number of photons can be shown to be (n+1), with the one extra photon being responsible for the spontaneous emission. In the classical limit n>>1, the difference between the number (n+1/2) and the quantum mechanical number (n+1) is immaterial. The next section will show how to find a correct quantum mechanical transformation.

D. The Fictitious Spin-1/2 Operators for the Spin-Radiation Interaction

By analogy to the procedure given in Sec.B, $\{|n,+\rangle, |n+1,-\rangle\}$ will be chosen as the complete basis set for the coupled two-level system. Fictitious spin-1/2 operators for the coupled system of the spin and radiation may be constructed by utilizing the identity

$$\hat{T} = \sum_{\ell,m} |\ell\rangle T_{\ell m} \langle m| . \tag{2.54}$$

Then there results a new set of operators ℓ_x, ℓ_y, and ℓ_z

$$\begin{aligned}
\ell_x &= 1/2(|n,+\rangle\langle n+1,-| + |n+1,-\rangle\langle n,+|), \\
\ell_y &= -i/2(|n,+\rangle\langle n+1,-| - |n+1,-\rangle\langle n,+|), \\
\ell_z &= 1/2(|n,+\rangle\langle n,+| - |n+1,-\rangle\langle n+1,-|).
\end{aligned} \tag{2.55}$$

which can esily be shown to satisfy the commutation rules for the angular momentum operators:

$$[\ell_x\ ,\ell_y\ ] = i\ell_z\ ,$$

$$[\ell_y\ ,\ell_z\ ] = i\ell_x\ , \tag{2.56}$$

$$[\ell_z\ ,\ \ell_x\ ] = i\ell_y\ .$$

Furthermore,

$$\ell_x^2 = \frac{1}{4}\left(|n,+\rangle\langle n,+| \ +\ |n+1,-\rangle\langle n+1,-| \right) = \frac{1}{4}, \tag{2.57}$$

where the closure relation

$$|\ n,+\rangle\langle n,+\ |\ +\ |\ n+1,-\rangle\langle n+1,-\ |\ = 1 \tag{2.58}$$

is used for the second equality. Similarly,

$$\ell_y^2 = \ell_z^2 = \frac{1}{4}. \tag{2.59}$$

It follows that the operators can be regarded as fictitious spin-1/2 operators. Finally, we can relate these operators to a, $a^\dagger$ and the <u>original</u> spin-1/2 operators, by using Eq.(2.54) and the matrix elements

$$\langle n+1,-|\ aI_+|\ n,+\rangle = 0$$

$$\langle n,+|\ a^\dagger I_-\ |\ n+1,-\rangle = 0$$

$$\langle n,+|\ aI_+\ |\ n+1,-\rangle = \sqrt{(n+1)}$$

$$\langle n+1,-|\, a^{\dagger}I_{-} \,|\, n,+\rangle = \sqrt{(n+1)} \tag{2.60}$$

$$\langle n+1,-|\, I_z \,|\, n+1,-\rangle = -\frac{1}{2}$$

$$\langle n,+|\, I_z \,|\, n,+\rangle = \frac{1}{2}$$

Thus the following set of fictitious spin-1/2 operators results

$$\ell_x = \frac{1}{2\sqrt{(n+1)}}(aI_{+} + a^{\dagger}I_{-})$$

$$\ell_y = \frac{-i}{2\sqrt{(n+1)}}(aI_{+} - a^{\dagger}I_{-}) \tag{2.61}$$

$$\ell_z = I_z$$

and it is easy to verify that these are the correct set of fictitious spin-1/2 operators. Implicit in Eq.(2.61) is that the total excitation number operator[23]

$$\hat{N} = a^{\dagger}a + I_z \tag{2.62}$$

is a constant for the spin-radiation interaction Hamiltonian given by Eq.(2.30), because both aI_{+} and $a^{\dagger}I_{-}$ conserve $\hat{N}$. Consequently, $\hat{N}$ must commute with both the unperturbed Hamiltonian and $\mathcal{H}_{SR}$. The commutation can easily be shown. Furthermore, it can be shown that the numerical value of $\hat{N}$ is equal to (n+1/2) as follows:

(i) Spin "up"

The corresponding state must be $|\, n,+\rangle$. Thus

$$\langle +|\, I_z \,|\, +\rangle = 1/2$$

and

$$\langle n \mid a^{\dagger}a \mid n\rangle = n.$$

Therefore, the expectation number of $\hat{N}$ is equal to n+1/2.

(ii) Spin "down"

The state is $\mid n+1,-\rangle$, so

$$\langle - \mid I_z \mid - \rangle = -1/2,$$

$$\langle n+1 \mid a^{\dagger}a \mid n+1\rangle = n+1$$

and thus

$$\langle \hat{N} \rangle = 1/2.$$

E. The Transition Probability

With the fictitious spin-1/2 operators ℓ_α (α = x,y,z) the "switched" Hamiltonian given by Eq.(2.32) can easily be calculated. From now on $\hbar$ will be set equal to 1 and the subscript "off" will be suppressed for convenience. Thus

$$\begin{aligned} \tilde{\mathcal{H}} &= e^{it\lambda/(n+1)\ell_x}\, \Delta\omega\ell_z\, e^{-it\lambda/(n+1)\ell_x} \\ &= \Delta\omega\left(\ell_z \cos\lambda/(n+1)t + \ell_y \sin\lambda/(n+1)t\right). \end{aligned} \tag{2.63}$$

The first two terms in the average Hamiltonian then becomes

$$\bar{\mathcal{H}}^{(0)} = \frac{-\Delta\omega}{\lambda\sqrt{(n+1)}\tau}\left\{\ell_z \sin\lambda\sqrt{(n+1)}\tau + \ell_y(1-\cos\lambda\sqrt{(n+1)}\tau\right\}$$

$$\bar{\mathcal{H}}^{(1)} = \frac{(\Delta\omega)^2}{2\lambda\sqrt{(n+1)}}\ell_x\left\{1 - \frac{\sin\lambda\sqrt{(n+1)}\tau}{\lambda\sqrt{(n+1)}\tau}\right\}. \tag{2.64}$$

Suppose the spin is continuously irradiated and measurements are made at time t such that

$$\lambda\sqrt{(n+1)}t = 2m\pi \quad (m = 0,1,2,\ldots), \tag{2.65}$$

then the average Hamiltonian terms become

$$\bar{\mathcal{H}}^{(0)} = 0 \tag{2.66}$$

and

$$\bar{\mathcal{H}}^{(1)} = \frac{(\Delta\omega)^2}{2\lambda\sqrt{(n+1)}}\ell_x. \tag{2.67}$$

The evolution operator in the interaction picture may thus be approximated as

$$U(t) \approx e^{-it\lambda\sqrt{(n+1)}\ell_x}\, e^{-it\left(\bar{\mathcal{H}}^{(0)} + \bar{\mathcal{H}}^{(1)}\right)}$$

$$= e^{-it\left\{\lambda\sqrt{(n+1)} + \frac{(\Delta\omega)^2}{2\lambda\sqrt{(n+1)}}\right\}\ell_x}. \tag{2.68}$$

We also assume the initial state is $|n,+\rangle$. The state at time t is then

$$|\Psi(t)\rangle = U(t)|n,+\rangle$$

$$= \cos\frac{\Omega t}{2} \mid n,+> - i \sin\frac{\Omega t}{2} \mid n+1,->, \tag{2.69}$$

where

$$\Omega = \lambda\sqrt{(n+1)} + \frac{(\Delta\omega)^2}{2\lambda\sqrt{(n+1)}}. \tag{2.70}$$

The transition probability is thus

$$P = |\, <n+1,-| \Psi(t)> \,|^2 = \sin^2 \frac{t}{2}\left[\lambda\sqrt{(n+1)} + \frac{(\Delta\omega)^2}{2\lambda\sqrt{(n+1)}}\right], \tag{2.71}$$

while upon using Eqs.(2.20)-(2.27) the exact solution is found to be

$$P = \frac{\lambda^2(n+1)}{(\Delta\omega)^2 + \lambda^2(n+1)} \sin^2 \frac{t}{2} \left\{ \lambda^2(n+1) + (\Delta\omega)^2 \right\}^{1/2} \tag{2.72}$$

When $\lambda\sqrt{(n+1)} >> \Delta\omega$, which is implicit in the transformation given by Eq.(2.34), to a good approximation

$$\frac{\lambda^2(n+1)}{(\Delta\omega)^2 + \lambda^2(n+1)} \approx 1, \tag{2.73}$$

and

$$\left\{ \lambda^2(n+1) + (\Delta\omega)^2 \right\}^{1/2} \approx \lambda\sqrt{(n+1)}\left\{1 + \frac{1}{2}\left[\frac{\Delta\omega}{\lambda\sqrt{(n+1)}}\right]^2\right\}. \tag{2.74}$$

Then Eq.(2.72) reduces to

$$p \approx \sin^2 \frac{t}{2}\left[\lambda\sqrt{(n+1)} + \frac{1}{2}\,\frac{(\Delta\omega)^2}{\lambda\sqrt{(n+1)}}\right], \tag{2.75}$$

which is identical to the approximate solution, Eq.(2.71).

A comparison between the semiclassical and quantum mechanical transition probabilities[23,24] establishes the correspondence

$$\lambda\sqrt{(n+1)} \longleftrightarrow \omega_1 .$$

In the next section the theory will be extended to include double-quantum transitions.

F. The Double-Quantum Transition

A simple three-level system is generated by placing a spin-1 in the static field. The energy scheme is depicted in Fig. 2.2. The Hamiltonian can be shown to be[9] with a slight modification

$$\mathcal{H} = \omega_0 I_z + \tfrac{1}{3}\omega_Q Q_z + \omega a^\dagger a + \frac{\lambda}{\sqrt{2}}(aI_+ + a^\dagger I_-) \qquad (2.76)$$

where the basis operators for the spin-1 in Table 2.3 have been used, along with $\omega_{12} + \omega_{23} = 2\omega_0$ and $\omega_{23} - \omega_{12} = 2\omega_Q$.

In the frame defined by Eq.(2.29) the Hamiltonian becomes

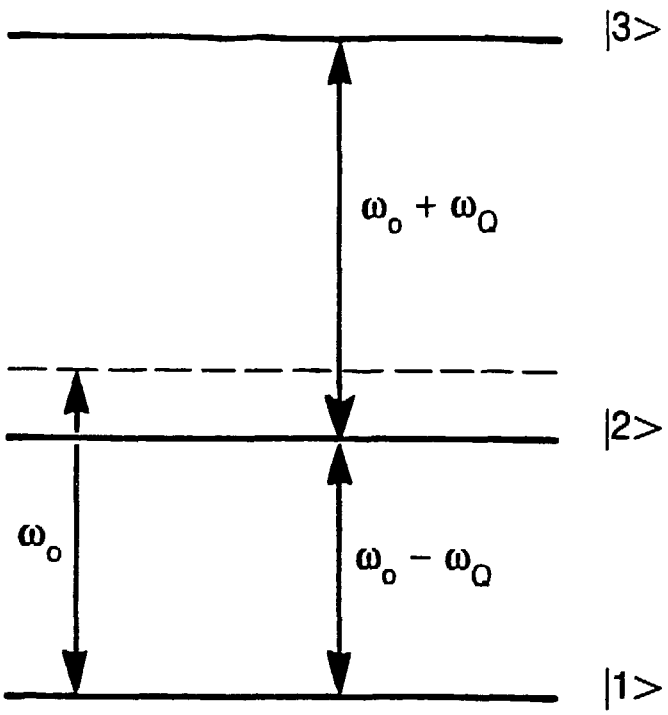

Fig. 2.2 Three-level diagram for a spin I = 1. The original energy levels are determined by the Larmor frequency ω_0, and they are perturbed by the quadrupole interaction. ω_Q is the quadrupole coupling constant.

$$\mathcal{H} = \frac{1}{3}\omega_Q Q_z + \frac{\lambda}{\sqrt{2}}(aI_+ + a^\dagger I_-). \tag{2.77}$$

Supposing that $\omega_Q \gg \lambda\sqrt{(n+1)}$, we may transform to a second interaction frame, where the switched Hamiltonian is given by

$$\tilde{\mathcal{H}} = e^{i\omega_Q t Q_z}\left\{\frac{\lambda}{\sqrt{2}}(a+a^\dagger)I_x + \frac{i\lambda}{\sqrt{2}}(a-a^\dagger)I_y\right\}e^{-i\omega_Q t Q_z} \tag{2.78}$$

With $\omega_Q \tau = 2m\pi$ ($m = 1,2,\ldots$) and after some algebra using the commutation relations among the basis operators for the spin-1 given in Table 2.3 one can show that

$$\bar{\mathcal{H}}^{(0)} = 0, \tag{2.79}$$

and

$$\bar{\mathcal{H}}^{(1)} = -\frac{\lambda^2}{\omega_Q}(a^2 Q_{+2} - a^{\dagger 2} Q_{-2}), \tag{2.80}$$

where terms leading to non-conservation of the total number of particles are ignored. The identical result can also be obtained by an operator perturbation method.[9] One thus can see that the double-quantum transition is associated with the application of a^2 and $a^{\dagger 2}$ operators.

II.5. Remarks

In this chapter it was shown that simple cases of a spin

interacting with the electromagnetic field can be treated on a consistent full-quantum mechanical footing, by employing the second quantization method and a correct transformation which yields fictitious-spin operators. The AHT, a tool widely used in treating many complex dynamical phenomena in NMR, is also employed to deal with the fully-quantum mechanical cases with, to a good approximation, identical results. As a result, it is possible to make a connection between semiclassical and quantum mechanical quantities such as the field strength and the number of photons in the field.

The direct appearance of photon creation and annihilation operators in the expressions may allow one to "see" the spectroscopic dynamics microscopically. The treatment, hopefully, will cast some light on schemes that require such a microscopic observation. Especially, it may be of help to clarify the relation of NMR to quantum optics, in which the use of quantized radiation field is a common practice. In fact much of the development of optical spectroscopy has capitalized on the close analogy to NMR, and some sophisticated NMR techniques have benefited from developments in quantum optics. A possible application of the above treatment may be to analyze the spin dynamics during multiple pulse and multiple quantum experiments.

In most routine NMR experimental conditions it is possible to create enormous number of photons in a unit frequency range with low power due to the smallness of the frequencies involved in these transitions and high accuracy of frequency generated. Thus in these conditions the classical limit $n \longrightarrow \infty$ is applicable with virtually no errors. Consequently, in the discussions to follow the spontaneous

emission will be neglected and the magnitude ω_1 and the phase ϕ of the radiation will simultaneously be assigned.

The convention for the direction of pulses adopted in this Dissertation is as follows: According to classical mechanics the equation of motion of a spin magnetic dipole moment is given by

$$\frac{d\vec{\mu}}{dt} = \gamma \vec{\mu} \times \vec{B} \ . \tag{2.81}$$

The moment is related to angular momentum by

$$\vec{\mu} = \gamma \vec{I} \tag{2.82}$$

and the Hamiltonian for the interaction of the spin and $\vec{B}$ is

$$\mathcal{H} = - \vec{\mu} \cdot \vec{B} = - \gamma \vec{B} \cdot \vec{I} = \vec{\omega} \cdot \vec{I} \ . \tag{2.83}$$

If

$$\vec{B} = B_1 \hat{x}, \tag{2.84}$$

then

$$\mathcal{H} = \omega_1 I_x. \tag{2.85}$$

Consequently, when the term "x pulse" is used it means that the pulse is applied in such a way that the direction of the pulse field is along the positive x axis. Thus the pulse is associated with the rotation operator

$$R_x = \exp\left(-it\omega_1 I_x\right) \tag{2.86}$$

and the rotation is clockwise if γ is positive.

References

1. P. A. M. Dirac, Proc. Roy. Soc. (London) A 114, 243 (1927).

2. P. Jordan and E. P. Wigner, Z. Physik 47, 631 (1928).

3. See, for example, A. A. Abrikosov, L. P. Gorkov, and I. E. Dzyaloshinski, Methods of Quantum Field Theory in Statistical Physics, (Prentice-Hall, Inc., Englewood Cliffs, New Jersey, 1963).

4. U. Haeberlen and J. S. Waugh, Phys. Rev. 175, 453 (1968).

5. U. Haeberlen, High Resolution NMR in Solids: Selective Averaging, (Academic, New York, 1976).

6. S. Vega and A. Pines, J. Chem. Phys. 66, 5624 (1977).

7. S. Vega, J. Chem. Phys. 68, 5518 (1979).

8. A. Wokaun and R. R. Ernst, J. Chem. Phys. 67, 1752 (1977).

9. A. Pines, in Proceedings of the 100th Fermi School on Physics (B. Maraviglia, Ed.), in press.

10. P. Hohenberg and W. Kohn, Phys. Rev. 136, B864 (1964).

11. D. Pines, Elementary Excitations in Solids, (Benjamin, New York, 1963).

12. E. T. Jaynes and F. W. Cummings, Proc. I. E. E. E. 51, 89 (1963).

13(a). B. Buck and C. V. Sukumar, Phys. Lett. 81A, 132 (1981).

13(b). B. Buck and C. V. Sukumar, J. Phys. A17, 877 (1984)

14(a). P. L. Knight and P. M. Radmore, Phys. Rev. A26, 676 (1982); Phys. Lett. 90A, 342 (1982).

14(b). S. M. Barnet and P. L. Knight, Opt. Acta 31, 435 (1984); 31, 1203 (1984); Phys. Rev. A33, 2444 (1986).

15. G. S. Agarwal, Phys. Rev. Lett. 53, 1732 (1984).

16. See, for example, M. Mehring, High Resolution NMR in Solids, (Springer-Verlag, Berlin, 1983).

17. W. S. Warren and A. H. Zewail, J. Chem. Phys. 78, 2279 (1983); ibid. 78, 3583 (1983).

18. W. S. Warren, D. P. Weitekamp, and A. Pines, J. Chem. Phys. 73, 2084 (1980).

19. F. J. Dyson, Phys. Rev. 75, 486 (1949).

20. L. Susskind and J. Glogower, Physics 1, 49 (1964).

21. R. Loudon, The Quantum Theory of Light, 2nd ed.(Clarendon Press, Oxford, 1983).

22. J. J. Sakurai, Advanced Quantum Mechanics, (Addison-Wesley, Reading, 1967).

23. L. Allen and J. H. Eberly, Optical Resonance and Two-Level Atoms, (John Wiley & Sons, Inc., 1975).

24. W. H. Louisell, Quantum Statistical Properties of Radiation, (Wiley, New York, 1973).

CHAPTER III. Orchestration of Multiple-Pulses in 15-Dimensional Spin Space in Solids.

III.1 Introduction

This and later chapters will concentrate on more complicated systems: the system consists of many interacting spins, and they are under much more complicated external perturbations. Nearly all modern NMR experiments are performed in the time-domain; that is the external perturbations are applied such that the (internal) spin Hamiltonian is made appear time dependent. Provided that the time-dependence is fast enough, the modulated internal Hamiltonian can be time-averaged. With variety of external perturbations the experimenter can in principle make the spin Hamiltonian into any form he desires. This chapter concentrates on the multiple-pulse technique for the selective removal of various terms in the Hamiltonian. External perturbations are thus in the form of radio-frequency pulses and are applied on the spin coordinates, which are then time-averaged. The pulses can be either "hard" or "soft", the former nearly approximating the δ-funtion and the latter being windowless.

Magnetic-field pulses cause the spin to nutate about the direction of the axes along which the pulses are applied. From the transformation properties of various spin operators under these rotations some useful informations can be extracted. Especially, one of the goals of the high-field iterative schemes is the removal of various spin operators with low-power rf fields. In such condition the

resonance offset can cause the pulse to deviate strongly from the ideal pulse, and as a result variety of linear and bilinear terms are created. Same spin opertors appear in the low static field and multiple-pulse sequences for the removal of these spin operators can thus shed some light on the design of the high-field iterative schemes. In Chapter VI discussed is the averaging of various anisotropies by mechanical motions. It will be shown in the chapter that the transformation properties of the spin operators are also useful for the design of schemes for the averaging of these anisotropies.

III.2 The Spin Hamiltonian

One of the simplest multiple-pulse sequences is the WHH-4 sequence[1] designed to remove the homonuclear dipolar Hamiltonian in high field. The secular dipolar Hamiltonian may be written as

$$\mathcal{H}^{D}_{zz} = \sum_{i>i'} D_{ii'} \, (3I_{iz}I_{i'z} - \vec{I}_i \cdot \vec{I}_{i'}), \tag{3.1}$$

where

$$D_{ii'} = \frac{1}{2}\gamma^2\hbar(1 - 3\cos^2\theta_{ii'})/\, r^3_{ii'} \tag{3.2}$$

is a dipole coupling constant. The dipole Hamiltonian can be averaged to zero utilizing

$$\mathcal{H}^{D}_{xx} + \mathcal{H}^{D}_{yy} + \mathcal{H}^{D}_{zz} = 0, \tag{3.3}$$

and the WHH-4 sequence satisfies Eq.(3.3). Of course, the WHH-4 sequence is not the shortest sequence that satisfies Eq.(3.3), since the three-pulse sequence ($xy\bar{x}$) also satisfies Eq.(3.3). At any rate, these sequences all generate the same configurations {(X,Y,Z),(Y,Z,X),(Z,X,Y)} ignoring the sign, which is immaterial for quadratic terms. But what if there are more terms than those given in Eq.(3.1)? How many and which configurations are needed to remove all these terms? To answer these questions let us first write down the Hamiltonian that includes all possible linear and bilinear spin operators. The Hamiltonian can be obtained by placing a system of spins I in a static magnetic field which is too low to truncate dipole-dipole or quadrupole interactions. Thus it may be written as

$$\begin{aligned}\mathcal{H} &= \mathcal{H}_1 + \mathcal{H}_2 + \mathcal{H}_p(t) \\ &= \mathcal{H}_{int} + \mathcal{H}_p(t).\end{aligned} \tag{3.4}$$

Here

$$\mathcal{H}_1 = -\sum_j \gamma_j \vec{I}_j \cdot (1-\boldsymbol{\sigma}_j) \cdot \vec{B}_0 \tag{3.5}$$

contains terms linear in spin vaiable with $\boldsymbol{\sigma}$ denoting the chemical shift tensor. In contrast, the terms in

$$\mathcal{H}_2 = \sum_{j,k} \vec{I}_j \cdot C_{jk} \cdot \vec{I}_k \tag{3.6}$$

are bilinear in spin variable for which j≠k corresponds to the dipole interaction with a coupling tensor C_{jk} and j=k corresponds to quadrupole interaction with a coupling tensor C_{jj}. Finally,

$$\mathcal{H}_p(t) = -\sum_j \gamma_j \vec{I}_j \cdot \vec{B}_1(t) \tag{3.7}$$

denotes the pulsed magnetic field. For convenience, the coordinate system chosen is the laboratory system.

The evolution operator given by

$$U(t) = \mathcal{T}\exp\left[-i\int_0^t dt' \mathcal{H}(t')\right] \tag{3.8}$$

may be separated into two parts

$$\begin{aligned} U(t) &= U_p(t)\tilde{U}_{int}(t) \\ &= \mathcal{T}\exp\left[-i\int_0^t dt' \mathcal{H}_p(t')\right] \mathcal{T}\exp\left[-i\int_0^t dt' \tilde{\mathcal{H}}_{int}(t')\right] \end{aligned} \tag{3.9}$$

as discussed in Appendix 2. The "switched" Hamiltonian is

$$\tilde{\mathcal{H}}_{int}(t) = U_p^{\dagger}(t)\, \mathcal{H}_{int}\, U_p(t). \tag{3.10}$$

Assuming the cyclicity of $U_p(t)$ at time $t = t_c$, the cycle time, one can now calculate the average Hamiltonian $\bar{\mathcal{H}} = \bar{\mathcal{H}}^{(0)} + \bar{\mathcal{H}}^{(1)} + \ldots$ For simplicity, only the zeroth-order term will be considered. It is worth noting here that the density matrix ρ can be expanded in terms of

$N = (2I+1)^2$ basic operators. For example,

$$\rho(t) = \sum_{\alpha=x,y,z} a_\alpha(t) I_\alpha + a_0 1 \tag{3.11}$$

for I=1/2. For I = 1 there are eight basic hermitian operators, traceless and independent of each other. One such set of commonly encountered basis operators is given in Table 2.3. Also from the form of internal Hamiltonian given by Eq.(3.4), it can be noted that the same basic operators can be used to expand the internal Hamiltonian. Thus, with the following shorthand notations

$$\begin{aligned} A &= I_{j\alpha}, \\ AA &= I_{j\alpha} I_{k\alpha} - 1/3\ \vec{I}_j \cdot \vec{I}_k, \\ AB &= I_{j\alpha} I_{k\beta} + I_{j\beta} I_{k\alpha}, \end{aligned} \tag{3.12}$$

$$(A \neq B,\ A,B=X,Y,\text{ or } Z;\ \alpha \neq \beta,\ \alpha,\beta=x,y,\text{ or } z)$$

the internal Hamiltonian may be written as

$$\mathcal{H} = \sum_j \sum_A a_{jA} A + \sum_{j,k} \sum_{A,B} b_{jkAB} AB. \tag{3.13}$$

The time-dependent switched Hamiltonian given by Eq.(3.10), corresponding to the form for ρ, is then

$$\tilde{\mathcal{H}}(t) = \sum_j \sum_A a_{jA}(t) A + \sum_{j,k} \sum_{A,B} b_{jkAB}(t) AB. \tag{3.14}$$

Another way of writing Eq.(3.10) is to consider $\mathcal{H}_p(t)$ causing the time-dependence of the spin operators. The latter viewpoint is adopted for this chapter. The reason is that in the latter viewpoint the trajectory of the spin operators can easily be visualized, and this is of great use in designing certain experiments. In Chapter V these transformation properties will be fully exploited. However, the feasibility of monitoring the trajectory is due to the fact that there is no big offset term in the Hamiltonian. If there is an offset Hamiltonian with a size comparable to that of $\mathcal{H}_p$, it becomes very difficult to follow the trajectories and the form given by Eq.(3.14) is highly useful. This viewpoint will be exploited in the section on spin-decoupling problem in liquids. Thus, the form of $\tilde{\mathcal{H}}_{int}$ to be used in this chapter is

$$\tilde{\mathcal{H}}_{int}(t) = \sum_j \sum_A a_{jA} \tilde{A}(t) + \sum_{j,k} \sum_{A,B} b_{jkAB} \tilde{A}(t)\tilde{B}(t), \tag{3.15}$$

with

$$\tilde{A}(t) = U_p^{\dagger}(t)\, A\, U_p(t), \text{ etc.} \tag{3.16}$$

III.3 Transformation Properties of the Spin Opertors

In general, in the three-dimensional space spins can be rotated through any angle around any axis through the origin. These rotations then constitute a three-dimensional rotation group.[2] Here, though, only 90^0 rotations generated by pulses along three orthogonal axes x, y, and z are considered so that they constitute the octahedral group O. The group O has the axes of symmetry of a cube: three axes of the fourth

Table 3.1 24 configurations accessible in a right-handed coordinate system and operatons to reach them.

Configuration	Operation*
x y z	1
y z x	$\bar{x}\ \bar{z}$
z x y	z x
$\bar{x}$ z y	$\bar{x}$ z z, z z x
y $\bar{x}$ z	$\bar{z}$
z y $\bar{x}$	y
$\bar{y}$ x z	z
z $\bar{y}$ x	x z x, $\bar{x}\ \bar{z}\ \bar{x}$, z x z, $\bar{z}\ \bar{x}\ \bar{z}$
x z $\bar{y}$	$\bar{x}$
$\bar{z}$ y x	$\bar{y}$
x $\bar{z}$ y	x
y x $\bar{z}$	x x $\bar{z}$, z $\bar{x}$ $\bar{x}$
x $\bar{y}$ $\bar{z}$	x x
$\bar{z}$ x $\bar{y}$	z $\bar{x}$
$\bar{y}$ $\bar{z}$ x	x z
y $\bar{z}$ $\bar{x}$	x $\bar{z}$
$\bar{x}$ y $\bar{z}$	x z
$\bar{z}$ $\bar{x}$ y	$\bar{z}$ x
z $\bar{x}$ $\bar{y}$	$\bar{z}$ $\bar{x}$
$\bar{y}$ z $\bar{x}$	$\bar{x}$ z
$\bar{x}$ $\bar{y}$ z	z z
$\bar{x}$ $\bar{z}$ $\bar{y}$	x z z, z z $\bar{x}$
$\bar{y}$ $\bar{x}$ $\bar{z}$	x x z, $\bar{z}$ x x
$\bar{z}$ $\bar{y}$ $\bar{x}$	x $\bar{z}$ x, $\bar{x}$ z $\bar{x}$, $\bar{z}$ x $\bar{z}$, z $\bar{x}$ z

*Operations are given in chronological order with the following notation: $\alpha = (\pi/2)_{\alpha}$.

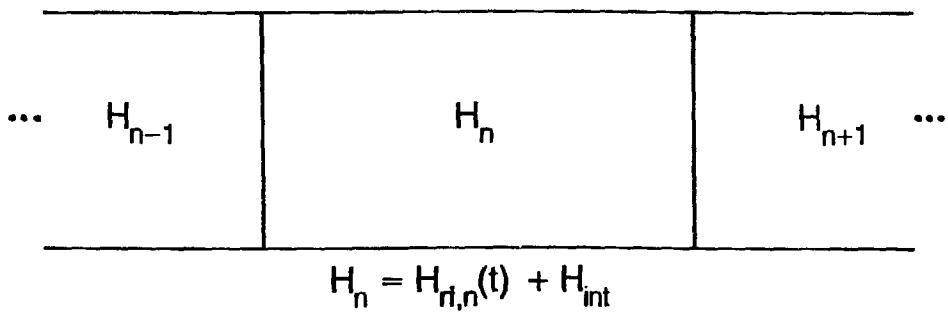

Fig.3.1 Schematic diagram showing the nth piecewise-constant Hamiltonian in the rotating frame.

order, four axes of the third order, and six axes of the second order. There are 24 elements which are divided into five classes: E, eight rotations C_3 and C_3^2, six rotations C_4 and C_4^3, three rotations C_4^2, and six rotations C_2. The switched Hamiltonian tranforms subject to these operations in the group. Table 3.1 lists all these 24 configurations accessible in the right-handed coordinate system.

When rotations are made using pulses having finite widths, it is no longer possible to use the interaction frame Hamiltonian sandwiched between pulses. Thus it is necessary to consider the transformation of each operator during each pulse. To this end, first consider the rotating frame Hamiltonian consisting of the internal part ($\mathcal{H}_{int}$) and $\mathcal{H}_{rf}$,

$$\mathcal{H}_n = \mathcal{H}_{rf,n}(t) + \mathcal{H}_{int}, \tag{3.17}$$

during a pulse as is drawn schemetically in Fig.3.1. n represents the n-th section of the sequence. The evolution operator for an n piecewise-constant pulse sequence is given by Eq.(3.9), and as usual may be approximated as

$$U(\tau) \approx U_{rf}(\tau)\, e^{-i\tau \left(\bar{\mathcal{H}}^{(0)} + \bar{\mathcal{H}}^{(1)} + ..\right)} \tag{3.18}$$

with

$$\bar{\mathcal{H}}^{(0)} = \frac{1}{\tau}\int_0^{\tau} U_{rf}^{\dagger}(t)\, \mathcal{H}_{int}\, U_{rf}(t)dt, \text{ etc.} \tag{3.19}$$

Eq.(3.19) can be decomposed into n integrals

$$\bar{\mathcal{H}}^{(0)} = \frac{1}{\tau}\sum_{k=1}^{n}\int_{t_{k-1}}^{t_k} U_{rf}^{\dagger}(t)\, \mathcal{H}_{int}\, U_{rf}(t)dt. \tag{3.20}$$

Table 3.2 Zeroth order average of linear and blinear operators during a $\pi/2$ pulse.

Pulse	Linear operators		
	I_x	I_y	I_z
$\pm x$	I_x	$(2/\pi)(I_y \mp I_z)$	$(2/\pi)(I_z \mp I_y)$
$\pm y$	$(2/\pi)(I_x \pm I_z)$	I_y	$(2/\pi)(I_z \mp I_x)$
$\pm z$	$(2/\pi)(I_x \mp I_y)$	$(2/\pi)(Iy \pm I_x)$	I_z

	Bilinear Operators					
	XY*	YZ	ZX	XX	YY	ZZ
$\pm x$	XY∓ZX	±(YY-ZZ)	(ZX±XY)	XX	(YY+ZZ)/2∓2YZ	(YY+ZZ)/2±2YZ
$\pm y$	XY±YZ	YZ∓ZX	±(ZZ-XX)	(XX+ZZ)/2±2ZX	YY	(ZZ+XX)/2∓2ZX
$\pm z$	±(XX-YY)/2	YZ±ZX	ZX∓YZ	(XX+YY)/2∓2XY	(XX+YY)/2±2XY	ZZ

*The following notations are used:

$XY \equiv (I_x I_{y'} + I_y I_{x'})2/\pi$, $XX = I_x I_{x'}$, and cyclic permutations.

It may further be rewritten as

$$\bar{\mathcal{H}}^{(0)} = \frac{1}{\tau}\sum_k U_{rf}^{\dagger}(t_{k-1}) \int_0^{\tau_k} U_{rf,k}^{\dagger}(t)\, \mathcal{H}_{int}\, U_{rf,k}(t)dt\, U_{rf}(t_{k-1}) \quad (3.21)$$

where $\tau_k = t_k - t_{k-1}$ and $U_{rf,k}(t)$ denotes kth pulse. Eq.(3.21) dictates that the integration over the trajectory during the pulse must be performed, while transformations due to pulses up to the (k-1)th segment in the sequence can be considered to occur instantaneously.

If the configuration α for a linear term transforms into α' ($\alpha \neq \alpha'$), it is said that the "transition"[3] from α to α' has occurred and the average of the linear term during the transition is $(2/\pi)(\alpha+\alpha')$. If the rotation axis is along the direction α, α stays invariant and during the pulse one has a "stationary" point. In table 3.2 are listed time averages of various operators during a 90^0 pulse.

In NMR (although it is equally applicable to other spectroscopic methods)[4] the rotations of a spin has frequently been described via a vector representation on the unit sphere. The trajectory of the magnetization vector in particular has been extensively used to model coherent and incoherent processes. Here an extension will be made to include all nine basic operators, and it will be utilized to describe the transformational behavior of all operators subject to sequences of pulses. It is particularly useful for discussing windowless sequences where averaging over trajectories is performed. Fig.3.2 is a vector representation of nine basis operators and the trajectories they travel under rotations around coordinate axes. Linear operators have a direct correspondence to unit vectors pointing at respective "vertices", where the coordinate axes and the unit sphere intersect. Bilinear quadratic

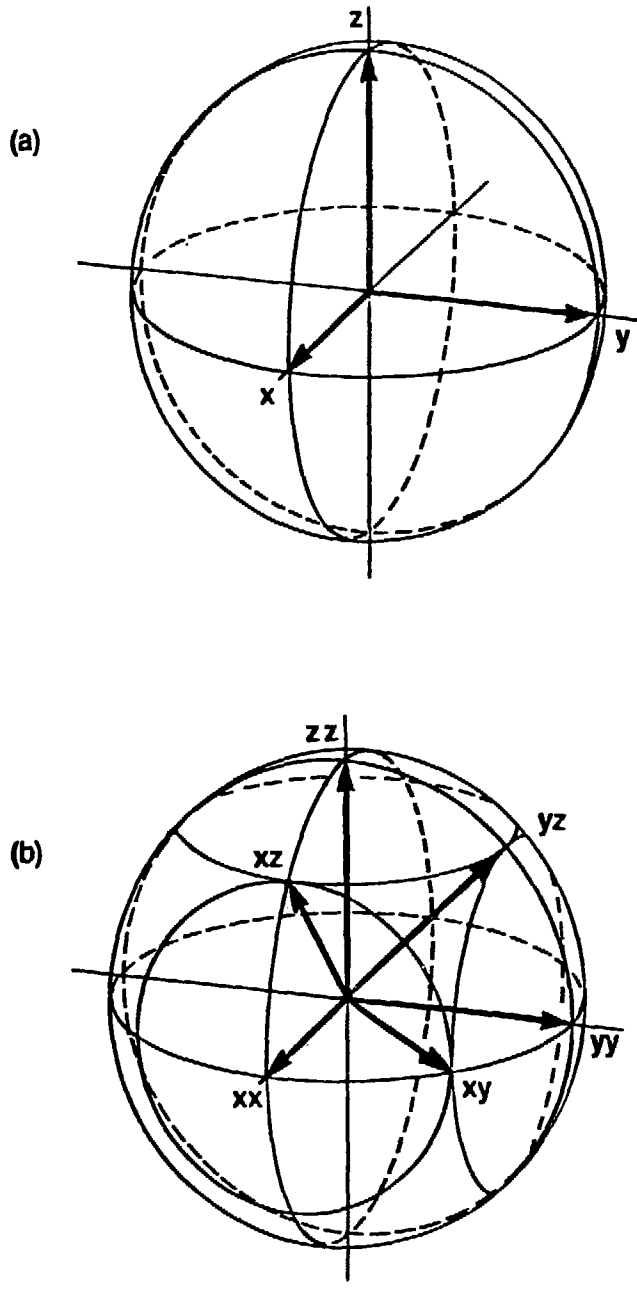

XBL 872-9572

Fig.3.2 Vector representation of the (a)linear and (b)bilinear spin operators. Curves denote the trajectories the operators follow under rotations about the coordinate axes.

terms XX, YY, and ZZ have the same correspondence to the vectors except that two opposite points on the sphere are identical. Bilinear cross terms point at the midway between two adjacent coordinate axes. Again points on the opposite sides of the sphere are equivalent.

If the rotations are made about the coordinate axes, the trajectories of the linear terms and bilinear quadratic terms would be certain segments of the great circles. The trajectories of the bilinear cross terms would be confined to circles with a radius $1/\sqrt{2}$, when only one component changes during the rotation, while they will be segments of great circles when the rotation axes are orthogonal to the direction of the operators.

With these tools is now possible to achieve various objectives such as averaging out the ZZ term.

(i) Z term

In high field, because of magnetic field inhomogeneity the spin isochromats undergo rapid dephasing. The inhomogeneity, which is proportional to Z, can be removed by pulse sequences such as the Carr-Purcell sequence. By a series of π pulses (or equivalently, two juxtaposed two $\pi/2$ pulses), the Z term in the interaction frame is periodically inverted: Z, $\bar{Z}$, Z, $\bar{Z}$,.... Thus the average is zero. Note that the ideal Carr-Purcell sequence generates the "perfect echo". It is obtained whenever

$$\bar{\mathcal{H}}^{(0)} = \bar{\mathcal{H}}^{(1)} = \ldots = \bar{\mathcal{H}}^{(n)} = \ldots = 0 \qquad (3.22)$$

because then

$$\rho(\tau) = U(\tau)\rho(0)U^{\dagger}(\tau) = e^{-i\bar{\mathcal{H}}\tau}\rho(0)e^{i\bar{\mathcal{H}}\tau} = \rho(0). \tag{3.23}$$

It is also possible to generate the perfect echo with a condition less stringent than Eq.(3.22), namely if either

$$[\ \bar{\mathcal{H}}_{int}\ ,\ \rho(0)\ ] = 0 \tag{3.24}$$

or

$$[\ \tilde{\mathcal{H}}_{int}\ ,\ \rho(0)\ ] = 0, \tag{3.25}$$

because then

$$\rho(\tau) = U(\tau)\rho(0)U^{\dagger}(\tau) = \rho(0)UU^{\dagger}(\tau) = \rho(0). \tag{3.26}$$

For the Carr-Purcell case, the initial density operator and the internal Hamiltonian are

$$\rho(0) = I_z \tag{3.27}$$

and

$$\mathcal{H}_{int} = \delta\omega I_z. \tag{3.28}$$

The switched internal Hamiltonian resulting from the Carr-Purcell sequence is

$$\tilde{\mathcal{H}}_{int}(t) = \pm\ \delta\omega I_z \tag{3.29}$$

with the sign depending on time. In this case Eqs.(3.24) and (3.25) as well as Eq.(3.22) is satisfied since

$$[\ \tilde{\mathcal{H}}(t),\tilde{\mathcal{H}}(t')\ ] = 0. \tag{3.30}$$

The heteronuclear interaction, after truncation, is proportional to $I_z S_z$. As long as γ_I and γ_S are sufficiently different for the pulses to affect only one spin species, the heteronuclear interaction can be removed by the same sequence. The removal of the Z term requires two configurations if δ pulses are employed.

With windowless sequences, any stationary point α is to be removed by adding another stationary point $-\alpha$. As given in Table 3.2 a transition gives an average $(2/\pi)(\alpha+\alpha')$ which is incommensurate with α and α', so it must be treated separately from stationary points. The number of times that α appears in transitions must be equal to the number of times $-\alpha$ appears. A minimum number of four $\pi/2$ rotations (or two π rotations) is required to remove the Z term.

(ii) All three linear terms

In zero-field experiments, it is difficult to attain the perfect zero-field because of a residual field and in general it has all three components. So the spin-residual field interaction term may be written as

$$\mathcal{H}_{res} = a_x I_x + a_y I_y + a_z I_z. \tag{3.31}$$

It therefore is necessary to remove all three linear terms to obtain the true zero-magnetic field. With δ pulses a minimum of four configurations, for example $\{(x,y,z),(x,\bar{y},\bar{z}),(\bar{x},\bar{y},z),(\bar{x},y,\bar{z})\}$ is required. These configurations are reached by the sequence of π rotations with equal delays between pulses: $(-\pi_x-\pi_y-\pi_x-\pi_y-)_n$. The sequence then is an zero-field analog of the Carr-Purcell sequence. However, in this case the perfect echo cannot be obtained because the

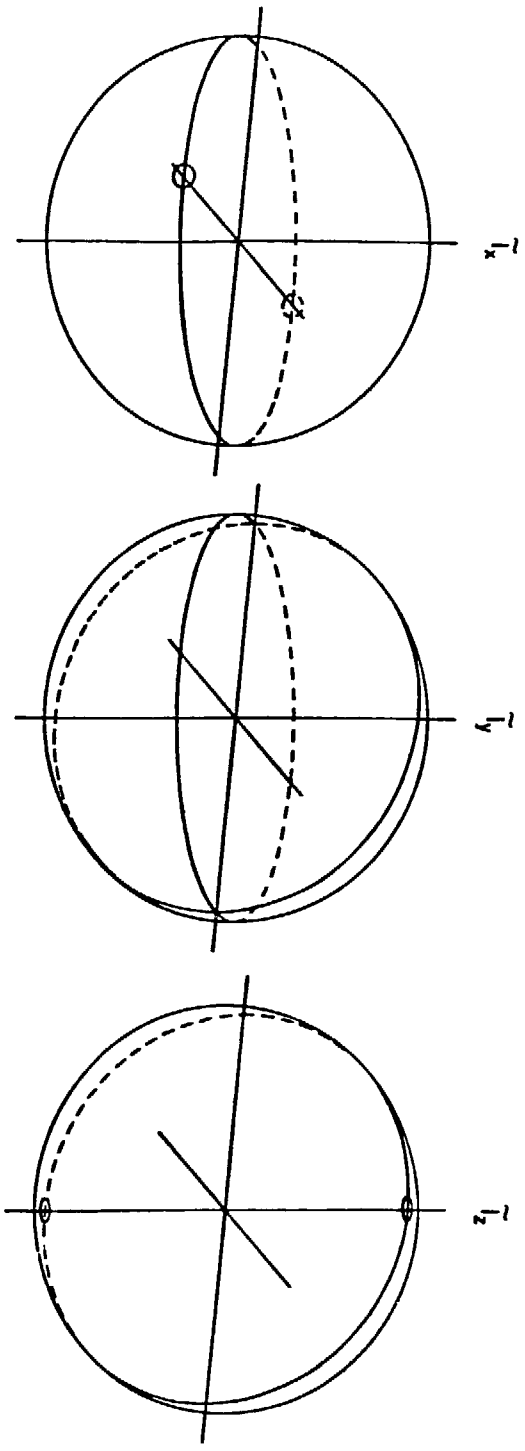

XBL 872 9571

Fig. 3.3 Trajectories of the three linear spin operators under the 16-pulse sequence (x x y y $\bar{x}$ $\bar{x}$ $\bar{y}$ $\bar{y}$ $\bar{x}$ $\bar{x}$ $\bar{y}$ $\bar{y}$ x x y y). The operators are eliminated by the sequence simultaneously. Small circles are stationary points.

Hamiltonians at different times do not commute with each other or with the initial density operator. For example, the Hamiltonian after the first pulse is $a_xI_x - a_yI_y - a_zI_z$ an it in general does not commute with $a_xI_x + a_yI_y + a_zI_z$.

The removal of all three terms with a windowless pulse sequence is much more complicated. It involves both stationary points and transitions. A minimum of 16 $\pi/2$ rotations (or eight π rotations) is required. An example of such a sequence is (x x y y $\bar{x}$ $\bar{x}$ $\bar{y}$ $\bar{y}$ $\bar{x}$ $\bar{x}$ $\bar{y}$ $\bar{y}$ x x y y). In Fig.3.3 the trajectories of three linear terms under the above sequence is shown.

(iii) ZZ term

As discussed at the beginning of this chapter, with δ pulses a minimum of three configurations, eg. {(x,y,z),(y,z,x),(z,x,y)}, is required to make the ZZ term vanish via the isotropic average

$$XX + YY + ZZ = 0, \tag{3.32}$$

since they cannot be inverted. The WHH-4 sequence is an example which satisfies Eq.(3.32). Incidentally, these three configurations also remove other quadratic terms YY and XX via Eq.(3.32). Therefore, in general, for any sequence to average the quadratic terms to zero it must average them over a multiple of three configurations.

A windowless anlog of the WHH-4 is the BLEW-6 sequence.[3] For quadratic terms $\alpha\alpha$, a transition $\alpha\alpha \rightarrow \beta\beta$ has the average Hamiltonian $(\alpha\alpha+\beta\beta)/2 + (1/\pi)\alpha\beta$ if $\alpha \neq \beta$ and $\alpha\alpha$ if $\alpha = \beta$. For the ZZ term the transition $ZZ \rightarrow \alpha\alpha$ has the average Hamiltonian

$$\bar{\mathcal{H}}^{(0)} = [\alpha,Z]^2/2 + \alpha Z/\pi \qquad (\alpha = x,y) \tag{3.33}$$

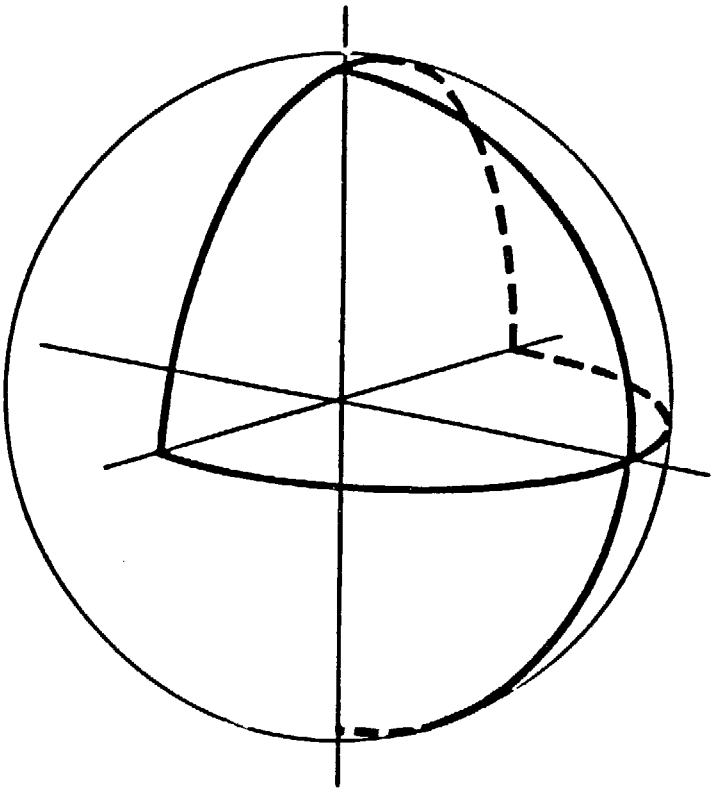

XBL 8711-5954

Fig. 3.4 A trajectory over which the ZZ term is averaged out.

whereas for $\alpha\alpha$ = ZZ

$$\bar{\mathcal{H}}^{(0)} = ZZ \ . \tag{3.34}$$

If pulses are to be applied only along the x, y, $\bar{x}$, and $\bar{y}$ directions Eq.(3.34) is irrelevant. The first term in Eq.(3.33) is a quadratic term and therefore must be averaged to zero via Eq.(3.32), whereas the second one is a cross term and must be balanced by a term proportional to $-\alpha Z$. These two averaging requirements are independent of each other, so a multiple of six steps is required to make $\bar{\mathcal{H}}^{(0)}$ to vanish. One such a trajectory is shown in Fig. 3.4.

It is observed that:

(a) To ensure the isotropic averaging, Eq.(3.32), a trajectory must traverse x, y, and z = $\pm$1 equal number of times, and

(b) Each quarter segment of a great circle must be balanced by an adjacent segment of the same circle.

There are eight trajectories equivalent to the one shown in Fig.3.4, associated with eight octants. There are six different ways of covering the trajectory in Fig.3.4. In terms of the notation of Burum et.al.[3] these are

$$(ZX)(XY)(Y\bar{X})(\bar{X}Z)(ZY)(Y\bar{Z})$$

$$(ZX)(XY)(YZ)(Z\bar{X})(\bar{X}Y)(Y\bar{Z})$$

$$(Z\bar{X})(\bar{X}Y)(YX)(XZ)(ZY)(Y\bar{Z})$$

$$(Z\bar{x})(\bar{X}Y)(YZ)(ZX)(XY)(Y\bar{Z})$$

$$(ZY)(YX)(XZ)(Z\bar{X})(\bar{X}Y)(Y\bar{Z})$$

$$(ZY)(Y\bar{X})(\bar{X}Z)(ZX)(XY)(Y\bar{Z})$$

all with a scaling factor equal to $2\sqrt{5}/3\pi$, identical to BLEW-6 sequences. Overall there are 8×6 = 48 sequences that are equivalent to

BLEW-6 sequences.

(iv) Other bilinear terms

Other quadratic terms XX and YY are also removed via the isotropic average if δ pulses are used. The configurations $\{(X,Y,Z),(Y,Z,X),(Z,X,Y)\}$ can be reached either by pairs of 90^0 rotations around the coordinate axes or by 120^0 rotations around the cube body axes.

Terms XX and YY are simply obtained from ZZ by 90^0 rotations around x or y axes respectively. Thus to average XX, for example, with windowless sequence one notes

$$\bar{\mathcal{H}}^{(0)}_{zz} = 0 = \int_0^\tau U^\dagger_{p,z}(t)\ ZZ\ U_{p,z}(t)dt - P_y^\dagger \int_0^\tau P_y U^\dagger_{p,z}(t) P_y^\dagger\ XX\ P_y U_{p,z}(t) P_y^\dagger\ dt\ P_y, \tag{3.35}$$

where P_y is a 90^0 rotation around y axis. Therefore, the trajectory of $\tilde{X}\tilde{X}(t)$ that satisfies

$$\bar{\mathcal{H}}^{(0)}_{xx} = \int_0^\tau U^\dagger_{p,x}(t)\ XX\ U_{p,x}(t)\ dt = 0 \tag{3.36}$$

may be obtained from

$$U_{p,x} = P_y\ U_{p,z}\ P_y^\dagger. \tag{3.37}$$

Thus the removal of any one of the three quadratic terms is simply related to the others and basically involves the same procedure. The removal of all three quadratic terms involves two stationary points

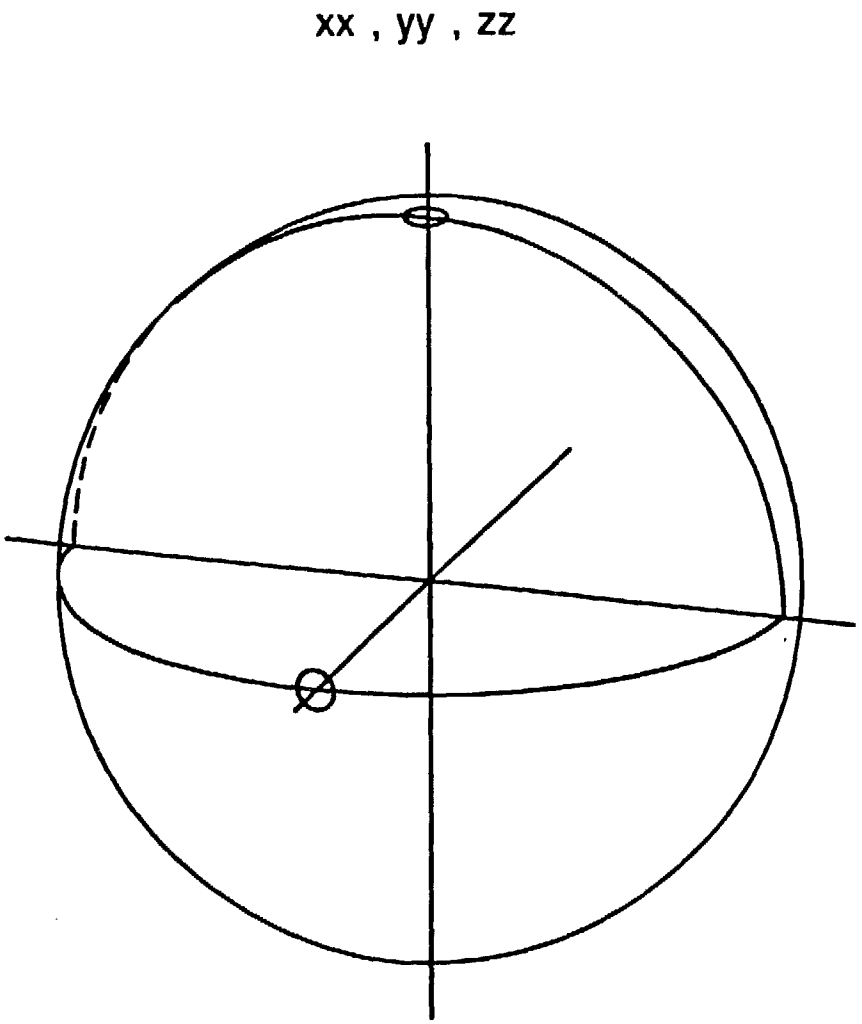

XBL 872-9569

Fig. 3.5 Trajectory the three bilinear operators XX, YY, and ZZ traverse under the windowless sequence $(x\ y\ z)^2$.

(a)

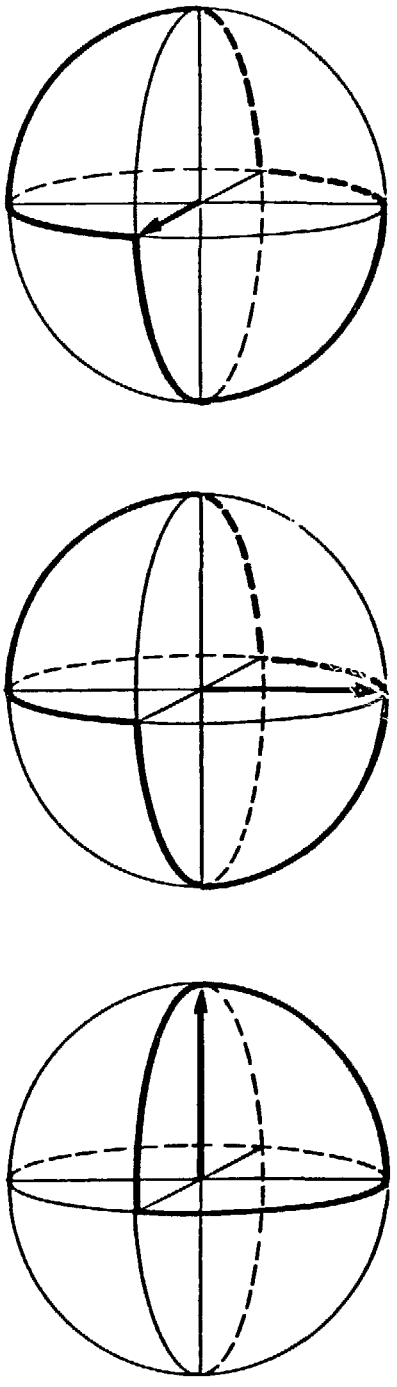

XBL 8711-5973

(b)

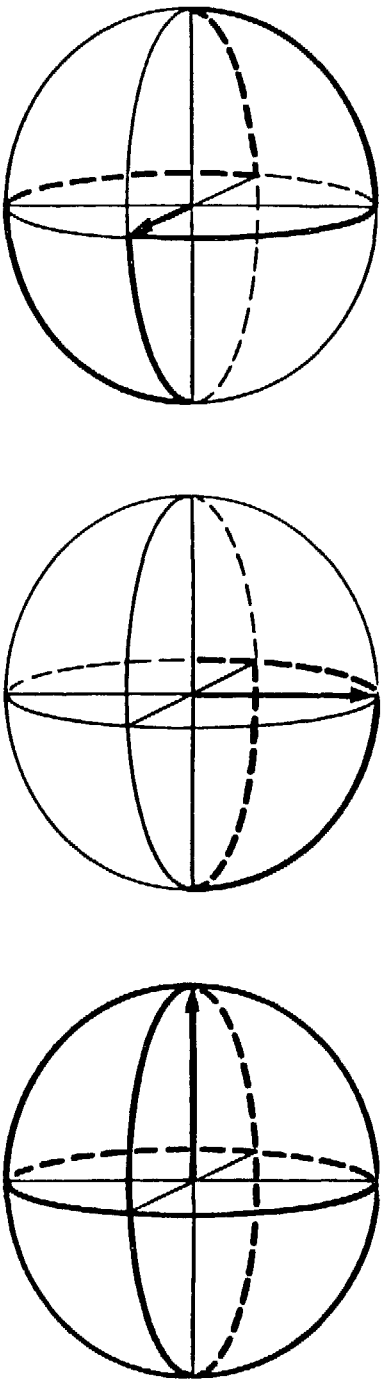

XBL 8711-5967

Fig. 3.6 Trajectories of the three linear spin operators under the 12 pulse sequences (a) $(\bar{y}\ x\ y\ \bar{x})^3$ and (b) $(x\ y\ \bar{x}\ y)^3$. The average of I_z under the first sequence is along the (1 1 1) axis, while it vanishes under the second sequence.

even though the same number of six steps are needed and Fig.3.5 shows one such trajectory, resulting from the sequence $(xyz)^2$.

A cross term is to be removed by adding an inverse. In any configuration (α,β,γ) the number of negative cross terms is either zero or two. In other words, it is an even number. Thus a multiple of four configurations is required to remove all three cross terms. The removal of all six bilinear operators requires therefore at least 12 configurations. The corresponding 12-pulse sequence is a zero-field analog of the WHH-4 sequence. If a windowless sequence is employed, 24 90^0 pulses are needed to remove all six bilinear terms, corresponding to BLEW-6 sequence for high field.

The use of 12-pulse sequences will be discussed in connection to decoupling experiments in a later chapter, and they deserve some more discussion which is given in the next section.

III.4 The 12-pulse sequences

There are three types of 12 90^0-pulse sequences which are zero-field analogs of the high-field WHH-4 sequence. The first group contains z and $\bar{z}$ pulses as well as pulses along x and y axes. A few examples are

$$(x\ y\ z\ x\ y\ \bar{z})^2,$$

$$(\bar{z}\ \bar{y}\ x\ z\ \bar{y}\ x)^2, \text{ and}$$

$$(y\ \bar{z}\ x\ y\ z\ x)^2.$$

The remaining two types of sequences have a common structure of

Table 3.3 Averaging of linear and bilinear operators under $(\bar{y}\ x\ y\ \bar{x})^3$ sequence.

	X	Y	Z	XY	YZ	ZX	XX-YY	YY-ZZ	ZZ-XX
$\bar{y}$	-Z	Y	X	-YZ	XY	-ZX	ZZ-XX	YY-XX	XX-ZZ
x	-Z	-X	Y	ZX	-XY	-YZ	ZZ-XX	XX-YY	YY-ZZ
y	Y	-X	Z	-XY	-ZX	YZ	YY-XX	XX-ZZ	ZZ-YY
$\bar{x}$	Y	Z	X	YZ	ZX	YX	YY-ZZ	ZZ-XX	XX-YY
$\bar{y}$	-X	Z	Y	-ZX	YZ	-XY	XX-ZZ	ZZ-YY	YY-XX
x	-X	-Y	Z	XY	-YZ	-ZX	XX-YY	YY-ZZ	ZZ-XX
y	Z	-Y	X	-YZ	-XY	ZX	ZZ-YY	YY-XX	XX-ZZ
$\bar{x}$	Z	X	Y	ZX	XY	YZ	ZZ-XX	XX-YY	YY-ZZ
$\bar{y}$	-Y	X	Z	-XY	ZX	-YZ	YY-XX	XX-ZZ	ZZ-YY
x	-Y	-Z	X	YZ	-ZX	-XY	YY-ZZ	ZZ-XX	XX-YY
y	X	-Z	Y	-ZX	-YZ	XY	XX-ZZ	ZZ-YY	YY-XX
$\bar{x}$	X	Y	Z	XY	YZ	ZX	XX-YY	YY-ZZ	ZZ-XX
	0	0	SI_{111}	0	0	0	0	0	0

$s = 1/\sqrt{3}$

$I_{111} = (I_x+I_y+I_z)/\sqrt{3}$

Table 3.4 Summary of averaging of operators for windowless sequences

Sequence*	X	Y	Z	XY	YZ	ZX	XX-YY	YY-ZZ	ZZ-XX	
$(x\bar{y}x\bar{y})^3$	0	$I^{\ddagger}_{11\text{-}1}$	0	0	0	0	$-4A^{\#}_{11\text{-}1}$	$2A_{11\text{-}1}$	$2A_{11\text{-}1}$	
$(x\bar{y}xy)^3$	$I_{\text{-}111}$	0	0	0	0	0	$4A_{\text{-}111}$	$-2A_{\text{-}111}$	$-2A_{\text{-}111}$	Group
$(xy\bar{x}y)^3$	0	$I_{1\text{-}11}$	0	0	0	0	$-4A_{1\text{-}11}$	$2A_{1\text{-}11}$	$2A_{1\text{-}11}$	(a)
$(xyx\bar{y})^3$	I_{111}	0	0	0	0	0	$4A_{111}$	$-2A_{111}$	$-2A_{111}$	
$(\bar{x}\bar{y}xy)^3$	0	0	$I_{1\text{-}11}$	0	0	0	0	$-6A_{1\text{-}11}$	$6A_{1\text{-}11}$	
$(\bar{x}yx\bar{y})^3$	0	0	$I_{11\text{-}1}$	0	0	0	0	$-6A_{11\text{-}1}$	$6A_{11\text{-}1}$	Group
$(x\bar{y}\bar{x}y)^3$	0	0	I_{111}	0	0	0	0	$-6A_{111}$	$6A_{111}$	(b)
$(xy\bar{x}\bar{y})^3$	0	0	$I_{\text{-}111}$	0	0	0	0	$-6A_{\text{-}111}$	$6A_{\text{-}111}$	

*Only representative sequences in each group are given.

$^{\ddagger}I_{11\text{-}1} = (I_x + I_y + I_z)/3$, etc.

$^{\#}A_{11\text{-}1} = (I_xI_y + I_yI_{\bar{z}} + I_{\bar{z}}I_x)/12$, etc.

$(\alpha\ \beta\ \alpha'\ \beta')^3$, with α and β being orthogonal and applied along $\pm x$ or $\pm y$ axes. α may or may not be equal to α'. So is with β and β'. These have intimate connection to the broadband decoupling sequences to be discussed in the next chapter. Two representative pulse sequences, one from each group, are $(\bar{y}\ x\ y\ \bar{x})^3$ and $(x\ y\ \bar{x}\ y)^3$, and corresponding trajectories for linear terms are given in Fig.3.6.

It can easily be seen that for the sequence $(\bar{y}\ x\ y\ \bar{x})^3$, $\bar{I}_x = \bar{I}_y = 0$ and $\bar{I}_z = S\ I_{111}$. The scaling factor S is $1/\sqrt{3}$ for the δ pulse case and $4/(\pi\sqrt{3})$ for the windowless case. The averaging for this sequence is shown in Table 3.3. For the sequence $(x\ y\ \bar{x}\ y)^3$, $\bar{I}_x = \bar{I}_y = 0$ and $\bar{I}_y = S\ I_{-11-1}$, with $S = 1/\sqrt{3}$ and $1/\sqrt{3}(2/\pi+1/2)$ for δ and windowless cases respectively. Table 3.3 also lists configurations reached during the sequence. The average values of various terms resulting from windowless sequences are summarized in Table 3.4.

It is interesting to note that the average value of quadratic terms $\alpha\alpha - \beta\beta$ $(\alpha,\beta = x, y, \text{or } z)$ all have the same form $(\alpha\beta + \beta\gamma + \gamma\alpha)$ if the trajectory of the nonvanishing linear term is in an octant spanned by $(\alpha\ \beta\ \gamma)$. It is also seen that even though each 12-pulse windowless sequence does not remove the bilinear terms, it is possible to do so by combining two suitably chosen sequences such as $(\bar{x}\ y\ x\ y)^3(x\ y\ x\ \bar{y})^3$, thus creating the desired 24 configurations as discussed in the previous section. However, no two sequences from group (b) can make all the bilinear term vanish. However, it can be shown that 36-pulse sequences such as

$$(\bar{y}\ \bar{x}\ y\ x)^3(z\ y\ \bar{z}\ \bar{y})^3(x\ \bar{z}\ \bar{x}\ z)^3$$

can make all bilinear terms vanish. For clarity, a few examples of

Table 3.5 Average values of operators resulting for group (b) sequences

	X	Y	Z	XY	YZ	ZX	XX-YY	YY-ZZ	ZZ-XX
$(\bar{y}x\bar{y}x)^3$	0	0	$I^{\ddagger}_{111}$	0	0	0	0	-6*	6
$(\bar{x}z\bar{x}z)^3$	0	I_{111}	0	0	0	0	-6	6	0
$(\bar{z}y\bar{z}y)^3$	I_{111}	0	0	0	0	0	6	0	-6
	.....								
$(y\bar{x}\bar{y}x)^3$	0	0	I_{-1-11}	0	0	0	0	-6	6
$(xz\bar{x}\bar{z})^3$	0	$-I_{-1-11}$	0	0	0	0	-6	6	0
$(\bar{z}\bar{y}zy)^3$	$-I_{-1-11}$	0	0	0	0	0	6	0	-6

‡Same as in Table 3.4.

*$A_{\alpha\beta\gamma}$ is suppressed for simplicity.

sequences with average values of operators are listed in Table 3.5.

In order to see the relationship between 12-pulse sequences and high-field iterative pulse schemes, it is necessary to have a brief review on the latter, which is the subject of the next chapter.

References

1(a). J. S. Waugh, L. M. Huber and U. Haeberlen, Phys. Rev. Lett. 20, 180 (1968).

1(b). U. Haeberlen and J. S. Waugh, Phys. Rev. 175, 453 (1969).

2. M. Hammermesh, Group Theory and its Application to Physical Problems, (Addison-Wesley, Reading, 1962).

3. D. P. Burum, M. Linder and R. R. Ernst, J. Mag. Res. 44, 173 (1981).

4. For an excellent introduction see, J. D. Macomber, The Dynamics of Spectroscopic Transitions, (Wiley, New York, 1976).

CHAPTER IV. Iterative Schemes in NMR

IV.1. Introduction

In NMR iterative schemes have been widely used ranging from the design of error compensated pulses for broadband excitation to selective multiple-quantum excitation. There are several extensive reviews available.[1-6] Consequently this chapter will focus on only some limited aspects of the iterative schemes: basic ideas behind broadband decoupling schemes such as the MLEV,[7] and the Waugh schemes[8] for single-spin cases. Then an extension will be made to take the homonuclear spin-spin coupling into consideration.

In previous chapters the assumption has been made that the pulses are much stronger than internal Hamiltonian terms. Mathematically, it corresponds to

$$\|\mathcal{H}_{int}\| t_c \ll 1, \tag{4.1}$$

where t_c is the cycle time of the sequence. Even for windowless sequences experimental results on high field dipole-coupled systems[9] show that the 90^0 pulses with widths up to 6 μsec were successful before the quality of the experimental results degraded. That corresponds to approximately 40 kHz for proton decoupling field strength. However, there are many samples which are polar or ionic so that the "lattice" of the sample absorbs the energy from the decoupling field. The heat thus generated in the sample not only damages the sample but also causes decoupling field inhomogeneity via thermal expansion of the decoupler coil. The temperature effect will be discussed in more detail later in a

section on spin-decoupling in liquids.

In order to achieve better resolution spectrometers with higher fields are being used. This means that the spread of chemical shifts to be decoupled is bigger. Consequently, the goal of modern decoupling schemes is to decouple broader bandwiths with minimal expenditure of decoupler power.

As the lower decoupler level is used, the magnitude of the resonance offset term becomes comparable to that of the decoupling field. Using AHT with the offset term included in the internal Hamiltonian would quickly become inaccurate as $\Delta\omega/\omega_2$ gets bigger. For this reason, it is desirable to consider the offset term as an additional external field. In the next section a closer look at this external Hamiltonian is given.

IV.2. Offset-incorporated Pulses

When there exists an offset with a size comparable to that of $\mathcal{H}_{rf}$, the total Hamiltonian for the perturbing field may be written as

$$\mathcal{H}_1 = \Delta\omega I_z + \omega_2 I_x, \tag{4.2}$$

where the decoupling field B_2 is assumed to be applied along the rotating frame x-direction and $\omega_2 = \gamma_I B_2$. The actual rotation due to the effective Hamiltonian $\mathcal{H}_1$ is

$$\begin{aligned} \hat{n}\cdot\underline{I}\,\beta^* &= -\omega_2^* t_p\, \hat{n}\cdot\underline{I} \\ &= -t_p(\Delta\omega I_z + \omega_2 I_x), \end{aligned} \tag{4.3}$$

where t_p is the pulse width. The magnitude and the direction of the

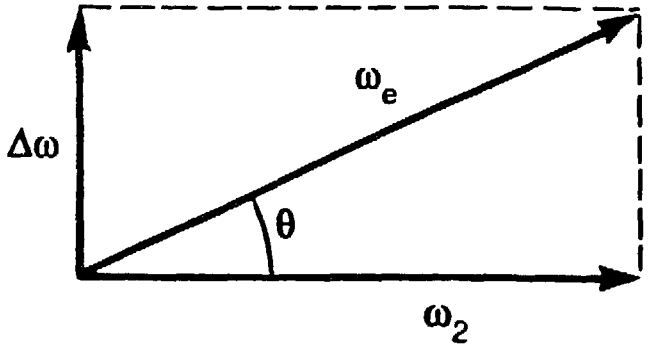

Fig. 4.1 The direction and the magnitude of the effective field resulting from the rf pulse and the resonance offset.

field is shown in Fig.4.1. Eq.(4.3) may be rewritten as

$$\hat{n}\cdot\underset{\sim}{I}\,\beta^{*} = t_p\sqrt{\Delta\omega^2+\omega_2^2}\left(\frac{\Delta\omega I_z}{\sqrt{\Delta\omega^2+\omega_2^2}} + \frac{\omega_2 I_x}{\sqrt{\Delta\omega^2+\omega_2^2}}\right)$$

$$= t_p\,\omega_e\left(\cos\theta\, I_x + \sin\theta\, I_z\right)$$

$$= t_p\,\omega_e\,\exp\left(i\theta I_y\right) I_x \exp\left(-i\theta I_y\right), \tag{4.4}$$

where

$$\tan\theta = \Delta\omega/\omega_2. \tag{4.5}$$

Eq.(4.4) can further be reduced to

$$\hat{n}\cdot\underset{\sim}{I}\,\beta^{*} = \omega_2 t_p \sec\theta \exp\left(i\theta I_y\right) I_x \exp\left(-i\theta I_y\right)$$

$$= \beta \sec\theta \exp\left(i\theta I_y\right) I_x \exp\left(-i\theta I_y\right). \tag{4.6}$$

Hence, if $\mathcal{H}_{rf}$ is applied along x-direction such that

$$\beta = \omega_2 t_p, \tag{4.7}$$

the net rotation angle is

$$\beta^{*} = \omega_2^{*} t_p = \beta \sec\theta \tag{4.8}$$

and the rotation axis is

$$\hat{n} = \hat{i}\cos\theta + \hat{k}\sin\theta. \tag{4.9}$$

More generally, when the pulse is applied along an axis rotated by a phase angle ϕ, the evolution operator for describing the net rotation is

$$U(\beta;\phi) = \exp\left(i\beta^{*}\hat{n}\cdot\underline{I}\right)$$

$$= e^{i\theta I_y}\, e^{i\phi I_z}\, e^{-i\beta I_x}\, e^{-i\phi I_z}\, e^{-i\theta I_y}. \tag{4.10}$$

In practice ω_2 is not equal to the nominal decoupler level ω_2^0. In terms of nominal quantities labeled with the superscript "0", the actual rotation angle can be written as

$$\beta^* = \beta^0 \frac{\omega_2}{\omega_2^0} \sec\theta = \beta^0 \left(1 + \frac{\delta\omega_2}{\omega_2^0}\right) \sec\theta, \tag{4.11}$$

where

$$\delta\omega_2 = \omega_2 - \omega_2^0. \tag{4.12}$$

IV.3. Iterative Schemes for Linear Operators

Because the effective angle β^* is different from the nominal value β^0 and the net rotation axis is not along the direction of the original pulse, it becomes very difficult to visualize the net effect of the sequence of such pulses. This is largely due to the $\Delta\omega$ term and also partly due to pulse imperfections such as $\delta\omega_2$. Thus it is important to design a scheme to offset the effect of these causes of pulse imperfection, and this is the main goal of designing composite pulses.

Now suppose a composite pulse R is designed such that the net effect of R is an approximate inversion of z-magnetization over a wide range of $\Delta\omega$:

$$R^\dagger I_z R \approx - I_z. \tag{4.13}$$

Then RR(= c) is an approximate cycle in the sense that

$$C^\dagger I_z C \approx I_z. \tag{4.14}$$

Two common operations for constructing more highly compensated cycles are phase shift and cyclic permutation of a certain segment of the sequence to the either ends of the sequence. The phase shift by 180^0 is an operation which inverts the phases of all constituent pulses, and is denoted as $\bar{C}$. It can be shown[3,8] that $\bar{C}$ leaves the net rotation angle

and the z-component of the rotation of the rotation axis unchanged but reverts x- and y-components of the rotation axis. Thus, provided that the z-component is very small, $\bar{C}$ is nearly the opposite rotation of C. A sequence C^P generated by cyclically permuting R, an approximate 180^0, nearly inverts the z-component of the rotation axis provided that it is predominantly bigger than x- and y- components.

Linear spin operators can be averaged out by using these operations, and Fig.4.2 shows a systematic cancellation scheme. In Fig.4.2.(a), the big resonance offset term is shown. The effect is approximately removed by the composite 180^0 pulse R. In (b), RR is thus a cycle with rotation axis almost in the x-y plane. Then RR is combined with $\overline{RR}$ in (c) to give the rotation axis along z (MLEV-4). Then $\overline{R}RR\overline{R}$, which is obtained by cyclically permuting a $\bar{R}$ and which approximately inverts the z-components, is added to give a net rotation axis predominantly in the x-y plane (MLEV-8), part (d). Finally, a phase inverted 8-pulse cycle is added to cancel x-y components, leaving only a small z-component (MLEV-16). MLEV-4 is the first member of the family of the MLEV sequences which has vanishingly small rotations. Hence it makes the linear I_z operator in

$$\mathcal{H}_{int} = (J\ S_z)I_z \tag{4.15}$$

vanish, thereby leading to heteronuclear decoupling.

IV.4 Connection to the Average Hamiltonian Theory

The switched Hamiltonian $\tilde{\mathcal{H}}_{int}$ resulting from the irradiation on the I spin with the composite pulse R in general has all three

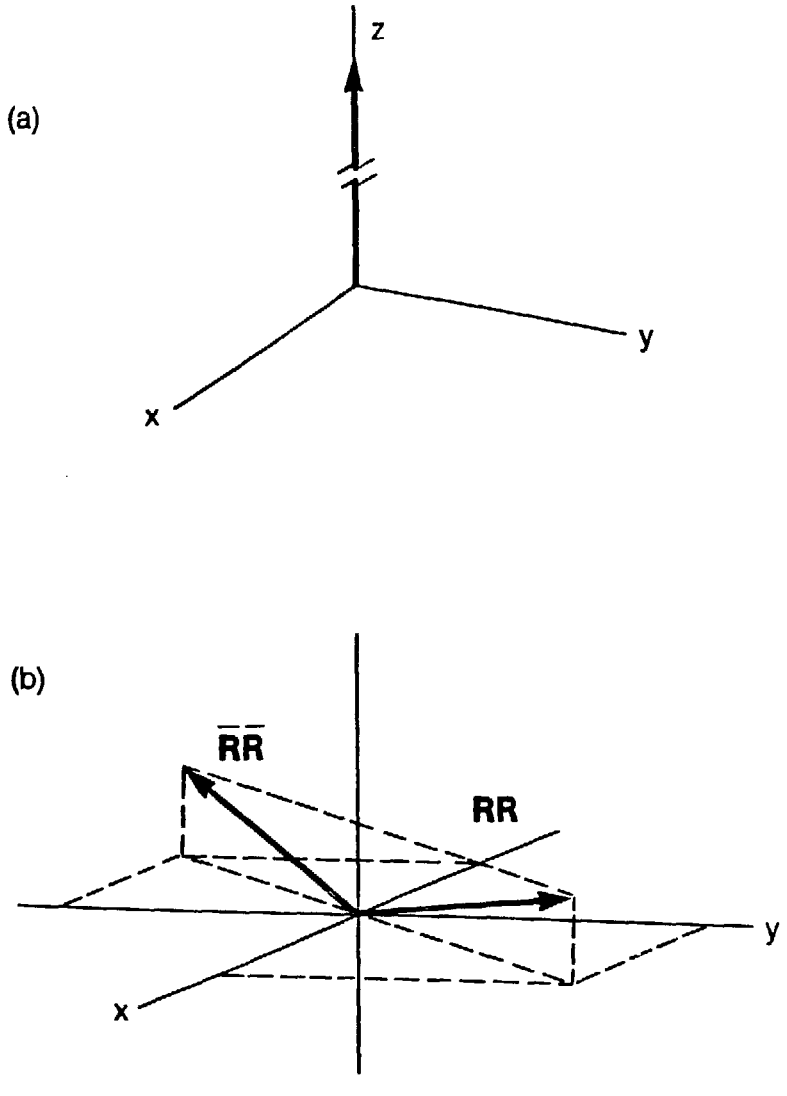

XBL 8711-5951

Fig. 4.2 Diagrams showing cancellation of errors by systematic concatenation of sequences related to each other by phase shifts and permutation of parts of the sequence. In (c) θ denotes a very small angle.

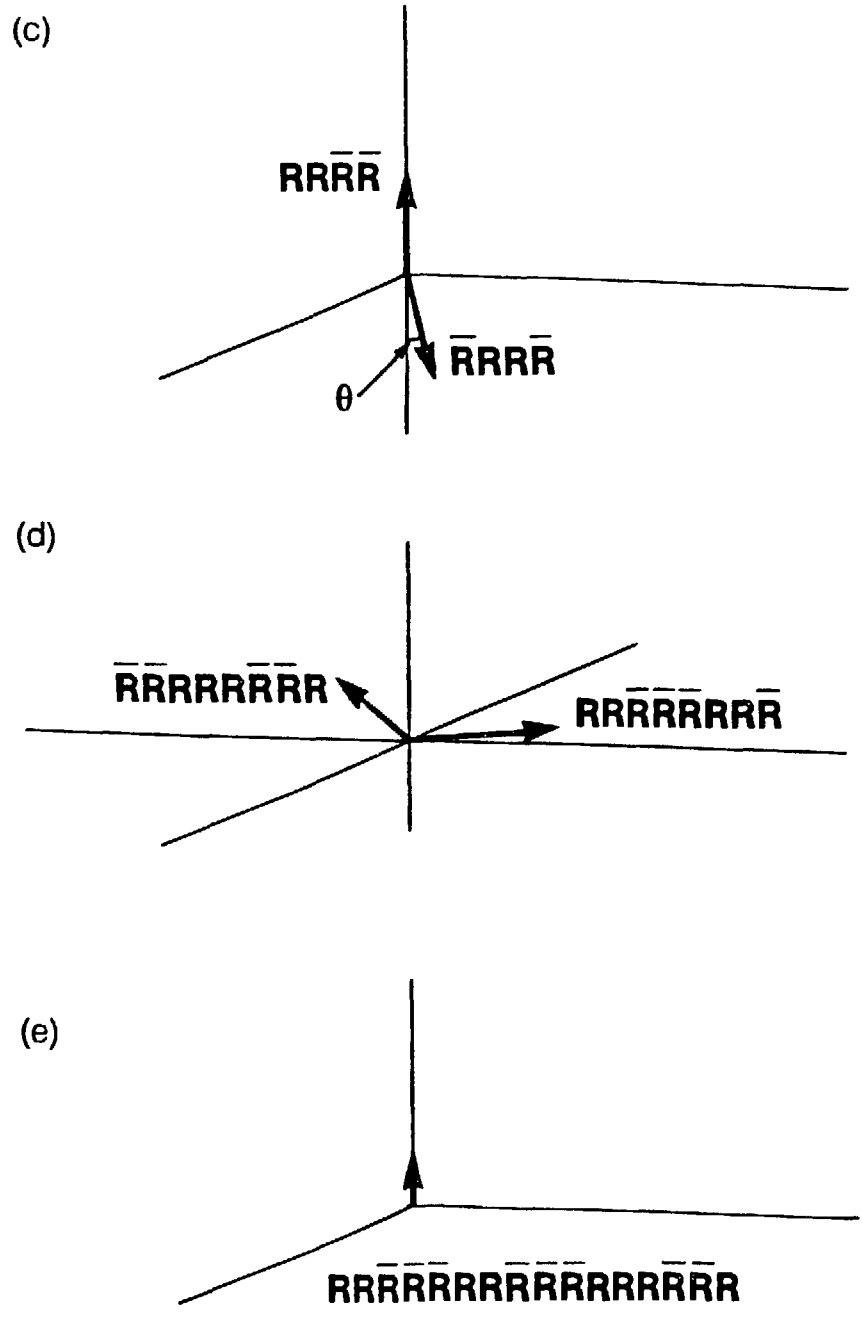

XBL 8711-5952

components

$$\bar{\mathcal{H}}_{int} = JS_z\left\{a(t)I_x + b(t)I_y + c(t)I_z\right\}, \tag{4.16}$$

where a(t), b(t), and c(t) are constants. The average Hamiltonian is

$$\bar{\mathcal{H}}_{int} = JS_z\left(aI_x + bI_y + cI_z\right), \tag{4.17}$$

where a, b, and c are time-independent constants and are not in general time-averages of a(t), b(t), and c(t). The quantity in the parenthesis in Eq.(4.17) has the same form as the residual field appearing in zero-field experiments. As discussed in Chapter III, it can be removed with a minimum of four configurations such as those obtained by applying the zero-field analog of the Carr-Purcell sequence, $(-\pi_x-\pi_z-\pi_x-\pi_z-)_n$.

For the case of MLEV-4 sequence $RR\bar{R}\bar{R}$, the total average Hamiltonian is

$$\bar{\mathcal{H}}^{(0)} = \frac{1}{4}\left\{\bar{\mathcal{H}}_{int} + R^{\dagger}\bar{\mathcal{H}}_{int}R + e^{i\pi I_z}\,\bar{\mathcal{H}}_{int}e^{-i\pi I_z} + e^{i\pi I_z}R^{\dagger}\,\bar{\mathcal{H}}_{int}Re^{-i\pi I_z}\right\}. \tag{4.18}$$

with $\bar{\mathcal{H}}_{int}$ given by Eq.(4.17).

In general the composite 180^0 pulse can be written as

$$R \approx e^{-i\theta I_z}\, e^{-i\pi I_x}\, e^{i\theta' I_z}, \tag{4.19}$$

where θ and θ' are offset dependent. In other words, the rotation axis is on the x-y plane and the phase may vary depending upon the offset. With the assumption that Eq.(4.19) holds exactly, Table 4.1 is drawn up to show the cancellation of terms. a' and b' are in general different from a and b due to Eq.(4.19).

For the zero-field sequence $(-\pi_x-\pi_z-\pi_x-\pi_z-)_n$ shown in Fig.4.3(a), the corresponding average of the Hamiltonian is

Table 4.1 Cancellation of linear terms with R R $\bar{R}$ $\bar{R}$

Pulse	I_x	I_y	I_z
R	a	b	c
R	a'	b'	-c
$\bar{R}$	-a	-b	c
$\bar{R}$	-a'	-b'	-c

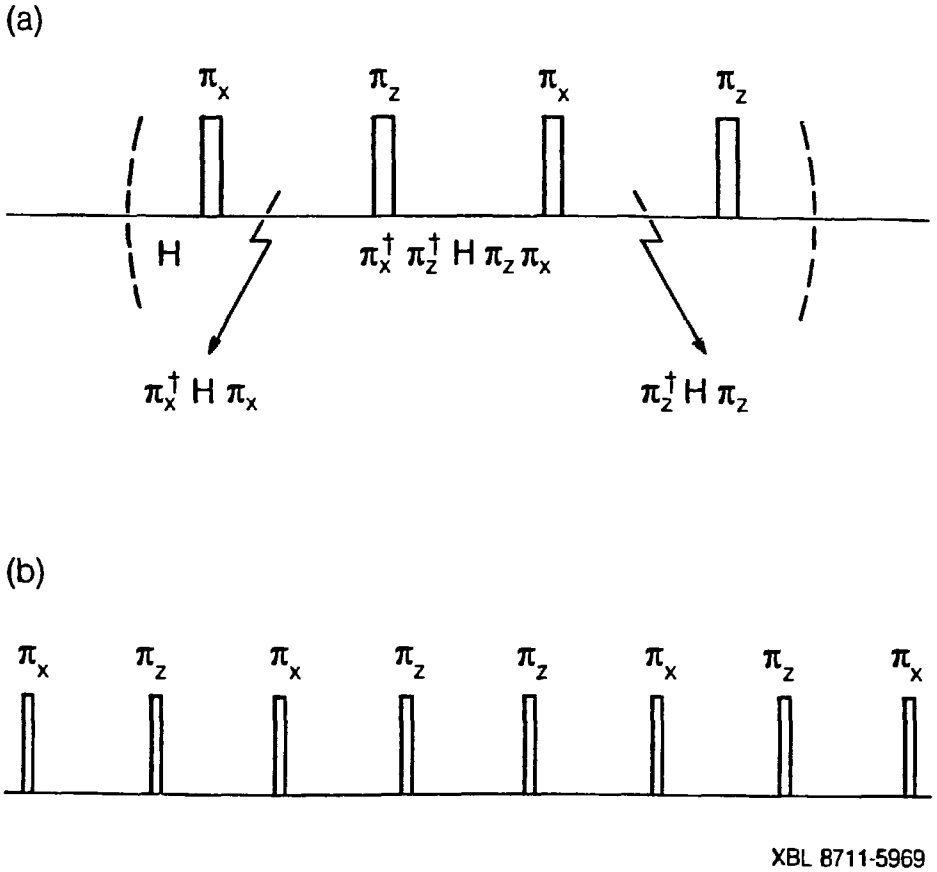

Fig. 4.3 Pulse sequences for the removal of linear terms. (a) A four pulse sequence to remove the terms to zeroth order. (b) Expanded sequence to remove the terms to first order.

$$\bar{\mathcal{H}}^{(0)} = \frac{1}{4}\left(\mathcal{H} + \pi_x^{-1}\mathcal{H}\,\pi_x + \pi_x^{-1}\pi_z^{-1}\mathcal{H}\,\pi_z\pi_x + \pi_x^{-1}\pi_z^{-1}\pi_x^{-1}\mathcal{H}\,\pi_x\pi_z\pi_x\right). \qquad (4.20)$$

Because $\pi_z\pi_x = \pi_x\pi_z$ and with the third and fourth term switched, Eq.(4.20) can be reduced to

$$\bar{\mathcal{H}}^{(0)} = \frac{1}{4}\left(\mathcal{H} + \pi_x^{-1}\mathcal{H}\pi_x + \pi_z^{-1}\mathcal{H}\pi_z + \pi_z^{-1}\pi_x^{-1}\mathcal{H}\pi_x\pi_z\right), \qquad (4.21)$$

which is equivalent to Eq.(4.18), since in zero-field the phase does not enter and thus π_x is equivalent to R.

Making $\bar{\mathcal{H}}^{(1)}_{int} = 0$ can be achieved by symmetrizing the sequence, which is shown in Fig.4.3(b). As is discussed previously, R is equivalent to zero-field π_x. Then the second half of the eight-pulse sequence, $(-\pi_z\text{-}\pi_x\text{-}\pi_z\text{-}\pi_x\text{-})$ can be obtained from the original four-pulse sequence by permuting a π_x to the right end of the sequence, i.e.

$$\pi_x^{-1}(\pi_x\pi_z\pi_x\pi_z)\pi_x = \pi_z\pi_x\pi_z\pi_x. \qquad (4.22)$$

In the high-field language, Eq.(4.22) can be shown to reduce to

$$\bar{R}(R\bar{R}\bar{R}\bar{R})\bar{R}^{-1} = \bar{R}R\bar{R}\bar{R}. \qquad (4.23)$$

Hence the eight-pulse sequence is equivalent to the MLEV-8 sequence. The procedure can be carried out further to show that 16 steps are needed to average out the second order average Hamiltonian term which contains coefficients such as a^2b, ab^2, b^2c, etc. Showing the cancellation is straightforward, but will not be discussed in more detail.

While some connections have been made between high-field iterative schemes and zero-field multiple-pulse methods, the difference should also be noted. Firstly, the generalized Hamiltonian with the form given by Eq.(4.17) is a result of the pulse sequence rather than the original Hamiltonian. The original high-field Hamiltonian commutes with I_z, and thus is invariant to phase shifts. By contrast, the original

low-field Hamiltonian originationg from the residual field does not commute with I_z. This remark is true also for the Hamiltonian including bilinear terms.

Secondly, the connection was possible only for the δ-function pulse cases. It should be reminded that for the case of windowless sequences, a minimum of 16 configurations is needed to average out the linear terms to zeroth order, rather than four configurations. Hence it is difficult to make a connection between the high-field iterative schemes and the zero-field multiple pulse sequences. The most important difference arises, however, from the fact that the time-averaging of the coefficients of Eq.(3.14) is in general different from that of the switched spin operators given by Eq.(3.15). Except for some special cases such as discussed in the last few paragraphs the sequences for averaging the the basis spin operators are not the same as those for the coefficients of the spin operators. Furthermore, the sequences designed for decoupling spins in liquids and liquid crystals use low decoupler power to avoid excessive sample heating, so the arguments for the δ-function pulses are not suitable for these cases.

Finally, the design of multiple pulse sequences requires detailed calculation of terms appearing in the Magnus expansion,[10] whereas the modern decoupling schemes use certain machinary which guarantees better averaging, without detailed calculations as the sequences are expanded iteratively.

The iterative schemes for heteronuclear spin-decoupling developed to date are aimed at removing an isolated I-S spin pair. However, in decoupling heteronuclear spins there are cases when interactions between

homonuclear spins need to be removed as well. Schemes for the single spin cases are found to be inefficient in decoupling when there are homonuclear couplings. Therefore, the development of schemes for averaging linear and and bilinear operators is necessary, and it is the subject of the next section.

IV.5. Schemes for Removing Linear and Bilinear Operators

A. The construction of basic sequences

When there are bilinear terms, operations such as phase shift and cyclic permutation commonly employed in single-spin decoupling do not behave as simple rotations. Detailed average Hamiltonian calculation may be employed to design a highly compensated sequences. However, the calculation, considering that low rf-field is used, can quickly become unwieldy as one goes to higher order calculations.

A method to obviate these complicated calculations and obtain a scheme for averaging both linear and bilinear operators is to decompose the total propagator into rf part and the perturbation:

$$U(t) = U_{rf}(t)U_{v}(t). \tag{4.24}$$

The discussion on the specific form of U_{rf} is deferred to a later section. Here it suffices to state that U_{rf} is a some broadband composite pulse without phase gradient. To be more explicit, Eq.(4.24) can be written as

$$U(t) = U_{rf}(t)\ \mathcal{T}\exp\left(-i\int_0^t U_{rf}^{\dagger}(t')\ \mathcal{H}_{int}\ U_{rf}(t')\ dt'\right). \tag{4.25}$$

The exact form of $U_{v}(t)$ given by the second exponential in Eq.(4.25) may

not be known, but in general it can be expressed as a single exponential with the exponent expanded in terms of basis operators. If $\mathcal{H}_{int}$ contains a homonuclear coupling term between two spins I_1 and I_2 as well as the offset and heteronuclear coupling terms, the basis operators span a 15-dimensional space: six associated with linear operators and nine bilinear operators.

Now suppose the total evolution operator is composed of a product of n evolution operators having a same duration τ:

$$U(n\tau) = U_{rf,n}(\tau)U_{v,n}(\tau)\cdots\cdots U_{rf,1}(\tau)U_{v,1}(\tau). \tag{4.26}$$

Also suppose that the evolution operator for a composite pulse with an overall phase $\phi = 0$ can be written as

$$U(\tau) = U_{rf,0}(\tau)U_{v,0}(\tau). \tag{4.27}$$

Then with the notation

$$\phi_z = \exp(-i\phi I_z), \tag{4.28}$$

the evolution operator associated with a pulse having a phase ϕ becomes

$$\begin{aligned} U_\phi(\tau) &= U_{rf,\phi}(\tau)\, U_{v,0}(\tau) \\ &= U_{rf,\phi}(\tau)\, \mathcal{T}\exp\left(-i\int_0^\tau U_{rf,\phi}^\dagger(t)\, \mathcal{H}_{int}\, U_{rf,\phi}(t)\, dt\right) \\ &= \phi_z^\dagger\, U_{rf,0}(\tau)\, \phi_z \;\times \\ &\qquad \mathcal{T}\exp\left(-i\int_0^\tau \phi_z^\dagger\, U_{rf,0}^\dagger(t)\, \phi_z\, \mathcal{H}_{int}\, \phi_z^\dagger\, U_{rf,0}(t)\, \phi_z\, dt\right). \end{aligned} \tag{4.29}$$

Since $\mathcal{H}_{int}$ is a high field Hamiltonian,

$$[\, I_z\, ,\, \mathcal{H}_{int}\,] = 0, \tag{4.30}$$

and Eq.(4.29) reduces to

$$U_{\phi}(\tau) = \phi_z^{\dagger}\, U_{rf,0}(\tau)\, \phi_z \phi_z^{\dagger}\, \mathcal{T}\exp\left(-i\int_0^{\tau} U_{rf,0}^{\dagger}(t)\, \mathcal{H}_{int}\, U_{rf,0}(t)\, dt\right)\phi_z$$

$$= \left\{\phi_z^{\dagger}\, U_{rf,0}(\tau)\, \phi_z\right\}\left\{\phi_z^{\dagger}\, U_{v,0}(\tau)\, \phi_z\right\}. \qquad (4.31)$$

In passing, it is worth noting that Eq.(4.30) does not hold for the zero-field Hamiltonian. So the present approach can not be used for zero-field multiple-pulse calculations.

At any rate, each element of Eq.(4.26) is simply related to U_0 by the phase shift ϕ_z. The evolution operator $U(n\tau)$ can now be rearranged such that the total evolution operator due to the rf-field Hamiltonian appears on the left :

$$U = U_{\phi_n} U_{\phi_{n-1}} \cdots U_{\phi_1}$$

$$= U_{rf,\phi_n} U_{v,\phi_n} \cdots U_{rf,\phi_1} U_{v,\phi_1}$$

$$= \mathcal{T}\, U_{rf}^{(n)} \prod_{p=1}^{n} \left\{U_{rf}^{(p-1)}\right\}^{\dagger} U_{v,\phi_p} \left\{U_{rf}^{(p-1)}\right\}$$

$$= \mathcal{T}\, U_{rf}^{(n)} \prod_{p=1}^{n} \tilde{U}_{v,\phi_p}, \qquad (4.32)$$

where $\mathcal{T}$ is the time-ordering operator,

$$U_{rf}^{(n)} = U_{rf,\phi_n} \cdots U_{rf,\phi_1}, \qquad (4.33)$$

and

$$\tilde{U}_{v,\phi_p} = \left\{U_{rf}^{(p-1)}\right\}^{\dagger} U_{v,\phi_p} \left\{U_{rf}^{(p-1)}\right\} \qquad (4.34)$$

with

$$U_{rf}^{(0)} = 1. \qquad (4.35)$$

Since U_v are assumed to be small perturbations, the time-ordered product

in Eq.(4.32) can be expressed as a simple exponential using the Baker-Campbell-Hausdorff formula:[11]

$$\mathcal{T}\prod_k \exp(-iA_k) = \exp\left(-i\left(\sum_k A_k + \frac{1}{2}\sum_{k>j}[A_k, A_j] + \cdots\right)\right). \quad (4.36)$$

Thus to first order the condition for the heteronuclear-decoupling reduces to finding phases ϕ_k such that

$$\sum_k A_k = 0 \quad (4.37)$$

for single-spin systems. However it may not be necessary to satisfy Eq.(4.37) for two-spin systems (systems of two coupled homonuclear spins each of which is also coupled to a nuclear spin with a different gyromagnetic ratio). It has been argued[12] that a non-vanishing offset-independent Hamiltonian, having large components orthogonal to the residual offset term, could quench the offset term, making a more favorable situation for decoupling. Hence, a natural choice for the offset-independent Hamiltonian for systems having both linear and bilinear terms, for example, in liquids is

$$\sum_k A_k = 2\pi J \mathbf{I}_1 \cdot \mathbf{I}_2. \quad (4.38)$$

It would be instructive to discuss first the cancellation of linear terms only, since it would make a connection to the methods of iterative schemes discussed in the previous chapter. Consider the sequence $UU\bar{U}\bar{U}$, where U is a composite 180^0 pulse along the x-direction without phase distortion. The "imperfection" term U_v during the composite pulse U may in general be written as

$$U_v = \exp\left(\epsilon_x I_x + \epsilon_y I_y + \epsilon_z I_z\right). \quad (4.39)$$

The cancellation of these linear error terms during the sequence is shown in Table 4.2.

Table 4.2

Cancellation of Linear Spin Operators by the Sequence U U $\bar{U}$ $\bar{U}$

State	Operator		
	I_x	I_y	I_z
1	ϵ_x	ϵ_y	ϵ_z
2	ϵ_x	$-\epsilon_y$	$-\epsilon_z$
3	$-\epsilon_x$	$-\epsilon_y$	ϵ_z
4	$-\epsilon_x$	ϵ_y	$-\epsilon_z$

It may appear that the current method is equivalent to the methods discussed in the previous section. However, the current method has the following advantages:

1) Any compososite pulse can be substituted into U_{rf}.
2) The evolution operators with phase ϕ are simply related by Eq.(4.31).
3) No calculation is needed for U_v and sequences satisfying Eq.(4.37) can be found rather easily, and
4) sequences can be improved mechanically by some iterative schemes.

The advantage labeled 1) will fully be exploited in finding practical sequences, and 4) will be discussed later on. Due tc advantages labeled 2) and 3) sequences for removing linear and bilinear operators, except the scalar operator given by Eq.(4.38) have been easily found employing integer arithmatic on the computer.

If only 90^0 pulses along the four quadrature channels $\pm x$ and $\pm y$ are employed, there are 64 12-pulse sequences found that satisfy Eq.(4.38). No sequences with less than 12 pulses are found, agreeing with the ealier discussion that a minimum of 12 pulses is required to average all linear and bilinear operators except the scalar. If the pulse sequence begins with an x pulse, there are 16 sequences and these are listed in Table 4.3. The first four sequences consist of three identical subunits of four 90^0 pulses and the rest consist of two identical subunits of six 90^0 pulses. If there are no pulse imperfections present, the six pulse subunit consists of 180^0 rotations around the x, y, or z axis, while the four pulse subunit is equivalent to 120^0 rotations around one of the "magic" axes. It can be shown that

Table 4.3 Windowless Sequences of 90^0 Pulses Producing a Scalar Operator

(1)	$X\ Y\ \bar{X}\ Y\ X\ Y\ \bar{X}\ Y\ X\ Y\ \bar{X}\ Y$
(2)	$X\ Y\ X\ \bar{Y}\ X\ Y\ X\ \bar{Y}\ X\ Y\ X\ \bar{Y}$
(3)	$X\ \bar{Y}\ X\ Y\ X\ \bar{Y}\ X\ Y\ X\ \bar{Y}\ X\ Y$
(4)	$X\ \bar{Y}\ \bar{X}\ \bar{Y}\ X\ \bar{Y}\ \bar{X}\ \bar{Y}\ X\ \bar{Y}\ \bar{X}\ \bar{Y}$
(5)	$X\ Y\ X\ Y\ \bar{X}\ Y\ X\ Y\ X\ Y\ \bar{X}\ Y$
(6)	$X\ Y\ \bar{X}\ Y\ X\ Y\ X\ Y\ \bar{X}\ Y\ X\ Y$
(7)	$X\ Y\ X\ \bar{Y}\ X\ \bar{Y}\ X\ Y\ X\ \bar{Y}\ X\ \bar{Y}$
(8)	$X\ \bar{Y}\ X\ Y\ X\ \bar{Y}\ X\ \bar{Y}\ X\ Y\ X\ \bar{Y}$
(9)	$X\ \bar{Y}\ X\ \bar{Y}\ X\ Y\ X\ \bar{Y}\ X\ \bar{Y}\ X\ Y$
(10)	$X\ \bar{Y}\ \bar{X}\ \bar{Y}\ \bar{X}\ \bar{Y}\ X\ \bar{Y}\ \bar{X}\ \bar{Y}\ \bar{X}\ \bar{Y}$
(11)	$X\ Y\ X\ Y\ X\ \bar{Y}\ X\ Y\ X\ Y\ X\ \bar{Y}$
(12)	$X\ Y\ X\ \bar{Y}\ X\ Y\ X\ Y\ X\ \bar{Y}\ X\ Y$
(13)	$X\ \bar{Y}\ X\ Y\ X\ Y\ X\ \bar{Y}\ X\ Y\ X\ Y$
(14)	$X\ Y\ \bar{X}\ Y\ \bar{X}\ Y\ X\ Y\ \bar{X}\ Y\ \bar{X}\ Y$
(15)	$X\ \bar{Y}\ X\ \bar{Y}\ \bar{X}\ \bar{Y}\ X\ \bar{Y}\ X\ \bar{Y}\ \bar{X}\ \bar{Y}$
(16)	$X\ \bar{Y}\ \bar{X}\ \bar{Y}\ X\ \bar{Y}\ X\ \bar{Y}\ \bar{X}\ \bar{Y}\ X\ \bar{Y}$

the sequences (1)-(4) are simply related to each other by phase shifts and cyclic permutations. If these operations are assumed to be fairly accurate, the sequences (1)-(4) would give identical performance. The same is true with sequences (5)-(10) and (11)-(16). Consequently, there are three distinct representative sequences

$(xy\bar{x}y)^3$, $(xyxy\bar{x}y)^2$, $(xyxyx\bar{y})^2$.

To see how these sequences work, take an example of $(xy\bar{x}y)^3$. Table 4.4 shows the systematic cancellation of linear and bilinear cross terms while preserving the scalar during the sequence.

Eq.(4.38), however, cannot be satisfied with 180^0 rotations and 180^0 phase shifts because $I_{1\alpha}I_{2\alpha}$ are invariant to these operations, and with 180^0 shifts ϵ_{xx} is always tied to $I_{1x}I_{2x}$ throughout the sequence. So far no assumptions have been made about the size or the relationship among coefficients ϵ. If the composite 180^0 pulse has the property of making the coefficients associated with the quadratic terms $I_{1\alpha}I_{2\alpha}$ nearly equal, or there are some relationships among coefficients that are favorable for averaging these quadratic terms, one may as well use these sequences with 180^0 operations. Detailed discussion on these and other practical aspects are deferred to a later section.

B. Expansion Procedure

B.1. Single spin case

It was shown that $C_2 = U\,U\,\bar{U}\,\bar{U}$ removes errors of order ϵ, but errors of order ϵ^2 remain originating from the commutator in Eq.(4.36).

Table 4.4 Systematic cancellation of Spin Operators by the 12-Pulse Sequence (X Y $\bar{X}$ Y X Y $\bar{X}$ Y X Y $\bar{X}$ Y)

Operator											
x	y	z	xy	xz	yz	yx	zx	zy	xx	yy	zz
ϵ_x	ϵ_y	ϵ_z	ϵ_{xy}	ϵ_{xz}	ϵ_{yz}	ϵ_{yx}	ϵ_{zx}	ϵ_{zy}	ϵ_{xx}	ϵ_{yy}	ϵ_{zz}
$-\epsilon_y$	$-\epsilon_z$	ϵ_x	ϵ_{yz}	$-\epsilon_{yx}$	$-\epsilon_{zx}$	ϵ_{zy}	$-\epsilon_{xy}$	$-\epsilon_{xz}$	ϵ_{yy}	ϵ_{zz}	ϵ_{xx}
ϵ_z	$-\epsilon_x$	$-\epsilon_y$	$-\epsilon_{zx}$	$-\epsilon_{zy}$	ϵ_{xy}	$-\epsilon_{xz}$	$-\epsilon_{yz}$	ϵ_{yx}	ϵ_{zz}	ϵ_{xx}	ϵ_{yy}
$-\epsilon_x$	$-\epsilon_y$	ϵ_z	ϵ_{xy}	$-\epsilon_{xz}$	$-\epsilon_{yz}$	ϵ_{yx}	$-\epsilon_{zx}$	$-\epsilon_{zy}$	ϵ_{xx}	ϵ_{yy}	ϵ_{zz}
$-\epsilon_y$	ϵ_z	$-\epsilon_x$	$-\epsilon_{yz}$	ϵ_{yx}	$-\epsilon_{zx}$	$-\epsilon_{zy}$	ϵ_{xy}	$-\epsilon_{xz}$	ϵ_{yy}	ϵ_{zz}	ϵ_{xx}
ϵ_z	ϵ_x	ϵ_y	ϵ_{zx}	ϵ_{zy}	ϵ_{xy}	ϵ_{xz}	ϵ_{yz}	ϵ_{yx}	ϵ_{zz}	ϵ_{xx}	ϵ_{yy}
ϵ_x	$-\epsilon_y$	$-\epsilon_z$	$-\epsilon_{xy}$	$-\epsilon_{xz}$	ϵ_{yz}	$-\epsilon_{yx}$	$-\epsilon_{zx}$	ϵ_{zy}	ϵ_{xx}	ϵ_{yy}	ϵ_{zz}
ϵ_y	ϵ_z	ϵ_x	ϵ_{yz}	ϵ_{yx}	ϵ_{zx}	ϵ_{zy}	ϵ_{xy}	ϵ_{xz}	ϵ_{yy}	ϵ_{zz}	ϵ_{xx}
$-\epsilon_z$	$-\epsilon_x$	ϵ_y	ϵ_{zx}	$-\epsilon_{zy}$	$-\epsilon_{xy}$	ϵ_{xz}	$-\epsilon_{yz}$	$-\epsilon_{yx}$	ϵ_{zz}	ϵ_{xx}	ϵ_{yy}
$-\epsilon_x$	ϵ_y	$-\epsilon_z$	$-\epsilon_{xy}$	ϵ_{xz}	$-\epsilon_{yz}$	$-\epsilon_{yx}$	ϵ_{zx}	$-\epsilon_{zy}$	ϵ_{xx}	ϵ_{yy}	ϵ_{zz}
ϵ_y	$-\epsilon_z$	$-\epsilon_x$	$-\epsilon_{yz}$	$-\epsilon_{yx}$	ϵ_{zx}	$-\epsilon_{zy}$	$-\epsilon_{xy}$	ϵ_{xz}	ϵ_{yy}	ϵ_{zz}	ϵ_{xx}
$-\epsilon_z$	ϵ_x	$-\epsilon_y$	$-\epsilon_{zx}$	ϵ_{zy}	$-\epsilon_{xy}$	$-\epsilon_{xz}$	ϵ_{yz}	$-\epsilon_{yx}$	ϵ_{zz}	ϵ_{xx}	ϵ_{yy}

The next step of the expansion procedure is the cyclic permutation of $\bar{U}$ and concatenation with the original sequence to give

$$C_3 = U\ U\ \bar{U}\ \bar{U}\ \bar{U}\ U\ U\ \bar{U}. \tag{4.40}$$

It is easily verified that if the errors of $O(\epsilon^3)$ are neglected, the last four pulses are obtained from the original sequence of four pulses by 180^0 rotation around the x axis. Thus they should also cancel the linear terms. It is straightforward but tedious to calculate the commutator in Eq.(4.36). These are error terms of order ϵ^2 originating from the cross product of ϵ_α and it can be shown that they vanish for the sequence C_3, leaving errors of $O(\epsilon^3)$.

The analysis can in principle carried out further to show systematic cancellation of higher order terms. However, the procedure quickly becomes intractable: if symmetry of the commutator is not taken into account, there would be 360 commutators to calculate in the next stage of the expansion, i.e. the 16-pulse sequence.

A much more manageable and mechanical way of achieving cancellation is once again to group the residual errors in one exponential:

$$\begin{aligned} U\bar{U}\bar{U}U &= U_{rf}U_vU_{rf}U_v\bar{U}_{rf}\bar{U}_v\bar{U}_{rf}\bar{U}_v \\ &= U_{rf}U_{rf}\bar{U}_{rf}\bar{U}_{rf}U_v^{(2)} = U_v^{(2)}, \end{aligned} \tag{4.41}$$

where

$$U = \exp\left(-i\underline{\epsilon}^{(2)}\cdot\underline{I}\right) \tag{4.42}$$

with $\epsilon^{(2)}$ denoting the error of size $\|\epsilon^{(2)}\| = O(\epsilon^2)$. Eq.(4.40) can be considered as the first configuration in the Table 4.2. One problem in generating other configurations with the above method is that the

product of 180^0 rotations U_{rf} does not generate a fixed point[4,5,13] of next stage 180^0 rotation but generates an approximate unity operator instead. Thus the 180^0 rotation must be generated in some other way. One such a method is to approximate the 180^0 rotation by cyclically permuting $\bar{U}$:

$$\begin{aligned} \bar{U}\, U\, U\, \bar{U} &= \bar{U}\, (\, U\, U\, \bar{U}\, \bar{U}^{1})\, \bar{U} \\ &= \bar{U}_{rf}\, \bar{U}_{v}\; U_{v}^{(2)} \bar{U}_{v}^{-1}\, \bar{U}_{rf}^{-1} \\ &= \bar{U}_{rf}\, U_{v}^{(2)}\; \bar{U}_{rf}^{-1}, \end{aligned} \tag{4.43}$$

where the errors of $O(\epsilon^3)$ have been ignored. Eq.(4.43) corresponds to the second configuration in Table 4.2. However, $\epsilon^{(2)}$ are not arbitrary but have certain symmetry originating from the commutator in Eq.(4.36), which has been fully exploited in removing errors of $O(\epsilon^2)$ as discussed in the paragraph following Eq.(4.40). This point may also be argued from the observation that the sequence $\bar{U}\ \bar{U}\ U\ U$ can be derived from $U\ U\ \bar{U}\ \bar{U}$ by either a 180^0 phase shift or a cyclic permutation of $\bar{U}\ \bar{U}$. Consequently,

$$\bar{U}_{v}^{(2)} = \bar{U}\ \bar{U}\ U_{v}^{(2)}\ (\ \bar{U}\ \bar{U}\ )^{-1} \cong U_{v}^{(2)}, \tag{4.44}$$

neglecting errors of $O(\epsilon^3)$. For Eq.(4.44) to hold $\epsilon_x^{(2)}$ and $\epsilon_y^{(2)}$ must be much smaller than $\epsilon_z^{(2)}$. In other words, $\epsilon_x^{(2)}$ and $\epsilon_y^{(2)}$ are of $O(\epsilon^3)$ and $\epsilon_z^{(2)}$ is of $O(\epsilon^2)$. Also, the eight pulse $U\ U\ \bar{U}\ \bar{U}\ \bar{U}\ U\ U\ \bar{U}$ cancels $\epsilon_z^{(2)}$, leaving an error of $O(\epsilon^3)$.

The above arguments imply faster convergence of the present scheme. Namely, the third and fourth configurations in Table 4.2 are easily generated by an exact phase inversion and a cyclic permutation accompanied by a phase inversion (accurate to $O(\epsilon^3)$) respectively. The resulting sequence is

$$C_4 = U\,U\,\bar{U}\,\bar{U}\,\bar{U}\,U\,U\,\bar{U}\,\bar{U}\,\bar{U}\,U\,U\,U\,\bar{U}\,\bar{U}\,U, \tag{4.45}$$

the MLEV-16 sequence. The product of U_{rf} is again a unity operator. It can be proved[1,3] that the residual error is of $O(\epsilon^4)$. Therefore, the present expansion scheme $C_2 \longrightarrow C_4 \longrightarrow C_6$ (a 64 pulse sequence) $\longrightarrow \cdots$ makes the error term converge as rapidly as $O(\epsilon^2) \longrightarrow O(\epsilon^4) \longrightarrow O(\epsilon^6)$ $\longrightarrow \cdots O(\epsilon^{2n})$ after n-th iteration. The convergence is much more favorable than $O(\epsilon^{n+1})$ which would result by combining various subcycles in an arbitrary order.

B.2. Two-spin case

If an expansion procedure for the two-spin case is built upon the apparent analogy to the single-spin case, it would be a 12-fold one. However, it can be shown that the two operations of cyclic permutation and phase shift do not generate all 12 necessary states. More specifically, Eq.(4.44) does not hold. Even if the next stage of the expansion with 144 pulses is found, there will be of little practical use of it because other effects such as relaxation would become important for such a long sequence. It thus is desirable to find schemes to generate shorter sequences. Fortunately, analogous to the discussion following Eq.(4.40) for a single spin, there also exist relationships among coefficients ϵ for the two-spin case.

With cyclic permutations and phase shifts 64 12-pulse sequences are generated from the three representative sequences mentioned previously. Hence, for example, following constraints can be found for $(x\ y\ \bar{x}\ y)^3$ sequence:

$$\epsilon_x^{(2)} = -\epsilon_y^{(2)} = \epsilon_z^{(2)}$$

$$\epsilon_{xy}^{(2)} = \epsilon_{yz}^{(2)} = -\epsilon_{zx}^{(2)}$$

$$\epsilon_{yx}^{(2)} = \epsilon_{zy}^{(2)} = -\epsilon_{xz}^{(2)}$$

$$\epsilon_{xx}^{(2)} = \epsilon_{yy}^{(2)} = \epsilon_{zz}^{(2)}, \tag{4.46}$$

where errors of $O(\epsilon^3)$ are neglected. The relationship among the coefficients for the sequence $(x\ y\ x\ y\ x\ \bar{y})^2$ is:

$$\epsilon_x^{(2)} = \epsilon_z^{(2)} = 0. \tag{4.47}$$

This then implies the possibility of adding certain 12-pulse sequences in a spirit quite similar to the construction of MLEV-8. An example of a 24-pulse sequence constructed this way to satisfy Eq.(4.38) is $(x\ \bar{y}\ x\ \bar{y}\ x\ y)^2\ (\bar{x}\ y\ x\ y\ x\ y)^2$. There are other 24-pulse sequences which do not fit the category described above, but still satisfy Eq.(4.38). With a phase shift confined to 90^0 between each element, there are 511 sequences which are not related to each other by either cyclic permutations or phase shifts. They are listed in Appendix 3. Some examples are:

$$x\ y\ \bar{x}\ y\ \bar{x}\ y\ x\ y\ \bar{x}\ y\ \bar{x}\ \bar{y}\ x\ y\ x\ y\ x\ \bar{y}\ x\ y\ x\ y\ x\ y \tag{4.48}$$

which does not have an obvious structure, and

$$(x\ y\ \bar{x}\ y\ x\ y\ x\ y)^3 \tag{4.49}$$

$$(x\ \bar{y}\ x\ \bar{y}\ x\ y)^2(\bar{x}\ y\ x\ y\ x\ y)^2 \tag{4.50}$$

$$(x\ \bar{y})^3(\bar{x}\ \bar{y})^3(\bar{x}\ y)^3(x\ y)^3, \tag{4.51}$$

which have definite subunit structures.

The iterative schemes discussed in this chapter and the sequences given above will be utilized in the next chapter, where heteronuclear

decoupling in liquids and liquid crystals are treated.

References

1. M. H. Levitt, R. Freeman and T. Frenkiel, Adv. in Mag. Res. 11, 47 (1983).
2. M. H. Levitt, Prog. in NMR Spect. 18, 61 (1986).
3. A. J. Shaka and J. Keeler, Prog. in NMR Spect. 19, 47 (1987).
4. R. Tycko, Ph.D. thesis, University of California, Berkeley, 1984.
5. H. M. Cho, Ph.D. thesis, University of California, Berkeley, 1987.

6(a). D. P. Weitekamp, Adv. in Mag. Res. 11, 111 (1983).

6(b). M. M. Munowitz and A. Pines, Adv. in Chem. Phys. 66, 1 (1987).

7. M. H. Levitt ans R. Freeman, J. Mag. Res. 43, 502 (1981).
8. J. S. Waugh, J. Mag. Res. 50, 30 (1982).
9. D. P. Burum, M. Linder and R. R. Ernst, J. Mag. Res. 44, 173 (1981).
10. W. Magnus, Commun. Pure Appl. Math. 7, 649 (1954).
11. R. M. Wilcox, J. Math. Phys. 8, 962 (1967).
12. D. Suter, K. V. Shenker and A. Pines, J. Mag. Res. 72,90 (1987).
13. R. Tycko, A. Pines, and J. D. Guckenheimer, J. Chem. Phys. 83, 2775 (1985).

CHAPTER V. Broadband Heteronuclear Decoupling in the Presence of Homonuclear Interactions

V.1 General Theory of Heteronuclear Decoupling

The iterative schemes in the previous chapter have been discussed with a view to heteronuclear decoupling of a spin I from an S spin. S denotes the spin under observation and a typical example is a carbon-13, while I denotes the spin which is irradiated with a decoupling field and a typical example is a proton.

According to Waugh,[1] decoupling of an isolated I-S pair can be completely analyzed by observing the behavior of the I spin under the irradiation without the necessity of considering the S spin. The criterion for the efficiency of decoupling of I from S (I = S = 1/2) over a certain bandwidth is that the net rotation angle (ϕ) the spin I undergoes should be insensitive to the offset (δ) within the bandwidth. Mathematically, the residual splitting of the S spin spectrum is given by

$$\Delta S(\delta) = J_{IS} \frac{1}{t_r} \frac{\partial \phi}{\partial \delta} = J_{IS} \frac{\partial \Omega}{\partial \delta} \tag{5.1}$$

where J_{IS} is a coupling constant between spins I and S, t_r the net time of the periodic sequence, and Ω the average frequency during t_r.

If there are interactions between two I spins-1/2 or if there is a quadrupole interaction for the spin $I \geq 1$, it is no longer possible to treat the behavior of the system of I spin(s) as a three-dimensional

rotation. Since the average frequency Ω is equal to the energy times $1/\hbar$, the most general decoupling criterion should be expressed in terms of the effective energy or equivalently of the average Hamiltonian over the irradiation period t_r.

In the past few years some of the important developments in heteronuclear decoupling for multi-level systems have been made. The following is a general theory of heteronuclear decoupling in a form somewhat different than the treatments of references 2 and 3.

First consider the Hamiltonian in a rotating frame on resonance for the S spin given by

$$\mathcal{H} = \mathcal{H}_I + \mathcal{H}_{II} + \mathcal{H}_{IS} + \mathcal{H}_I^{rf}(t). \tag{5.2}$$

Now suppose the initial density operator for the S spin is given by

$$\rho(0) = S_x, \tag{5.3}$$

then the signal of the S spin S^- suitable for the quadrature detection is given by

$$S^-(nt_r) = Tr\left\{\left(S_x - i\,S_y\right) U(nt_r)\, S_x\, U^\dagger(nt_r)\right\}. \tag{5.4}$$

Since the terms depending only on the I spin commute with the S spin operators, these can be factored out of Eq.(5.4) by using the transformation

$$U(t) = U_I(t)U_{IS}(t), \tag{5.5}$$

where

$$U_I(t) = \mathcal{T} \exp\left(-i\int_0^t \left\{\mathcal{H}_I + \mathcal{H}_{II} + \mathcal{H}_I^{rf}(t')\right\}dt'\right) \tag{5.6}$$

is the pure I spin propagator and

$$U_{IS}(t) = \mathcal{T} \exp\left(-i\int_0^t U_I^{\dagger}(t')\, \mathcal{H}_{IS}\, U_I(t')dt'\right). \tag{5.7}$$

Eq.(5.4) now reduces to

$$\begin{aligned} S^{-}(nt_r) &= Tr\left\{\left(S_x - i\, S_y\right) U_I^n(t_r)\, U_{IS}^n(t_r)\, S_x\, U_{IS}^{\dagger n}(t_r)\, U_I^{\dagger n}(t_r)\right\} \\ &= Tr\left\{\left(S_x - i\, S_y\right) U_{IS}^n(t_r)\, S_x U_{IS}^{\dagger n}(t_r)\right\}. \end{aligned} \tag{5.8}$$

Perfect decoupling is achieved when

$$U_{IS}(t_r)\, S_x\, U_{IS}^{\dagger}(t_r) = S_x. \tag{5.9}$$

This in turn means

$$[\, U_{IS}\, ,\, S_x\,] = 0, \tag{5.10}$$

which can be satisfied only when $U_{IS} = 1$. This is because $\mathcal{H}_{IS}$ in the

high field Hamiltonian in Eq.(5.7) may be written in the form

$$\mathcal{H}_{IS} = \left(\sum_j J_j I_{jz}\right) S_z \ , \tag{5.11}$$

and the evolution operator in terms of an average Hamiltonian defined by

$$U_{IS}(t_r) = \exp\left(-it_r \bar{\mathcal{H}}_{IS}\right) = \exp\left(-it_r \bar{h}_I S_z\right) \tag{5.12}$$

satisfies Eq.(5.10) only when $\bar{h}_I = 0$, and then the Fourier transform of S^- will consist of a single peak.

To facilitate the calculation of the spectrum under a less perfect decoupling condition, it is desirable to divide the average Hamiltonian $\bar{\mathcal{H}}_{IS}$ into two commuting parts:

$$\bar{\mathcal{H}}_{IS} = \bar{h}_I S_z = p_+ h_+ + p_- h_- , \tag{5.13}$$

where

$$p_\pm = \frac{1 \pm 2S_z}{2} \tag{5.14}$$

is the S spin projection operator, and

$$h_\pm = \pm \frac{1}{2} \bar{h}_I . \tag{5.15}$$

Then, with the properties

$$p_+^n = p_+ , \ p_-^n = p_- , \ p_+ p_- = p_- p_+ = 0, \tag{5.16}$$

it can be shown that

$$U_{IS}(t_r) = p_+ \exp(-it_r h_+) + p_- \exp(-it_r h_-)$$

$$= p_+ U_+ + p_- U_- . \tag{5.17}$$

Eq.(5.8) now becomes

$$S^-(nt_r) = Tr\left\{(S_x - i\,S_y)(p_+ U_+^n + p_- U_-^n) S_x (p_+ U_+^{\dagger n} + p_- U_-^{\dagger n})\right\}, \tag{5.18}$$

where

$$(p_+ U_+ + p_- U_-)^n = p_+ U_+^n + p_- U_-^n \tag{5.19}$$

is used. With some algebra it can be shown that

$$S^-(nt_r) = Tr(U_+^n U_-^{\dagger n}). \tag{5.20}$$

Thus S^- is known once $\bar{h}_I$ is calculated in the basis set which diagonalizes $\bar{h}_I$, or calculated perturbatively in the eigenbasis set of the Hamiltonian generating the evolution operator U_I. The result is (in $\hbar$ units)

$$S^-(nt_r) = \sum_{k=1}^{N} \exp\left\{-i\, t_r(\mathcal{E}_{k+} - \mathcal{E}_{k-})\right\} \tag{5.21}$$

where N is the total number of states and $\mathcal{E}_{k\pm}$ are eigenvalues of $h_\pm$ in the k-th state. Thus the spectrum consists of maximum N peaks positioned at $(\mathcal{E}_{k+} - \mathcal{E}_{k-})$.

Suppose for simplicity all J_j are equal and equal to J_{IS} in Eq.(5.11), and approximate U_{IS} to first order, i.e.

$$U_{IS}^{(0)}(t_r) = e^{-it_r \bar{h}_I^{(0)} S_Z} = \exp\left(-i \int_0^{t_r} U_I^\dagger(t)\, \mathcal{H}_{IS}\, U_I(t)\, dt\right). \tag{5.22}$$

The righthand side of Eq.(5.22) is in fact the first order correction[4] to the (fictitious) I spin Hamiltonian defined by

$$U_I(t_r) = \exp\left(-it_r \bar{\mathcal{H}}^I\right). \tag{5.23}$$

The total I spin Hamiltonian may be written in terms of this fictitious Hamiltonian as

$$\begin{aligned} \mathcal{H}^I &= \bar{\mathcal{H}}^I + \bar{\mathcal{H}}_{IS} \\ &= \bar{\mathcal{H}}^I + J_{IS}\, h_{IS}. \end{aligned} \tag{5.24}$$

From the Rayleigh-Schrödinger perturbation theory[5] the energy for $\mathcal{H}^I$ in k-th state Ψ_k may be expanded as a power series of J_{IS}:

$$E_k = E_k^{(0)} + J_{IS}E_k^{(1)} + \frac{J_{IS}^2}{2!} E_k^{(2)} + \cdots \tag{5.25}$$

Similar to Eq.(5.13), Eq.(5.24) may be rewritten as

$$\mathcal{H}^I = p_+\mathcal{H}_+ + p_-\mathcal{H}_-, \tag{5.26}$$

where

$$\mathcal{H}_\pm = \bar{\mathcal{H}}^I \pm 1/2\ J_{IS}I_z \tag{5.27}$$

with corresponding energies in k-th state

$$E_{k\pm} = E_k\left(\delta_I \pm \frac{J_{IS}}{2}\right). \tag{5.28}$$

Here δ_I is a shorthand notation for offsets $\{\delta_1, \delta_2, \cdots, \delta_j, \cdots\}$. The total energy may be expanded as

$$E_k(\delta_I + J_{IS}S_z) = p_+E_k(\delta_I + \frac{J_{IS}}{2}) + p_-E_k(\delta_I - \frac{J_{IS}}{2})$$

$$= p_+\left\{E_k(\delta_I) + \left[\frac{\partial E_k}{\partial \delta_I}\right]\frac{J_{IS}}{2} + \cdots\right\} + p_-\left\{E_k(\delta_I) - \left[\frac{\partial E_k}{\partial \delta_I}\right]\frac{J_{IS}}{2} + \cdots\right\}$$

$$= E_k(\delta_I) + J_{IS}\left[\frac{\partial E_k}{\partial \delta_I}\right]S_z + \frac{J_{IS}^2}{2!}\left[\frac{\partial^2 E_k}{\partial \delta_I^2}\right] + \cdots . \qquad (5.29)$$

From Eqs.(5.22), (5.25), and (5.29) it follows that

$$\langle\Psi_k^{(0)}|\ \bar{h}_I^{(0)}S_z\ |\Psi_k^{(0)}\rangle = J_{IS}E_k^{(1)} = J_{IS}\left[\frac{\partial E_k}{\partial \delta_I}\right]S_z. \qquad (5.30)$$

The generalized scaling factor λ_k may be defined as[2]

$$\lambda_k = \left[\frac{\partial E_k}{\partial \delta_I}\right]. \qquad (5.31)$$

In view of Eq.(5.21), the expectation value $\langle\Psi_k^{(0)}|\ \bar{h}_I^{(0)}\ |\Psi_k^{(0)}\rangle$ in Eq.(5.30), although approximate, determines the position of the peaks. Consequently, once again the scaling factor λ_k is the measure of the splitting in the S spin spectrum. Within the validity of the λ-approximation, perfect decoupling requires $\lambda_k = 0$ for all offsets $\delta_I = \{\delta_1, \delta_2, \cdots, \delta_j, \cdots\}$. In other words, the decoupling sequence must create a fictitious Hamiltonian which is offset-independent. Furthermore, as discussed in section IV.5 the offset-independent fictitious Hamiltonian does not have to vanish.

Theoretically speaking, Eq.(5.31) requires a multi-dimensional calculation. However, any decoupling sequence which performs well within

its decoupling bandwidth should create offset-independent fictitious Hamiltonian. Therefore, only the slice

$$\delta_1 = \delta_2 = \cdots = \delta_k = 0 \quad (k \neq j) \tag{5.32}$$

needs to be investigated. For a single-spin case there is only one index in Eq.(5.32), and consequently there are two eigenvalues originating from a (2 × 2) matrix. With the identity $E_k = \Omega_k$ for this case, it is straightforward to show that

$$\lambda_k = \frac{\partial \Omega_k}{\partial \delta} \qquad k = 1,2 \tag{5.33}$$

so there are two scaling factors, whereas there is only one Waugh scaling factor resulting from Eq.(5.1):

$$\lambda = \frac{\partial \Omega}{\partial \delta} \; . \tag{5.34}$$

The difference stems from the fact that the generalized scaling factor gives the actual line positions while the Waugh scaling factor gives the frequency difference between two parent lines.

V.2. Applications to Heteronuclear Decoupling for a I = 1 and S = 1/2 System in Liquid Crystal Samples.

Fung et. al.[6] have made an extensive comparison among various decoupling sequences developed for liquids by applying them to liquid crystal samples. They also suggested some decoupling sequences of their own, called ALPHA sequences. All sequences for the single-spin decoupling tested failed, and their sequences along with a few Waugh sequences[1,7] showed performance somewhat better than that of the single-spin decoupling sequences. Nontheless, the whole experimental results

are far from satisfactory and their sequences are not backed by theory.

Proper decoupling sequences for the above mentioned case can be developed by applying the principles founded in the previous sections. For concreteness, consider the Hamiltonian for a system consisting of an I =1 and a S = 1/2:

$$\mathcal{H} = - \delta I_z + \omega_Q (I_z^2 - \frac{2}{3}) + D_{IS} I_z S_z, \tag{5.35}$$

where δ is the offset, ω_Q the quadrupole coupling constant, and D_{IS} the heteronuclear dipole-coupling constant. Indirect coupling is neglected.

In principle, the Hamiltonian in Eq.(5.35) can be removed with the sequences developed in section IV.5. In practical applications, however, some questions arise. First, is it better to design a short, relatively crude 90^0 pulse and improve decoupling performance by expanding the sequence from a 12-pulse sequence to a 24-pulse sequence to a longer sequence, or is it best to design a relatively long 90^0 pulse and substitute it into the 12-pulse sequence? Second, how can a composite pulse best be optimized?

The answer to these questions should depend upon the particular system under consideration. Inspection of Table 4.4 reveals that the 12-pulse sequence is not efficient for eliminating the linear terms, requiring all 12 steps. Hence, when resonance offset is a predominant term, schemes based on the 12-pulses may not be suitable. Conversely, if the chemical shift range is small, as in the case of deuterium, and a relatively strong field has to be applied to overcome the quadrupolar interactions, schemes using a 12-pulse sequence may be appropriate.

Suppose the system of interest belongs to the latter category. This is typical for liquid crystal samples with parameters ω_2 = 10 kHz, ω_Q = 10 kHz, D_{IS} = 1 kHz, δ_I ~ 500 Hz, and the linewidth = 2 Hz. Then a scheme that is more efficient in reducing the big bilinear terms at the cost of reduced bandwidth should be the choice. In other words, a shorter composite pulse with a longer sequence is favorable as long as the overall cycling rate is not unacceptably small. The composite pulse should create less offset-dependent Hamiltonian within its bandwidth. The procedure for optimizing the composite pulse would require the construction of the surface with continuous variables δ and ω_Q, and the details will not be discussed here.

Shenker et. al.[8] came up with sequences called COMARO-n given by

$$\text{COMARO-2} = (y\ x)^3(\bar{y}\ x)^3$$

$$\text{COMARO-4} = (y\ x)^3(\bar{x}\ y)^3(\bar{y}\ x)^3(\bar{x}\ \bar{y})^3.$$

For the COMARO-2 sequence a calculation similar to the one given in Table 4.4 results

$$\sum_k A_k = -\frac{1}{3}\epsilon_x I_x - \frac{1}{3}(\epsilon_{yz} I_y I_z + \epsilon_{zy} I_z I_y) + \frac{\epsilon_{xx}+\epsilon_{yy}+\epsilon_{zz}}{3} I(I+1) \tag{5.36}$$

and shows quick averaging for the quadratic terms. The presence of the isotropically averaged term I(I+1) is common to all 12-pulse sequences explored in the previous chapter. For COMARO-2, however, still there are terms remaining after averaging unlike those 12-pulse sequences. COMARO-4 is, incidentally, indistinguishable to Eq.(4.50) and therefore should average all linear and bilinear terms to higher order than the 12-pulse sequences or the COMARO-2 sequence. Nontheless, COMARO-2 reportedly performs as well for $\omega_Q = 0.5\ \omega_1$ as COMARO-4 sequence, and outperforms

COMARO-4 for $\omega_Q = \omega_1$. Perhaps the superior performance of COMARO-2 over COMARO-4 is due to the remaining terms in the fictitious Hamiltonian, which are made insensitive to offset by the composite pulse[9,12]

$$385_0\ 320_{180}\ 25_0$$

partially aided by the scaling by 1/3. Or it may be due to the composite 90^0 pulse given above, which is optimized without including the quadrupole Hamiltonian, therby renders irregular performance. Thus the direct comparison between the two members of the COMARO family may not be legitimate. It would be interesting to optimize the composite pulse with the quadrupole Hamiltonian included in the total Hamiltonian and compare various 12- and 24-pulse sequences.

In the next section it will be shown how to optimize the composite pulse for isotropic liquids and how to remove various error terms by systematic expansions.

V.3. Heteronuclear Decoupling in Liquids for Scalar-Coupled Spins.

V.3.A. Introduction

Current broadband heteronuclear decoupling methods[1,10] assume that homonuclear interactions among I spins-1/2 as well as among S spins-1/2 are negligible. Under this assumption, the decoupling of an isolated I-S spin pair can be examined by looking at the behavior of the I spin alone under the decoupling field. A good decoupling sequence should create small net rotation angles $\beta(+)$ and $\beta(-)$ corresponding to states $S_z = \pm 1/2$, which the I spin undergoes under the decoupling sequence.

There are cases, however, where these neglected homonuclear scalar interactions cause visible residual splitting or broadening. The interaction would be important when very high resolution is required with low decoupler power, or when the coupling between abundant nonequivalent I spins are rather strong. For a system consisting of an S spin-1/2 and two homonuclear-coupled nonequivalent I spins-1/2 the dependence of the magnitude of the splitting on the various parameters is emperically given by[3]

$$\Delta S \cong \frac{J_{II}\, J_{IS}}{\left(\gamma B_2\right)^2} f(\Delta\omega_1 , \Delta\omega_2) \tag{5.37}$$

where J_{II} and J_{IS} are homo- and heteronuclear coupling constants. $f(\Delta\omega_1 , \Delta\omega_2)$ is a complicated function of chemical shifts and differs from one decoupling sequence to another. Later in this chapter the functional form of ΔS will be derived in a rigorous manner. Thus, given that the coupling constants and B_2 are the same, the residual splitting depends solely upon the decoupling sequence used.

In the previous section it was shown that the decoupling sequence creates a fictitious Hamiltinian and in liquids the fictitious Hamiltonian is given by Eq.(4.38). A less offset sensitive fictitious Hamiltonian means better decoupling performance of the sequence used. Table 4.4 shows, however, that the sequence itself largely contributes to making the fictitious Hamiltinian assume the scalar form, Eq.(4.38). In other words, the sequence does not alter the size of the coefficients but averages them. Consequently, it is the composite pulse that largely determines the coefficients and hence determines the offset dependence of the whole decoupling scheme. It therefore is important to design

composite pulses which make the fictitious Hamiltonian offset independent within their respective decoupling bandwidths to ensure good decoupling.

V.3.B. The design of composite pulses for two scalar-coupled spins - phase alternating composite pulses[1,7,11].

The approach taken for designing composite pulses is the use of the Average Hamiltonian Theory (AHT). While there are numerous approaches to the design of composite pulses for the single-spin cases, the design for the coupled-spin case lacks the diversity of approaches largely because the propagators manipulated with pulses can no longer be regarded as rotations in three-dimensional space. The AHT approach is a suitable tool for dealing with situations such as the one described above. Even though the calculation gets complicated, the calculation of higher order average Hamiltonian terms provides insights by showing explicit offset-dependent terms, thereby guiding the design of the composite pulses.

The relevant Hamiltonian for two coupled-spins I_1 and I_2, both spins-1/2, should in general be expressed in terms of two offsets δ_1 and δ_2. However, as argued in section V.1 examination of the surface $\delta_2 = 0$ is sufficient to evaluate performance of a decoupling scheme. Thus it can safely be assumed that the second spin is on resonance and the first spin is off resonance by δ_1. Then in the rotating frame the k-th piecewise-constant Hamiltinian during τ_k over which the decoupling rf-field is applied may be written as

$$\mathcal{H}_k = \mathcal{H}_{rf,k} + V, \tag{5.38}$$

where

$$\mathcal{H}_{rf,k} = (-1)^k \omega_2 I_x \tag{5.39}$$

and

$$V = \delta_1 I_{1z} + J\ I_1 \cdot I_2. \tag{5.40}$$

Eq.(5.39) indicates that the phases of the pulses with constant amplitude alternate between x or -x axis of the rotating frame. The phase alternating composite pulse, in the absence of J, has some useful properties[11(a)]: This class of pulses produces a propagator at $\tau = \Sigma_k \tau_k$ which approximates an ideal rf pulse, i.e.

$$U(\tau) = \prod_k \exp\left(-i\tau_k \mathcal{H}_k\right) \approx e^{i\alpha I_x} \tag{5.41}$$

within the bandwidth of a composite pulse, thus having no phase gradient. α can be selected at will. Pulses without phase distortions as a function of offset have many important applications.[12]

The transformation

$$U(\tau) = U_{rf}\, \mathcal{T} \exp\left(-i \int_0^\tau U_{rf}^\dagger\, V\, U_{rf}\, dt\right), \tag{5.42}$$

along with application of the AHT yields

$$V^{(0)} = J\ I_1 \cdot I_2 + \frac{\delta_1}{\omega_2} \sum_{j=1}^{m} (-1)^{(j+1)} \left\{ I_{2z}(\sin\Delta_j - \sin\Delta_{j-1}) + I_{2y}(\cos\Delta_{j-1} - \cos\Delta_j) \right\}. \tag{5.43}$$

Here Δ_n is defined by

$$\Delta_n = \sum_{k=0}^{n} (-1)^k \alpha_k, \tag{5.44}$$

with α_k being the k-th nominal flip angle in the phase-alternating sequence of m pulses $\alpha_1\bar{\alpha}_2\alpha_3\cdots$. The intial angle α_0 is assumed to be zero. To zeroth order all intense coherent irradiation will remove the terms under the summation, leaving the scalar interaction alone, thus achieving the goal. However, for the decoupler level ω_2 of about 2 kHz the zeroth order approximation is highly inaccurate. Hence higher order terms need to be considered. After some laborious calculations the first order correction is obtained as:

$$V^{(1)} = \frac{\delta_1^2}{\omega_2^2 \tau} I_{2x} \left(\sum_j^m a_j + \sum_{l>j}^m a_{lj} \right)$$

$$+ \frac{\delta_1 J}{\omega_2^2 \tau} (I_{1y}I_{2x} - I_{2y}I_{1x}) \left(\sum_j^m b_j + \sum_{l>j}^m b_{lj} \right) \tag{5.45}$$

$$+ \frac{\delta_1 J}{\omega_2^2 \tau} (I_{1x}I_{2z} - I_{1z}I_{2x}) \left(\sum_j^m c_j + \sum_{l>j}^m c_{lj} \right)$$

where the coefficients are

$$a_j = (-1)^j(\alpha_j - \sin\alpha_j) \tag{5.46}$$

$$a_{kj} = (-1)^{k+j} \left\{ \begin{array}{l} \sin(\Delta_k - \Delta_j) - \sin(\Delta_{k-1} - \Delta_j) \\ - \sin(\Delta_k - \Delta_{j-1}) + \sin(\Delta_{k-1} - \Delta_{j-1}) \end{array} \right\} \tag{5.47}$$

$$b_j = 2\sin\Delta_{j-1} - 2\cos\Delta_j + (-1)^j\alpha_j(\sin\Delta_j + \sin\Delta_{j-1}) \tag{5.48}$$

$$b_{kj} = (-1)^{j+1}\alpha_k(\sin\Delta_j - \sin\Delta_{j-1}) + (-1)^k\alpha_j(\sin\Delta_k - \sin\Delta_{k-1}) \tag{5.49}$$

$$c_j = 2\sin\Delta_{j-1} - 2\sin\Delta_j + (-1)^{j+1}\alpha_j(\cos\Delta_j - \cos\Delta_{j-1}) \tag{5.50}$$

$$c_{kj} = (-1)^{j}\alpha_k(\cos\Delta_j - \cos\Delta_{j-1}) + (-1)^{k+1}\alpha_j(\cos\Delta_k - \cos\Delta_{k-1}) \quad (5.51)$$

It is observed that the linear cross terms are created by the sequences which were absent in the original Hamiltonian. Eqs.(5.44) and (5.46)-(5.51) are the primary equations used for designing composite pulses so that the offset dependent terms may be minimized.

Since in general the Hamiltonian resulting from a sequence of pulses contains all linear and bilinear terms, it would be instructive to consider the next order correction term at least qualitatively to see how offset dependence enters for various spin operators. To facilitate the calculation some useful commutation rules are given in Appendix 4. The operators that appear in $V^{(2)}$ are: I_{1z} and I_{1y} with coefficients proportional to δ_1^3/ω_2^3; the operators $I_{1x}I_{2x}$, $I_{1y}I_{2y}$, $I_{1z}I_{2z}$, $I_{1y}I_{2z}$, and $I_{1z}I_{2y}$ with coefficients varying as $\delta_1^2 J/\omega_2^3$ and the operators I_{1y}, I_{2y}, I_{1z}, and I_{2z} varying as $\delta_1 J^2/\omega_2^3$. Here the quadratic terms begin to deviate from scalar and linear spin operators for the second spin, which were absent in the original Hamiltonian, are produced. Theses linear terms can be regarded as arising from the interaction of the first spin with the small field produced by the rf field. In the previous section the criterion for good decoupling was discussed; the sequence should produce an offset-insensitive average Hamiltonian, and a natural choice for liquids is $J\, I_1 \cdot I_2$ as the remaining Hamiltonian. Now the average Hamiltonian calcultion dictates that for a composite pulse to render a perfect decoupling, which corresponds to making all δ_1-dependent terms vanish, it is inevitable to

have $JI_1 \cdot I_2$ remaining. It therefore appears that achieving homonuclear decoupling and heteronuclear decoupling simultaneously is an unrealistic goal.

Contrary to the liquid crystal case, in the decoupling of liquids the most dominant terms are the linear terms with δ_1 of $O(10^3)$ Hz first appearing in Eq.(5.43) whereas J is of $O(10^1)$ Hz. Thus the composite pulse should be optimized to remove the (offset-dependent) linear terms first. Incidentally, the minimization of offset dependence should also render a reasonably good scalar with J having a slow offset dependence.

The strategy for designing composite pulses is to select reasonably good candidates using Eqs.(5.44)-(5.51) and then optimize these initial candidates to achieve larger bandwidths by direct computation of the propagator $U(\tau)$ given by Eq.(5.42). The method is analogous to the single-spin case.[11(a)] It was discussed at the end of Section V.3.A that the offset dependence of the coefficient of the scalar interaction term is largely due to the composite pulse, rather than the schemes for expanding the sequences. The reason for this can be explained clearly in terms of the average Hamiltonian calculations. A composite pulse which accomplishes perfect decoupling would have to satisfy $V^{(0)} = JI_1 \cdot I_2$, and $V^{(1)} = V^{(2)} = \cdots = 0$. Thus the slope $\partial J(\tau_1)/\partial\delta_1$ would be zero. However, it is questionable that any solution which satisfies all these constraints exists. Numerical optimization, on the other hand, is performed such that the figure-of-merit function is minimal. Inevitably then the optimal pulses found may not remove all offset dependent terms from Eqs.(5.44)-(5.51), but minimize overall offset dependence. As a result, for a composite pulse with a given

number of constituent pulses there seems to exist a "natural" offset-dependence associated with the minimal value of the merit function. This is quite similar to the "natural" bandwidth one may find for a single-spin case.[11(a)]

V.3.C. The evolution of spin operators under scalar interaction.

Suppose a decoupling sequence managed to make all linear and bilinear cross terms vanishingly small and a good scalar term was obtained. Also suppose because of the nonideality of the composite pulse sequence that the scalar coupling constant obtained is slightly offset-dependent. Then the evolution operator under these conditions may be written as

$$U(\tau) = \exp\left(-i\tau\, Jf(\delta_1)\; I_1 \cdot I_2\right). \tag{5.52}$$

The resulting S-spin spectrum under this evolution operator can be predicted by calculating the scaling factor given by Eq.(5.31). For the two-spin case with a Hamiltonian given by Eq.(5.52) the position of the spectral lines can be calculated to give

$$\omega_j = J_{IS} J \left\{\frac{\partial f(\delta_1)}{\partial \delta_1}\right\} (I_1 \cdot I_2)_{jj} \qquad j = 1, \cdots, 4. \tag{5.53}$$

The matrix $(I_1 \cdot I_2)_{jj}$ can be obtained by diagonalizing the 4 x 4 matrix with the product basis $\{\alpha\alpha,\ \alpha\beta,\ \beta\alpha,\ \beta\beta\}$:

$I_1 \cdot I_2$	$\alpha\alpha$	$\alpha\beta$	$\beta\alpha$	$\beta\beta$
$\alpha\alpha$	$\frac{1}{4}$	0	0	0
$\alpha\beta$	0	$-\frac{1}{4}$	$\frac{1}{2}$	0
$\beta\alpha$	0	$\frac{1}{2}$	$-\frac{1}{4}$	0
$\beta\beta$	0	0	0	$\frac{1}{4}$

Diagonalization of the submatrix gives four eigenvalues

$$\alpha_1 = -\frac{3}{4} \quad , \quad \alpha_k = \frac{1}{4} \qquad (k = 2,3,4). \tag{5.54}$$

Therefore, the S-spin spectrum consists of four lines at the frequencies

$$\omega_j = J_{IS} J \frac{\partial f(\delta_1)}{\partial \delta_1} \alpha_j \quad , \qquad j=1,2,3,4 \ . \tag{5.55}$$

If the derivative $\partial f/\partial \delta_1$ is zero, corresponding to the perfect decoupling, the four lines collapse into a single line. On the other hand, if the derivative is sufficiently small so that the splitting between any pair of lines within the triplet manifold is smaller than the natural line width, then the three lines in this manifold collapse into a single peak, giving a spectrum consisting of two peaks with an intensity ratio 3:1. This situation is illustrated in Fig.5.1.

As a third type of situation, suppose the composite pulse produces a fictitious Hamiltonian, which contains small but non-trivial linear and bilinear cross terms and a reasonably good scalar interaction term. Under these conditions the effective Hamiltonian has the symmetry approaching closer to spherical symmetry than the cylindrical symmetry,

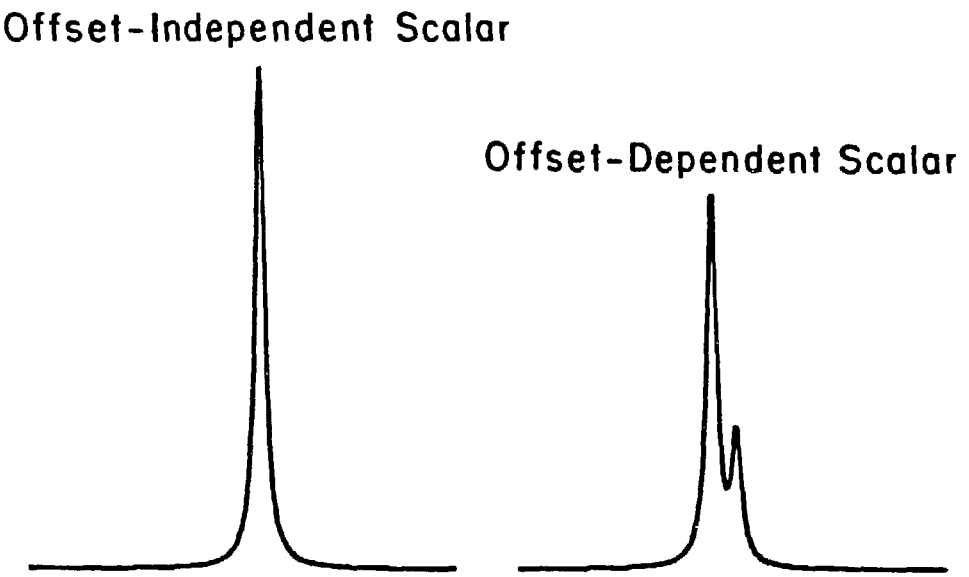

XBL 876-2673

Figure 5.1 The expected form of the S-spin spectrum under a decoupling sequence that produces an underlying Hamiltonian that is a pure scalar operator $2\pi J\mathbf{I}_1\cdot\mathbf{I}_2$. If the effective coupling constant is offset-independent then a sharp singlet is observed. When the coupling constant is offset-dependent a 3:1 pattern emerges, in which the S spin experiences the local field of the triplet or singlet states, respectively.

which the original unmodulated Hamiltonian possesses. Therefore, it becomes more convenient to use operators expressed in the spherical basis than in the Cartesian basis. The spherical basis for the bilinear operators are listed in Table 5.1 and for linear operators the ± combination

$$I_{\alpha\pm} = I_{1\alpha} \pm I_{2\alpha} \qquad \alpha=x,y,z \tag{5.56}$$

is convenient.

With the commutation rules in Appendix 4, it can be shown that for bilinear opeators

$$[A_{00} , A_{1k}] \neq 0 \qquad k = 0,\pm1 \tag{5.57}$$

$$[A_{00} , A_{2k}] = 0 \qquad k = 0,\pm1,\pm2 \tag{5.58}$$

and for linear terms

$$[A_{00} , I_{\alpha+}] = 0 \tag{5.59}$$

$$[A_{00} , I_{\alpha-}] = 0. \tag{5.60}$$

The significance of these commutation relations becomes apparent when the sequence is to be improved by expansion using the cyclic permutation and phase shifts. To be more specific, first separate the scalar part from the rest (denoted as $\bar{\mathcal{H}}'$ in the following) in the fictitious Hamiltonian such that

$$U(\tau) = e^{-i\tau\, Jf(\delta 1)\, I1\cdot I2} \; e^{-i\tau\, \bar{\mathcal{H}}'} = U_J U'. \tag{5.61}$$

Secondly, expand the sequence by combining various evolution operators and collecting U_J on the left:

Table 5.1 Spherical Basis Set of Bilinear Spin Operators

$$T_{00} = -\frac{1}{\sqrt{3}} I_1 \cdot I_2$$

$$T_{10} = -\frac{1}{2\sqrt{2}} \left(I_{1+}I_{2-} - I_{1-}I_{2+}\right)$$

$$T_{1\pm1} = \frac{1}{2} \left(I_{1z}I_{2\pm} - I_{1\pm}I_{2z}\right)$$

$$T_{20} = \frac{1}{\sqrt{6}} \left(3\, I_{1z}I_{2z} - I_1 \cdot I_2\right)$$

$$T_{2\pm1} = \mp\frac{1}{2} \left(I_{1z}I_{2\pm} + I_{1\pm}I_{2z}\right)$$

$$T_{2\pm2} = \frac{1}{2} I_{1\pm}I_{2\pm}$$

$$U(n\tau) = \exp\left(-in\tau\, Jf(\delta_1)\, I_1\cdot I_2\right)\, (U_J^{\dagger})^{n-1}\, U_n'\, U_J^{n-1} \cdots$$

$$\cdots\, U_J^{\dagger 2}\, U_3'\, U_J^2\, U_J^{\dagger}\, U_2'\, U_J\, U_1' \,. \qquad (5.62)$$

The operators O^+ in U_k' which commute with U_J can be made vanish to zeroth order in the BCH expansion by phase shifts and cyclic permutations:

$$\sum_{k=1}^{n} U_J^{\dagger}\, \epsilon_k O_k^{\dagger}\, U_J \;-\; U_J^{\dagger}\left(\sum_{k=1}^{n}\epsilon_k O_k^{\dagger}\right)U_J \;= 0. \qquad (5.63)$$

In contrast, operators O^- which do not commute with U_J evolve under U_J, making cyclic permutation and phase shifts ineffective in removing these terms. Thus they may pose problems as $n\tau$ increases. However, because the operators do not commute with $I_1\cdot I_2$, to first order they do not shift the energy levels produced by $I_1\cdot I_2$. The effect of O^- and the deviation from scalar on the spectrum may be shown by performing the degenerate-perturbation calculation. To be more specific, consider the 3×3 matrix which determines the first order energy correction to the triplet manifold. The singlet state has no dynamics, and thus can be ignored. Eigenfunctions to be used are:

$$\phi_1 = \alpha\alpha, \quad \phi_2 = \frac{\alpha\beta + \beta\alpha}{\sqrt{2}}, \quad \phi_3 = \beta\beta \qquad (5.64)$$

and the secular determinant is

Table 5.2 Matrix Elements of Operators O^- and $I_{1\alpha}I_{2\alpha}$.

$O^-_{ij} = 0 \qquad i,j = 1,2,3.$

x_1x_2	ϕ_1	ϕ_2	ϕ_3
ϕ_1	0	0	$\frac{1}{4}$
ϕ_2	0	$\frac{1}{4}$	0
ϕ_3	$\frac{1}{4}$	0	0

y_1y_2	ϕ_1	ϕ_2	ϕ_3
ϕ_1	0	0	$-\frac{1}{4}$
ϕ_2	0	$-\frac{i}{4}$	0
ϕ_3	$-\frac{1}{4}$	0	0

z_1z_2	ϕ_1	ϕ_2	ϕ_3
ϕ_1	$\frac{1}{4}$	0	0
ϕ_2	0	$-\frac{1}{4}$	0
ϕ_3	0	0	$-\frac{1}{4}$

$$\begin{vmatrix} \langle\phi_1|\,0\,|\phi_1\rangle - \lambda & \langle\phi_1|\,0\,|\phi_2\rangle & \langle\phi_1|\,0\,|\phi_3\rangle \\ \langle\phi_2|\,0\,|\phi_1\rangle & \langle\phi_2|\,0\,|\phi_2\rangle - \lambda & \langle\phi_2|\,0\,|\phi_3\rangle \\ \langle\phi_3|\,0\,|\phi_1\rangle & \langle\phi_3|\,0\,|\phi_2\rangle & \langle\phi_3|\,0\,|\phi_3\rangle - \lambda \end{vmatrix} = 0. \quad (5.65)$$

Table 5.2 lists matrix elements of 0^- and quadratic terms which are not removed by Eq.(5.63).

Since all matrix elements are zero for 0^- operators it can be concluded that they do not affect the first order spectrum. The presence of the scalar interaction of $0(J)$, therefore, quenches the saml1 terms and the decoupling performance is little affected. This is another situation where the offset-dependent small terms are stabilized by a larger offset-insensitive residual term, as discussed in a previous chapter.

Because $I_{1\alpha}I_{2\alpha}$ (α=1,2,3) do have matrix elements, the deviation from the scalar may be problematical. However, as long as the composite pulse produces a good scalar, the deviation from the scalar should be small, and further refinements in making a better scalar can be achieved by expanding the sequence with phase shifts and cyclic permutations.

V.3.D. Evaluation of decoupling schemes

Schemes using 90 degree pulses

With Sections V.3.B and V.3.C as a guideline, various composite pulses are found: Using $V^{(0)}$ and $V^{(1)}$ we find the initial candidates, then these candidates are optimized by numerically calculating the

Table 5.3 Phase-Alternating Composite 90^0 Pulses for Two Coupled Spins-1/2.

Label	Sequence	Bandwidth[a]	Length[b]
P_1	$395\ \overline{330}\ 25$	±0.15	750
P_2	$40\ \overline{290}\ 380\ \overline{40}$	±0.2	750
P_3	$55\ \overline{280}\ 310\ \overline{65}\ 305\ \overline{285}\ 50$	±0.3	1350
P_4	$20\ \overline{100}\ 335\ \overline{170}\ 300\ \overline{35}\ 140\ \overline{335}\ 170\ \overline{315}\ 80$	±0.6	2000

[a] Given in terms of the parameter $\Delta\omega/\omega_2$.

[b] Total rotation of the composite pulse in degrees.

underlying Hamiltonian around $\delta_1 = 0$. A criterion is to reduce the deviation from the scalar as a function of offset. Then they are further optimized by the method suggested by Waugh[1,7] which has been much used for improving composite pulses for decoupling,[13] which allows bandwidth extension without making the Hamiltonian deviate much from the scalar. Table 5.3 lists pulses with 90^0 flip angle along x axis and they are labeled P_1-P_4. The lengh of each pulse is given in degrees, with overbars denoting a 180^0 phase shift, and the bandwidths are given as a fraction of ω_2. All bandwidths are smaller than those of the single-spin case. This may be attributed to having more constraints Eqs.(5.44)-(5.51) in optimization.

This restricted bandwidth in principle may be expanded by using the 12-pulse based schemes. However, the schemes, as discussed in a previous chapter, are not efficient in removing the linear terms, although they are highly efficient in averaging the quadratic terms. Also from the experience in the single-spin case, it is well known that the use of nominally orthogonal channels are highly susceptible to the exact radio-frequency phase shifts. MLEV sequences with $90^0_x\ 180^0_y\ 90^0_x$ composite pulse are a good example.

Fig.5.2 shows the Waugh scaling factors for the $(x\ y\ \bar{x}\ y)^s$ sequence with the composite pulse P_3. A 5% reduction in ω_2 from the nominal value $\omega_2^0/2\pi = 2$ kHz significantly degrades the decoupling performance, showing that the sequence does not have sufficient compensation for the linear terms. Interestingly, however, the phase shift errors up to 1^0 do not have a perceptible effect on the decoupling

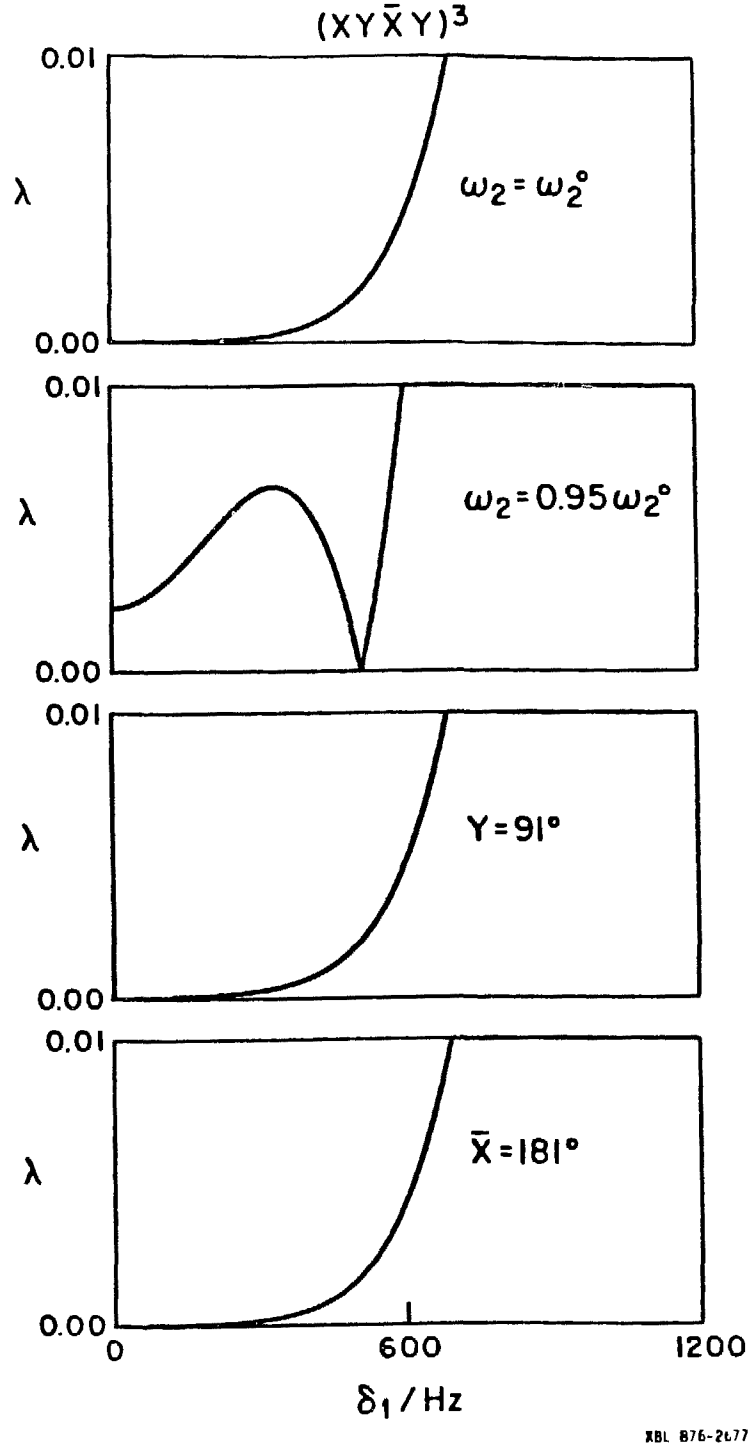
$(XY\bar{X}Y)^3$
0.01
λ
0.00
$\omega_2 = \omega_2^\circ$
0.01
λ
0.00
$\omega_2 = 0.95\omega_2^\circ$
0.01
λ
0.00
Y = 91°
0.01
λ
0.00
$\bar{X}$ = 181°
0
600
1200
δ_1 / Hz

XBL 876-2477

Figure 5.2 Sensitivity of $(X\ Y\ \bar{X}\ Y)^3$ to rf inhomogeneity or phase shift errors using the composite pulse P_3. The top plot shows the Waugh scaling factor for the correctly adjusted sequence. Directly underneath, the effect of a 5% reduction in $\omega_2/2\pi$ (to 1900 Hz) is shown. There is a significant degradation in performance. Phase shift errors as large as 1^0 on either Y (next trace) or $\bar{X}$ (bottom trace) channels are harmless, as a comparison with the correctly adjusted sequence shows.

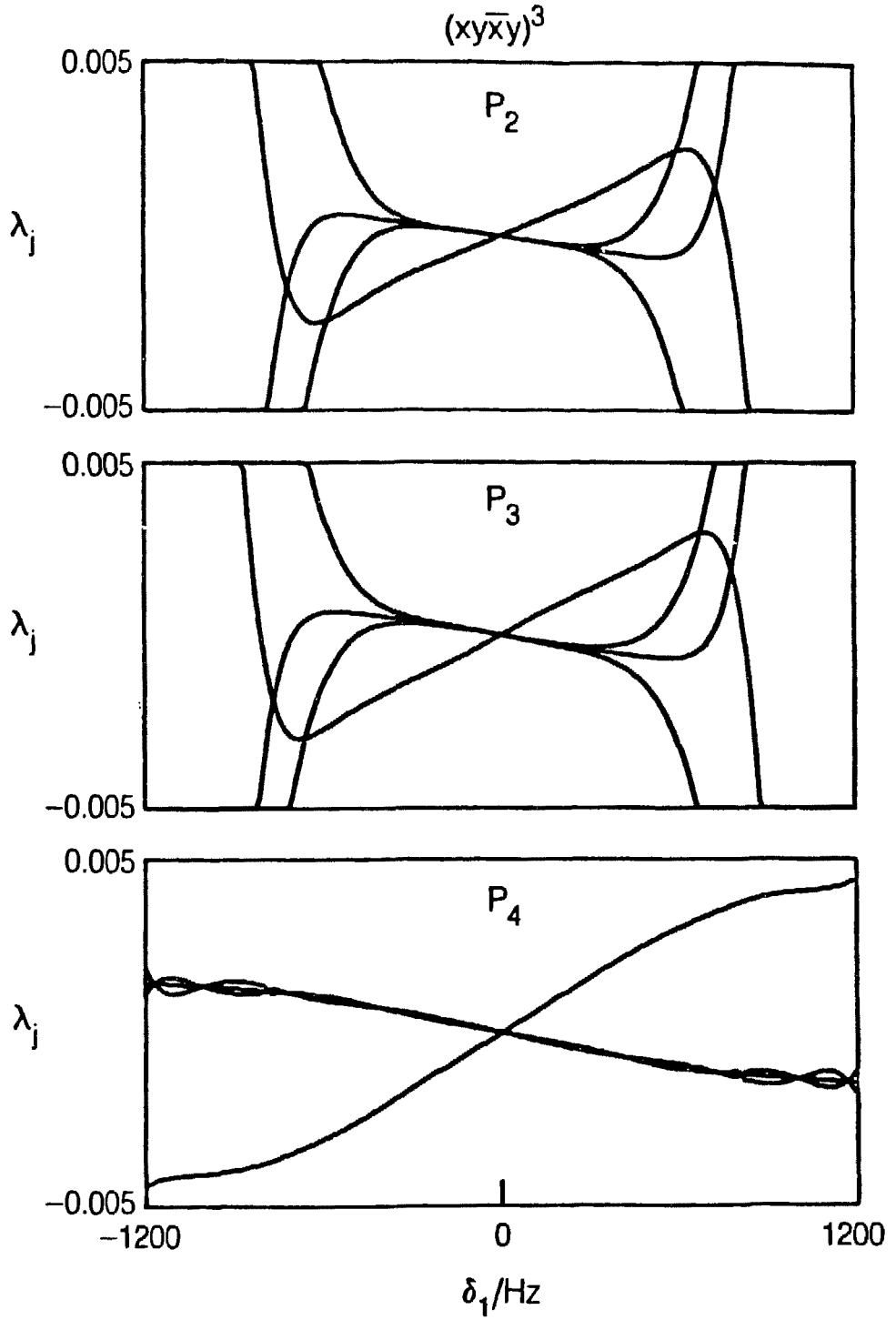

XBL 876-2771A

Fig. 5.3 Scaling factors for the indicated composite 90^0 pulses of Table 5.3 when used in the simple sequence $(X\ Y\ \bar{X}\ Y)^3$. The scaling factors are shown as a function of δ_1, the offset of the directly coupled I spin, for the case $\delta_2 = 0$, and assuming a homonuclear coupling of 10 Hz and a 2 kHz rf field. For small δ_1 the signature in each case is that of a pure scalar operator, but the effective bandwidth of the more elaborate composite pulses P_3 and P_4 is larger. Near the edge of the bandwidth the compensation fails and the "triplet" states are no longer degenerate.

performance. These behaviors are common to all composite 90^0 pulses in Table.5.2. Consequently, these may be considered the properties of the sequence itself.

Figure 5.3 shows the scaling factors given by Eq.(5.31) for the case of J = 10 Hz, $\omega_2/2\pi$ = 2 kHz, values typical to broadband proton decoupling in liquids. It is obvious from Table 5.3 and these Figures that the bandwidth is largely determined by the composite pulse and within their respective bandwidths the averaging of $I_{1\alpha}I_{2\alpha}$ is excellent.

If the $(x\ \bar{y}\ x\ \bar{y}\ x\ y)^2(\bar{x}\ y\ x\ y\ x\ y)^2$ sequence is used instead, there is a small improvement as Fig.5.4 shows. The sequence is also quite sensitive to the rf inhomogeneity. However, the sequence is insensitive to phase shift errors upto 1^0 unlike MLEV sequences.

Fig. 5.5 shows the scaling factors with 1^0 phase shift error in y and $\bar{x}$ channels for the above sequences when the composite pulse P_4 is used. Same ω_1 and J values are used.

In principle, a longer composite pulse with a 36- or 48-pulse sequence obtained by the expansion procedure developed in an earlier section can be used to get an improved result. However, at the low cycling rates of these longer sequences other imperfections due to, for example, sample spinning and relaxation would degrade the calculated decoupling performance.

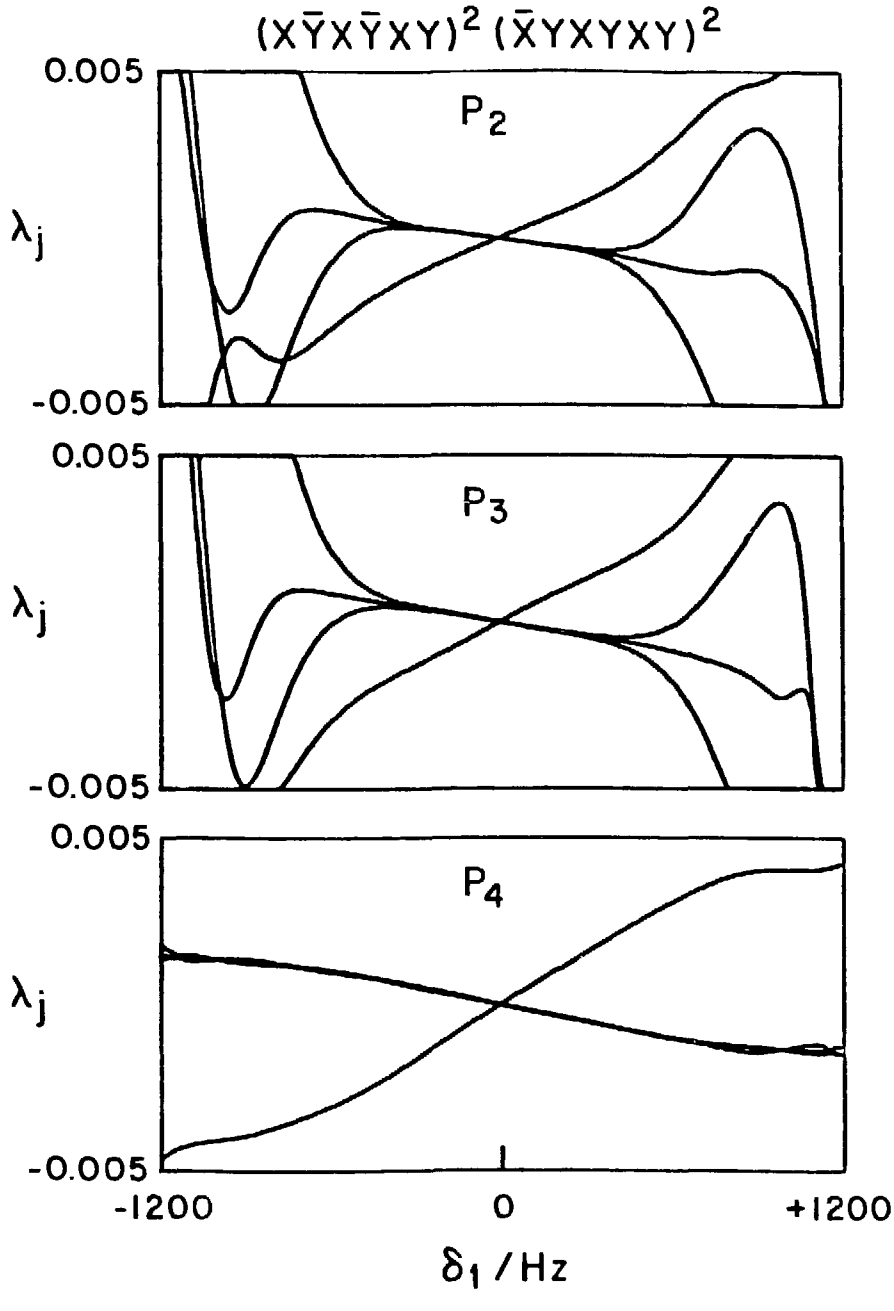
$(X\bar{Y}X\bar{Y}XY)^2\,(\bar{X}YXYXY)^2$
0.005
P_2
λ_j
-0.005
0.005
P_3
λ_j
-0.005
0.005
P_4
λ_j
-0.005
-1200
0
+1200
δ_1 / Hz

XBL 876-2670

Figure 5.4 Scaling factors for the 24-pulse sequence $(X\ \bar{Y}\ X\ \bar{Y}\ X\ Y)^2$ $(\bar{X}\ Y\ X\ Y\ X\ Y)^2$ under the same conditions as Fig.5.3. There is a slight improvement compared with the $(X\ Y\ \bar{X}\ Y)^3$ sequence.

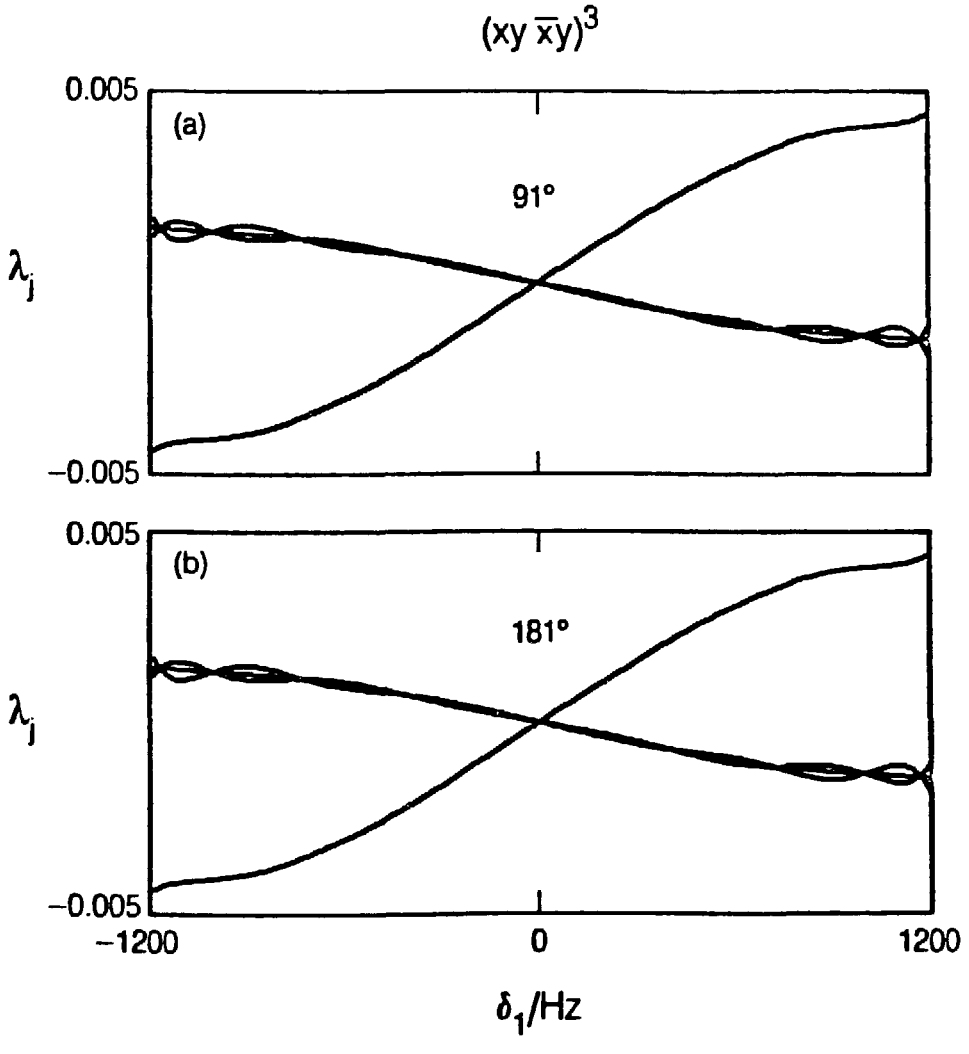

Figure 5.5(a) Scaling factors of the sequence $(x\ y\ \bar{x}\ y)^3$ with 1^0 phase shift error in $\bar{x}$ or y channel. The composite pulse used is P_4.

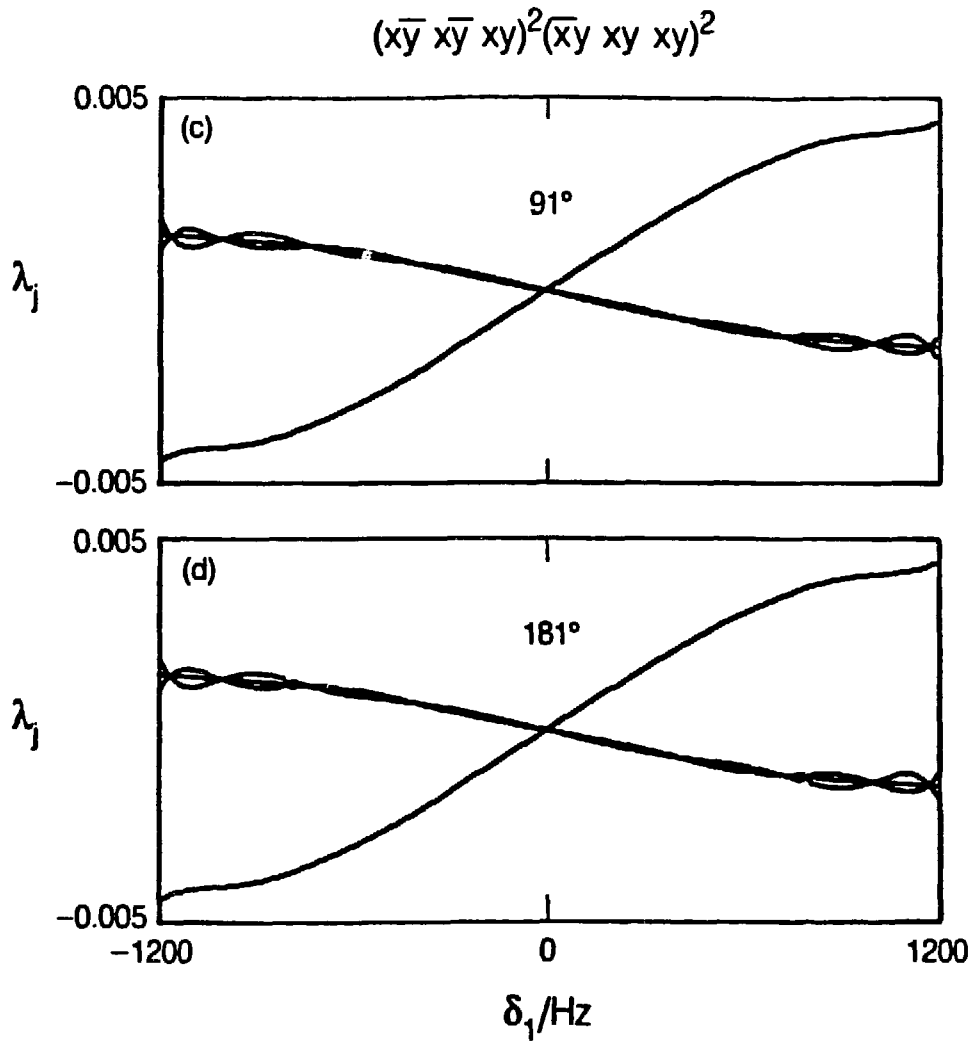

Fig. 5.5(b) Same as Fig. 5.5(a), except that the sequence $(x\ \bar{y}\ x\ \bar{y}\ x\ y)^2(\bar{x}\ y\ x\ y\ x\ y)^2$ is used instead.

Sequences using 180 degree pulses and 180 degree phase shifts

Table 5.4. lists phase alternating 180^0 composite pulses found using the same method as the one employed for the 90^0 pulses. These pulses then are assembled to have the form $U\bar{U}\bar{U}U$, which again reduces the linear and bilinear cross terms further. These are termed DIPSI ("Decoupling In the Presence of Scalar Interactions") sequences, and they are labeled by the index n, the same one used to label the composite pulses.

Waugh scaling factors for the DIPSI sequences are shown in Fig. 5.6. Also shown in the figure is the one for the WALTZ-16 sequence for comparison. WALTZ-16 sequence has the biggest bandwidth, reflecting that the less constraints were needed to design it. Within their respective bandwidths the DIPSI sequences are predicted to offer very good decoupling for the single-spin case, since λ are kept well below 10^{-3}. The cycling rate with $\omega_2/2\pi$ = 2 kHz is 130.4 Hz for DIPSI-1, so it has a length and complexity comparable to WALTZ-8. DIPSI-2 and -3 are comparable to WALTZ-16 and -32 respectively in cycling rate.

Fig.5.7 shows scaling factors for DIPSI-1, -2 and -3 sequences. The scaling factor for WALTZ-16 is also included for comparison. WALTZ-16 shows the largest deviation from the scalar for the most of its bandwidth. Thus it would give a spectrum consisting of four lines. DIPSI sequences, on the other hand, render very good scalars. Thus the spectrum would consist of a nearly degenerate "triplet" state and a singlet. Here again, it is possible to improve the degeneracy of the scalar by averaging the coefficients of $I_{1\alpha}I_{2\alpha}$. For example, Fig. 5.8

Table 5.4 Phase-Alternating Composite 180^{o} Pulses for Two Coulped Spins-1/2

Label	Sequence	Bandwidth[a]	Length[b]
R_1	$365\ \overline{295}\ 65\ \overline{305}\ 350$	± 0.4	1380
R_2	$320\ \overline{410}\ 290\ \overline{285}\ 30\ \overline{245}\ 375\ \overline{265}\ 370$	± 0.6	2590
R_3	$\overline{245}\ 395\ \overline{250}\ 275\ \overline{30}\ 230\ \overline{360}\ 245\ \overline{370}\ 340\ \overline{350}$ $260\ \overline{270}\ 30\ \overline{225}\ 365\ \overline{255}\ 395$	± 0.8	4890

[a] Given in terms of the parameter $\Delta\omega/\omega_2$.

[b] Total rotation in degrees.

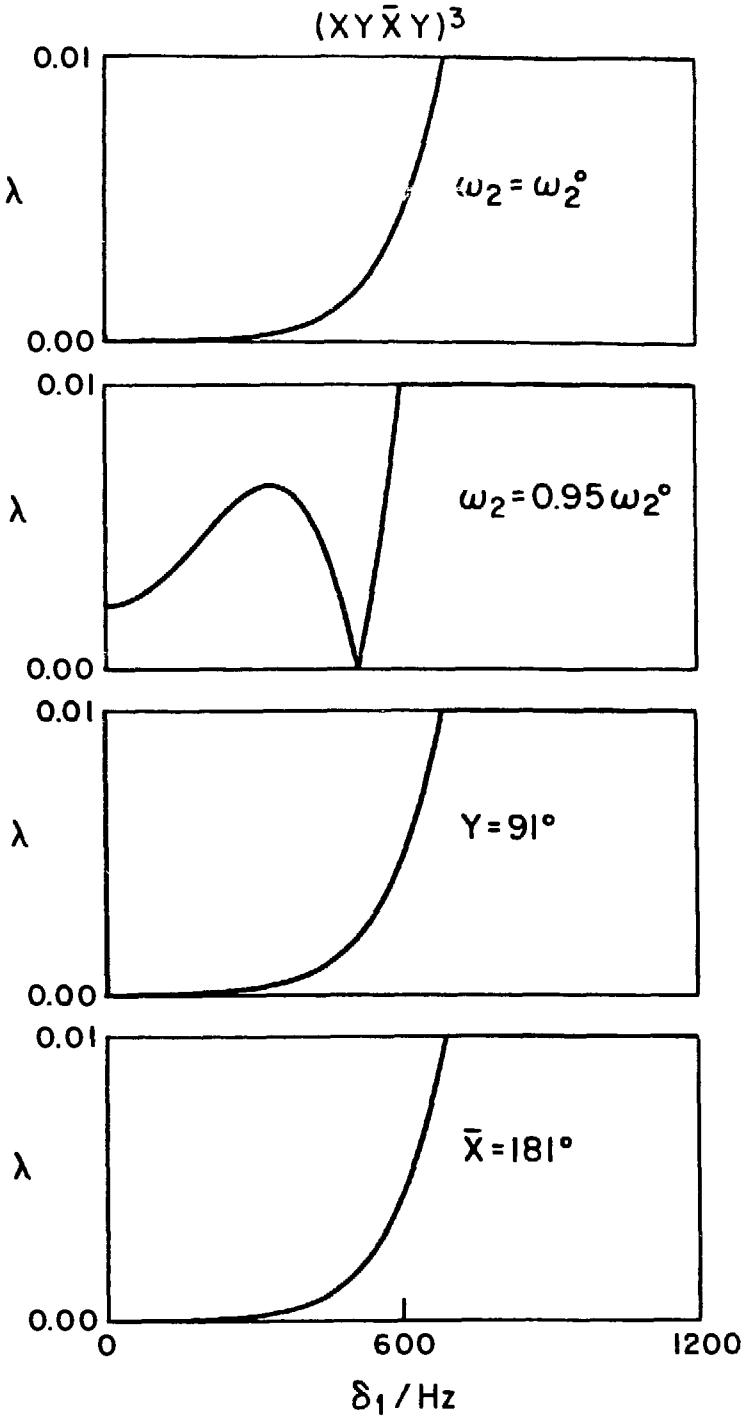
$(XY\bar{X}Y)^3$
0.01
λ
0.00
$\omega_2 = \omega_2^\circ$
0.01
λ
0.00
$\omega_2 = 0.95\,\omega_2^\circ$
0.01
λ
0.00
Y = 91°
0.01
λ
0.00
$\bar{X}$ = 181°
0
600
1200
δ_1 / Hz

XBL 876-2677

Figure 5.6 Single-spin scaling factors for DIPSI-1, -2, -3 and WALTZ-16. All the sequences offer excellent single-spin performance over their bandwidths, but WALTZ-16 gives the largest bandwidth.

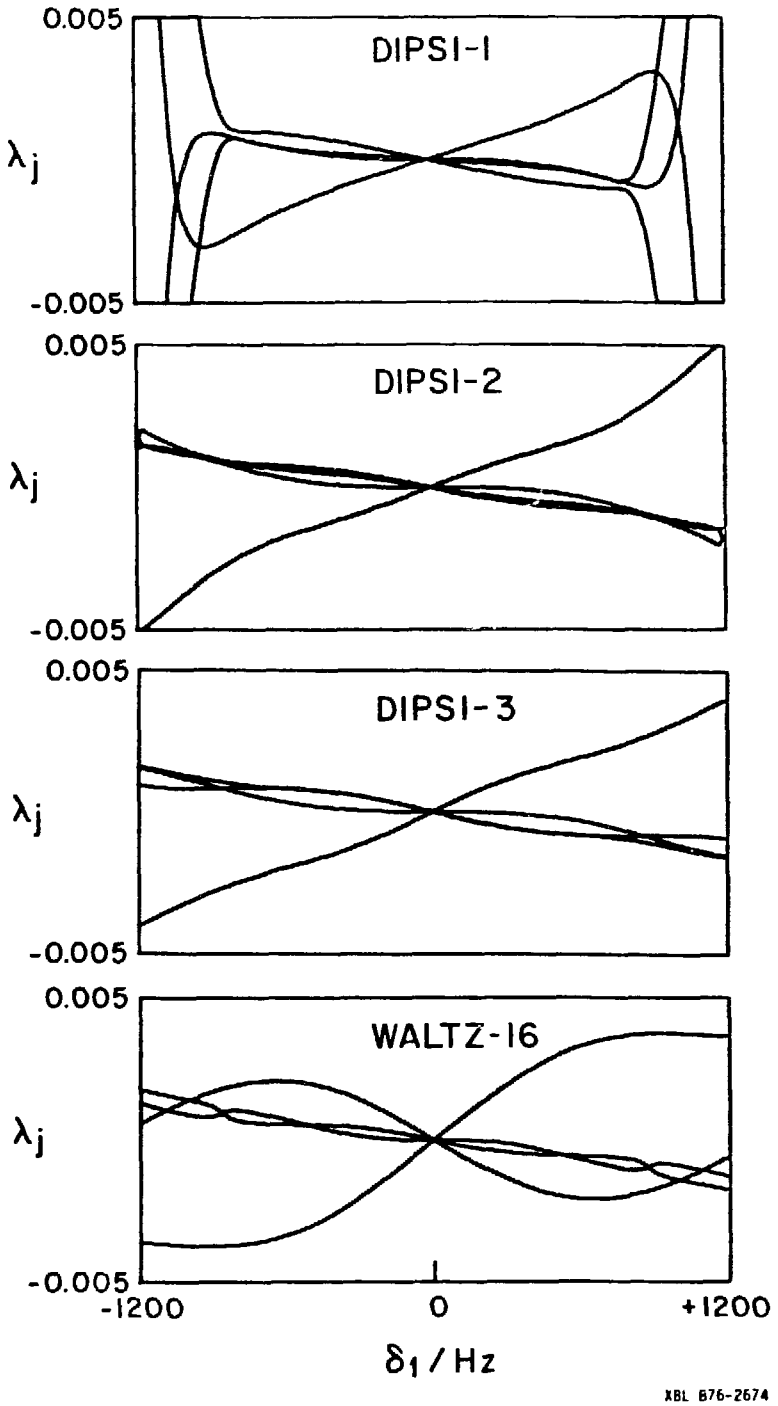
0.005
DIPSI-1
λ_j
-0.005
0.005
DIPSI-2
λ_j
-0.005
0.005
DIPSI-3
λ_j
-0.005
0.005
WALTZ-16
λ_j
-0.005
-1200
0
+1200
δ_1 / Hz

XBL 876-2674

Figure 5.7 Scaling factors for DIPSI-1, -2 , -3 and WALTZ-16, using the same conditions as in Fig. 5.3. Even though the DIPSI sequences use only 180^{0} phase shifts, a pure scalar propagator is approached quite closely. By contrast, WALTZ-16 gives a different signature, showing non-scalar behavior and resulting in four different transitions.

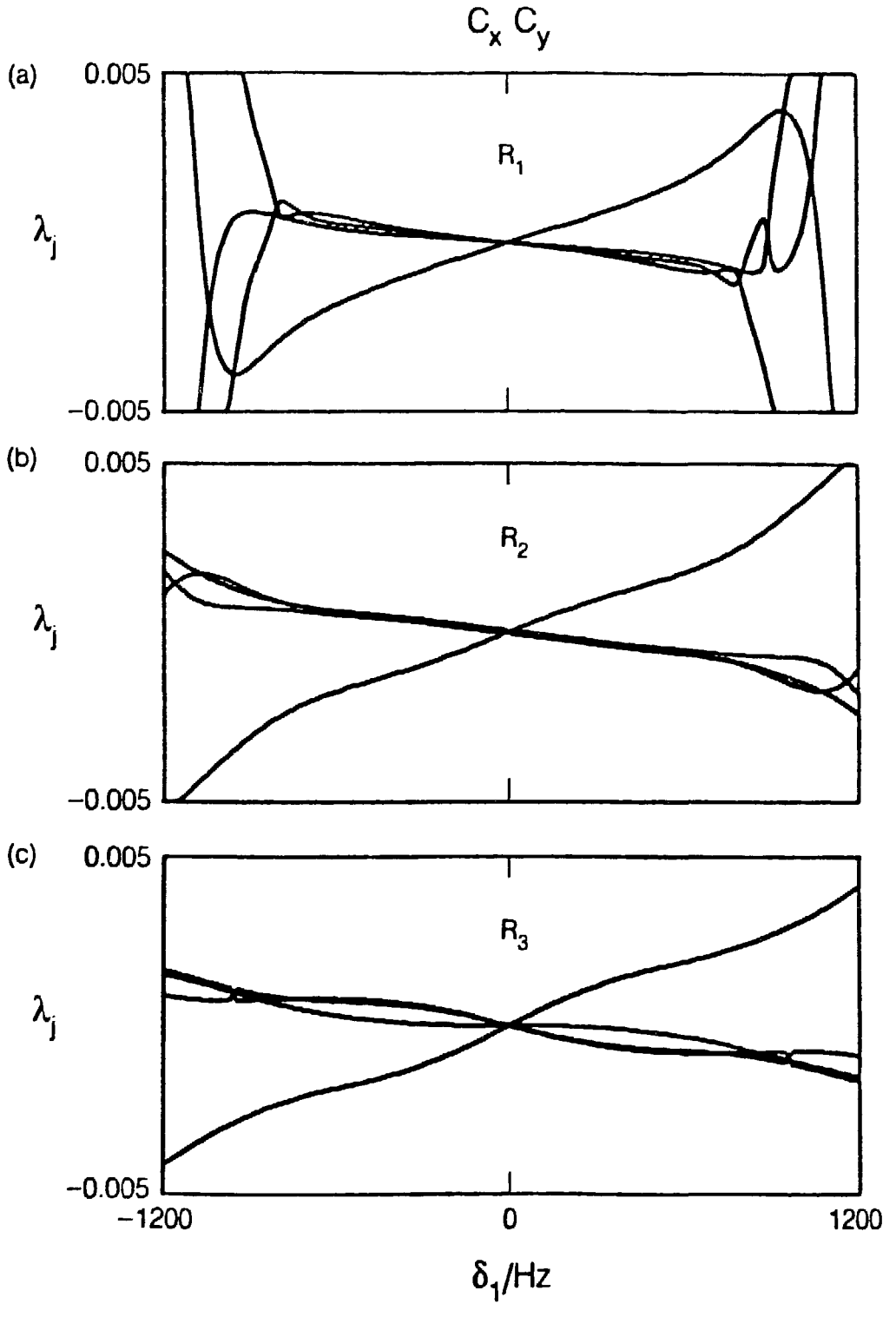

XBL 8711-5955

Fig. 5.8 Scaling factors for the expanded sequence C_xC_y with the composite pulses R_1, R_2, and R_3. It is seen that very good scalar operators result. However, the slopes of the scalars as a function of the offset do not change appreciably.

shows the averaging of the coefficients for the sequence C_xC_y, where C_α denote $R\bar{R}\bar{R}R$ with a composite 180^0 pulse R applied along α axis in the rotating frame. For most practical applications, however, small deviations from the scalar as in DIPSI sequences go unnoticed and the numerical value of the scalar does not change as the sequence is expanded. Furthermore, the sequence expanded using orthogonal phases may be very sesitive to imperfections such as phase shift errors and rf field inhomogeneity as well as other imperfections such as relaxation effects. Hence, in the experiments to be discussed in a later section, the regular DIPSI sequences are employed.

V.4. The Offset-Dependence of the Scalar Interaction.

The splitting (ΔS) given by Eq.(5.37) was first discovered emperically[3]. For a simple case of coherent-decoupling,[7,10,14,15] it is possible to derive a qualitative dependence of ΔS on parameters J_{IS}, J, ω_2, δ_1, and δ_2. First consider the Hamiltonian given by Eqs.(5.38)-(5.40). For coherent-decoupling the subscript k is immaterial. The evolution operator may be separated as

$$U(t) = \exp\left(-it(\omega_2 I_x + \delta_1 I_{1z})\right)\ \mathcal{T}\exp\left(-iJ\int_0^t \bar{I}_1\cdot\bar{I}_2\ dt'\right), \qquad (5.66)$$

where

$$\bar{I}_1\cdot\bar{I}_2 = \exp\left(it(\omega_2 I_x + \delta_1 I_{1z})\right)\ I_1\cdot I_2\ \exp\left(-it(\omega_2 I_x + \delta_1 I_{1z})\right). \qquad (5.67)$$

Since $\omega_2/2\pi$ is about 2 kHz and J is about 10 Hz, it is well to approximate U(t) such that

$$\mathcal{T}\exp\left(-iJ\int \bar{I}_1\cdot\bar{I}_2\ dt'\right) \approx \exp\left(-iJ\int \bar{I}_1\cdot\bar{I}_2\ dt'\right). \tag{5.68}$$

The calculation of Eq.(5.67) gives terms $I_{1\alpha}I_{2\alpha}$ as well as cross terms $I_{1\alpha}I_{2\beta}$ $(\alpha\neq\beta)$. Because only the qualitative offset-dependence of the scalar part is of interest, it may be well to consider terms $I_{1\alpha}I_{2\alpha}$. With Eqs.(4.4)-(4.7), the relevant part becomes

$$\begin{aligned}\bar{I}_1\cdot\bar{I}_2 \cong\ & I_{1x}I_{2x}(\cos^2\theta\ \cos\omega_e t + \sin^2\theta)\\ & + I_{1y}I_{2y}(\cos\omega_e t\ \cos w_2 t - \sin\omega_2 t\ \sin\omega_e t\ \sin\theta)\\ & + I_{1z}I_{2z}(\cos^2\theta\ \cos\omega_2 t + \sin^2\theta\ \cos\omega_e t\ \cos w_2 t).\end{aligned} \tag{5.69}$$

Furthermore, to see only the qualitative behavior it suffices to consider only the coefficient of any one of these operators. If the coefficient of $I_{1x}I_{2x}$, for example, is chosen with the understanding that $\omega_2\tau = 2\pi$ and in the limit $\omega_2 \gg \delta_1$, it reduces to $\tau(3/2)(\delta_1^2/\omega_2^2)$. Thus the splitting ΔS behaves as

$$\Delta S \sim J_{IS}\frac{\partial E}{\partial \delta_1} \sim \frac{J_{IS}}{\omega_2}\delta_1 \tag{5.70}$$

correctly showing the dependence on parameters J_{IS}, J, ω_2, and δ_1 as in Eq.(5.37). For this simple case $f(\delta) \sim \delta$.

In Section V.3.B the "natural" slope of $f(\delta_1)$ for each composite pulse was discussed. Furthermore, an inspection of Figures 5.3, 5.4,

5.7, and 5.8 shows an interesting feature; the slopes are nearly the same. The calculation based on the AHT is once again a good tool to assess the slopes. In the limit $\omega_2 \gg \delta_1$, a calculation up to $V^{(2)}$ is sufficient to show the offset-dependence of the scalar part, because $V^{(2)}$ is the first term in which deviations from the scalar operator appear. If the decoupling sequence makes linear and bilinear cross terms vanishingly small, or if consideration is confined only to the scalar part because linear and bilinear cross terms are not relevant to determining the slope, the evolution operator to second order becomes

$$U(\tau) = \prod_k \exp\left(-it_k\omega_k I_x\right) \exp\left[-it_k\left\{ J\, I_1\cdot I_2 + \frac{\delta_1^2 J}{6\,\omega_2^2} \right.\right. \times \left.\left. \left(c_x^{(k)} I_{1x}I_{2x} + c_y^{(k)} I_{1y}I_{2y} + c_z^{(k)} I_{1z}I_{2z}\right)\right\}\right], \tag{5.71}$$

where the following notations are used:

$$\begin{aligned}
\omega_k &= (-1)^k \omega_2 \,, \\
c_x^{(k)} &= -4 + 6\,\frac{s_{1k}}{\omega_k t_k} - 2\, c_{1k} \\
c_y^{(k)} &= -\frac{3}{2} - \frac{3}{4}\,\frac{s_{2k}}{\omega_k t_k} + \frac{3 s_{1k}}{\omega_k t_k} + \frac{c_{2k}}{4} \\
c_z^{(k)} &= -\frac{5}{2} + \frac{3}{4}\,\frac{s_{2k}}{\omega_k t_k} + \frac{3 s_{1k}}{\omega_k t_k} - \frac{c_{2k}}{4} - 2\, c_{1k}
\end{aligned} \tag{5.72}$$

with

$$s_{jk} = \sin(j\omega_k t_k)$$
$$c_{jk} = \cos(j\omega_k t_k). \tag{5.73}$$

Since $I_1 \cdot I_2$ commutes with the rest of the operators in Eq.(5.71), the evolution operator may be rewritten as

$$U(\tau) = \exp\left(-i\tau J\ I_1 \cdot I_2\right)\ P_k U_k \cdots P_1 U_1 \tag{5.74}$$
$$= U(\tau)\ P_k P_{k-1} \cdots P_1\ (P_{k-1} \cdots P_1)^{-1} U_k\ (P_{k-1} \cdots P_1) \cdots P_1^{-1} U_2 P_1 U_1,$$

where

$$P_k = \exp(-it_k \omega_k I_x). \tag{5.75}$$

With the definition

$$P^{(k)} = P_k \cdots P_1$$
$$= \exp\left(-i\Sigma_m^k\ t_m\ (-1)^m\ \omega_2 I_x\right)$$
$$= \exp\left(-i\ a^{(k)} I_x\right) \tag{5.76}$$

the transformation of U_k by $P^{(k-1)}$ becomes

$$\left(P^{(k-1)}\right)^{-1} U_k P^{(k-1)} = \exp\left[-it\ \frac{J\ \delta_1^2}{6\omega_2^2}\left[c_x^{(k)}\ I_{1x}\ I_{2x} + c_y^{(k)}\left\{\ I_{1y}I_{2y}\right.\right.\right.$$
$$\times \cos^2 a^{(k-1)} + I_{1z}I_{2z}\ \sin^2 a^{(k-1)} - \left(I_{1y}I_{2z} + I_{1z}I_{2y}\right)\ \sin\ a^{(k-1)}$$
$$\left.\left.\cos\ a^{(k-1)}\right\} + c_z^{(k)}\left\{I_{1z}I_{2z}\cos^2 a^{(k-1)} + I_{1y}I_{2y}\sin^2 a^{(k-1)} + \right.\right.$$
$$\left.\left.\left(I_{1y}I_{2z} + I_{1z}I_{2y}\right)\sin\ a^{(k-1)}\cos^{(k-1)}\right\}\right]. \tag{5.77}$$

Now the product of operators in Eq.(5.74) can be expressed in a single exponential form by using the BCH formula, once again ignoring the cross

terms. Then $U(\tau)$ reduces to

$$U(\tau) = U_J(\tau)\ P^{(k)}\ \exp\left[-i\frac{J\delta_1^2}{6\omega_2^2}\sum_k t_k\left\{ c_x^{(k)'}\ I_{1x}I_{2x} + c_y^{(k)'} I_{1y}I_{2y} + c_z^{(k)'} I_{1z}I_{2z}\right\}\right] \tag{5.78}$$

where

$$\begin{aligned} c_x^{(k)'} &= c_x^{(k)} \\ c_y^{(k)'} &= c_y^{(k)}\ \cos^2 a(k-1) + c_z^{(k)}\ \sin^2 a(k-1) \\ c_z^{(k)'} &= c_z^{(k)}\ \cos^2 a(k-1) + c_y^{(k)}\ \sin^2 a(k-1) \end{aligned} \tag{5.79}$$

If the sequence is to make a scalar,

$$\sum_k t_k c_x^{(k)'} = \sum_k t_k c_y^{(k)'} = \sum_k t_k c_z^{(k)'} \tag{5.80}$$

must hold. The numerical value of the coefficient for the scalar interaction is given by

$$\bar{c} = \frac{1}{3\tau}\sum_k t_k \left\{ c_x^{(k)'} + c_y^{(k)'} + c_z^{(k)'} \right\} . \tag{5.81}$$

Then Eq.(5.78) becomes

$$U(\tau) = U_J(\tau)\ P^{(k)}\ \exp\left[-i\tau\frac{J\delta_1^{2\bar{c}}}{6\omega_2^2}\ I_1\cdot I_2\right]. \tag{5.82}$$

Eq.(5.82) is the basis to estimate the "natural" offset dependence of the residual Hamiltonian associated with the composite pulses listed in Tables 5.3 and 5.4.

For the simple sequence $(360_x)(360_{\bar{x}})$, the residual Hamiltonian becomes

$$\bar{\mathcal{H}} = J\left[1 - \frac{2J\delta_1^2}{3\ \omega_2^2}\right] I_1\cdot I_2 \tag{5.83}$$

So the splitting is

$$\Delta S = \frac{4}{3}\frac{^J I S^J}{\omega_2^2}\ \delta_1 \qquad (\ \omega_2 \gg \delta_1) \tag{5.84}$$

For more complicated pulses, Eq.(5.82) is calculated using the computer. The result is listed in Table 5.5. It can be shown that all pulses listed give very similar but not identical slopes, confirming the earlier observation. The second order average Hamiltonian calculation predicts that the offset dependence of the splitting is linear:

$$\Delta S \sim \frac{^J I S^J}{\omega_2^2}\ \delta_1, \tag{5.85}$$

so that

$$f(\delta_1) \sim \delta_1 \tag{5.86}$$

as in the case of the simple coherent decoupling. The next term in the Magnus expansion which contains $I_{1\alpha}I_{2\alpha}$ term should be $V^{(4)}$, admixing terms proportional to δ_1^4. Thus in general, $f(\delta)$ can be expressed as a polynomial of odd powers of δ:

Table 5.5 Slopes* of the composite pulses P_1-P_4 and R_1-R_3

P_1	-1.2128733
P_2	-1.1255166
P_3	-1.1414866
P_4	-0.9625433
R_1	-1.2724800
R_2	-1.1944533
R^3	-1.1579233

*The slope is defined as the proportionality constant in Eq.(5.85).

$$f(\delta_1) = \sum_{k=1}^{\infty} a_{2k-1}\delta_1^{2k-1} \quad , (\delta_2 = 0, \text{ on resonance}). \qquad (5.87)$$

V.5. Experimental Details.

The sample used for decoupling experiments consists of a mixture of CH_3I and CH_3CH_2I in acetone-d_6. The acetone-d_6 is used as an internal lock. The protons in the methyl iodide, being equivalent, are used to test the single-spin bandwidths for the decoupling sequences. The linewidth of the carbon-13 of the molecule was used as an internal standard. A Brücker AM-400 with a 10 mm broadband probe was used for this search test under routine operating conditions. The effect of homonuclear coupling was examined by looking at the carbon-13 resonance of the methyl group in the ethyl iodide molecule. To observe fine structure in the carbon-13 spectra due to the homonuclear interaction a 5 mm broadband probe was used and the experiments were carried out on a Brücker AM-500. The AM-500 spectrometer turns out to have much better B_2 homogeneity than the AM-400.

A method for checking the spatial inhomogeneity of the B_2 field has been discussed in the literature.[13] Fig.5.9(a) shows an experimental spectrum of ^{13}C of the methyl iodide on the AM-400 with $180_x180_{\bar{x}}$ pulse sequence irradiating the proton spins in the molecule. A decoupler resonance offset of 200 Hz resulted 11.80 Hz splitting between peaks. With the measured value of J_{CH} = 151 Hz, the B_2 field was calibrated to give 2551.50 Hz. The distorted lineshape in the Figure results from the B_2 inhomogeneity. In Figure 5.9(b) a portion in Fig. 5.9(a) marked by an

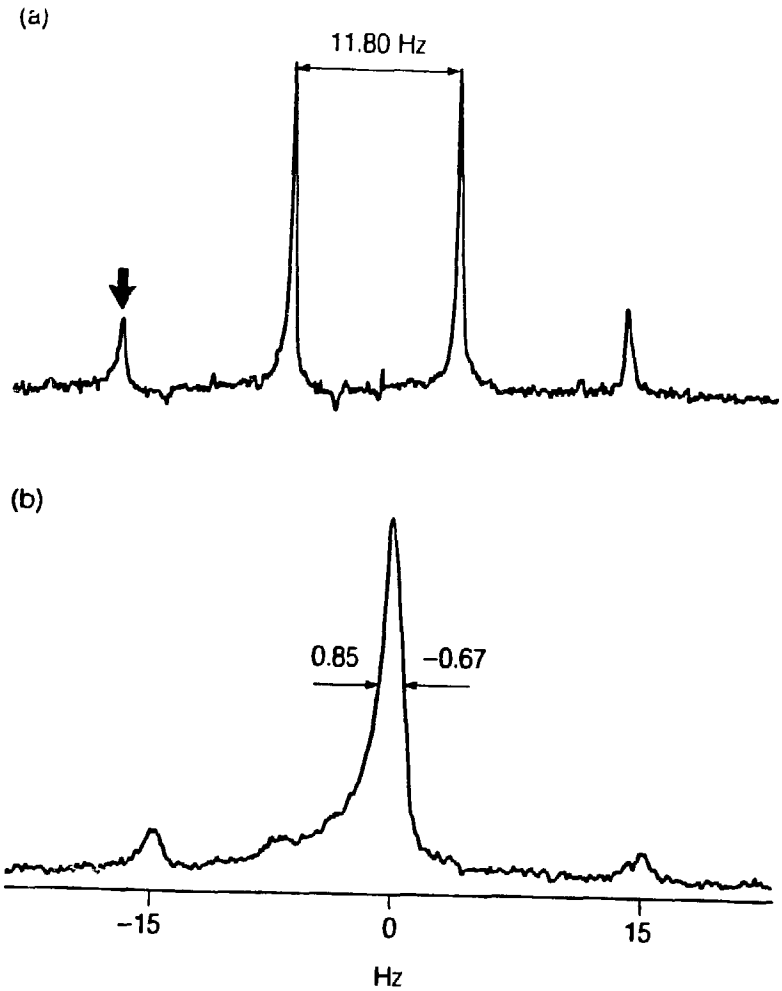

Fig. 5.9 (a) ^{13}C spectrum of the methyl iodide with proton decoupling. The splitting 11.80 Hz between two adjacent peaks results from a 200 Hz decoupler offset. (b) The expanded view of the peak marked by an arrow in (a). The B_2 field distribution at half of the maximum height around the nominal value 2551.50 Hz is 1.52 Hz. The small peaks at ± 15 Hz are spinning sidebands.

arrow is expanded to clearly show the distortion and to facilitate the extraction of the distribution of B_2 field from the line shape. A 1.52 Hz deviation from the nominal value at half of the maximum intensity is found.

For all decoupling experiments, care was taken to ensure a constant temperature around the sample. One reason is that the temperature change may cause a shift of resonance frequencies.[16] The temperature dependence of the C-13 peak of the methyl iodide in the sample is shown in Fig. 5.10. In the Figure, the peak at the far left corresponds to the reference peak with the decoupler level at 2551.50 Hz with the sample at 301^{0}. Then the temperature was suddenly raised to 307^{0} K. The signals were sampled at the interval of 5 minutes. The temperature change not only caused the shift of the resonance frequency, but also broadened the resonance linewidth. It is observed that about 15 minutes are required for the sample to reach the normal state. Another reason to keep the temperature constant is to prevent thermal expansion or contraction of the decoupler coil, which would lead to the fluctuation of the decoupler level. Irradiation of the decoupling field will invariably cause a temperature rise in the sample; a method for keeping the temperature stable is setting the temperature at a level higher than the room temperature by turning up the temperature control knob, so that the preheated N_2 gas may pass around the sample. Another advantage of turning up the temperature is that at higher temperatures the viscosity of the sample tends to decrease, a favorable condition for line narrowing. However, if the temperature is too high, the sample can evaporate. It was found that at 307 ^{0}K the temperature was most stable

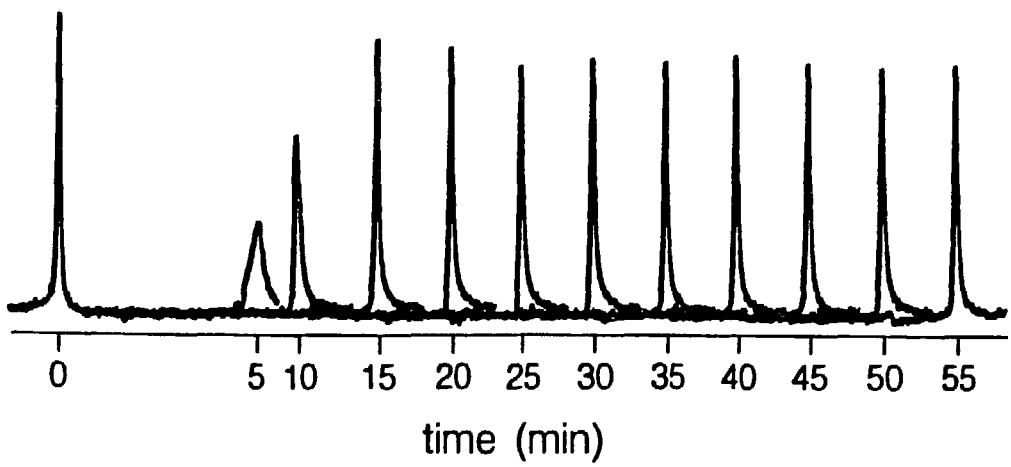

XBL 8711-5956

Fig. 5.10 The temperature dependence of the C-13 peak of the methyl iodide. The peak at the far left is the one before the temperature change, and after the temperature was changed signals were obtained at 5 minute intervals.

while the decoupler was on, and the sample did not evaporate. After the pulsing with decoupling sequences the cw decoupling field was turned on, because otherwise the temperature of the sample dropped under these conditions. Magnet shimming was also done at the same temperature. It was possible to shim the magnet to obtain a ^{13}C linewidth as narrow as 0.12 Hz with on-resonance proton decoupling.

Figure 5.11 shows the experimentally observed resonance of carbon-13 in methyl iodide (J_{CH} = 151 Hz) on the AM-400 as a function of proton decoupler offset for various decoupling sequences. The 10 mm sample tube was spun constantly at 6 Hz, because at high spinning rates the surface of the sample (in the bigger 10 mm tube) may be vortexing, which would introduce more inhomogeneity than what the spinning is intended to eliminate. Most of the time during the experiments the magnet was shimmed so that the on-resonance coherent decoupling gave linewidths within 0.2 Hz. To enhance the sensitivity, a line broadening of 0.5 Hz was added, giving a final linewidth of 0.25 Hz. The same setting was used for all the decoupling sequences. The decoupler level was calibrated using the method suggested by Ernst.[17] The decoupler level at 1480 Hz was used to perform a stringent test for each sequence. The decoupler offset was incremented in 200 Hz steps over the range ±1400 Hz about the exact resonance.

WALTZ-16, which was designed primarily for single-spin cases, gives the biggest bandwidth as expected. Bandwidths for WALTZ-16 and DIPSI-2 agree well with the theoretically predicted bandwidths. However, the bandwidth for the DIPSI-3 is less than the theoretical one. A cause for this discrepancy may be attributed to the low cycling rate of 27.2

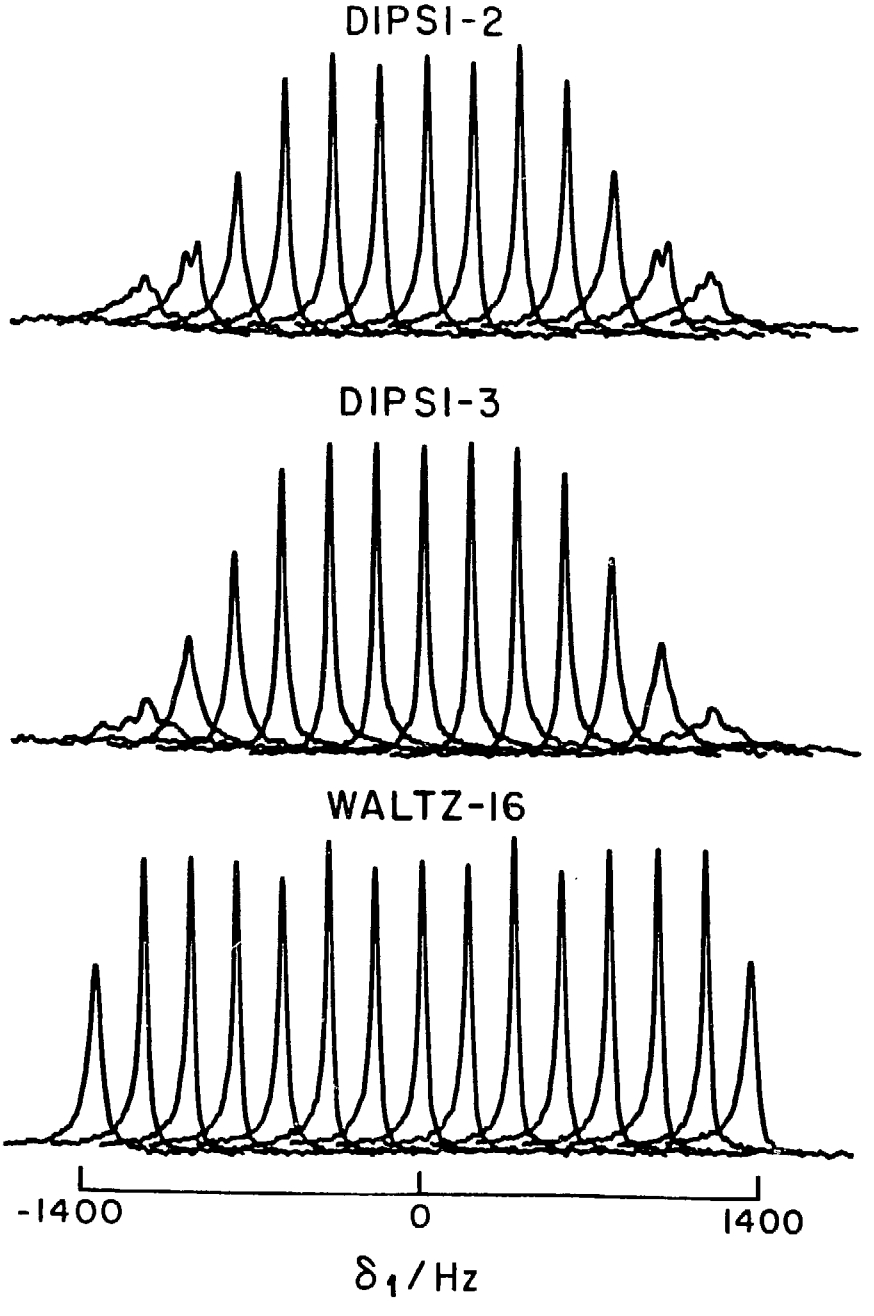

XBL 876-2669

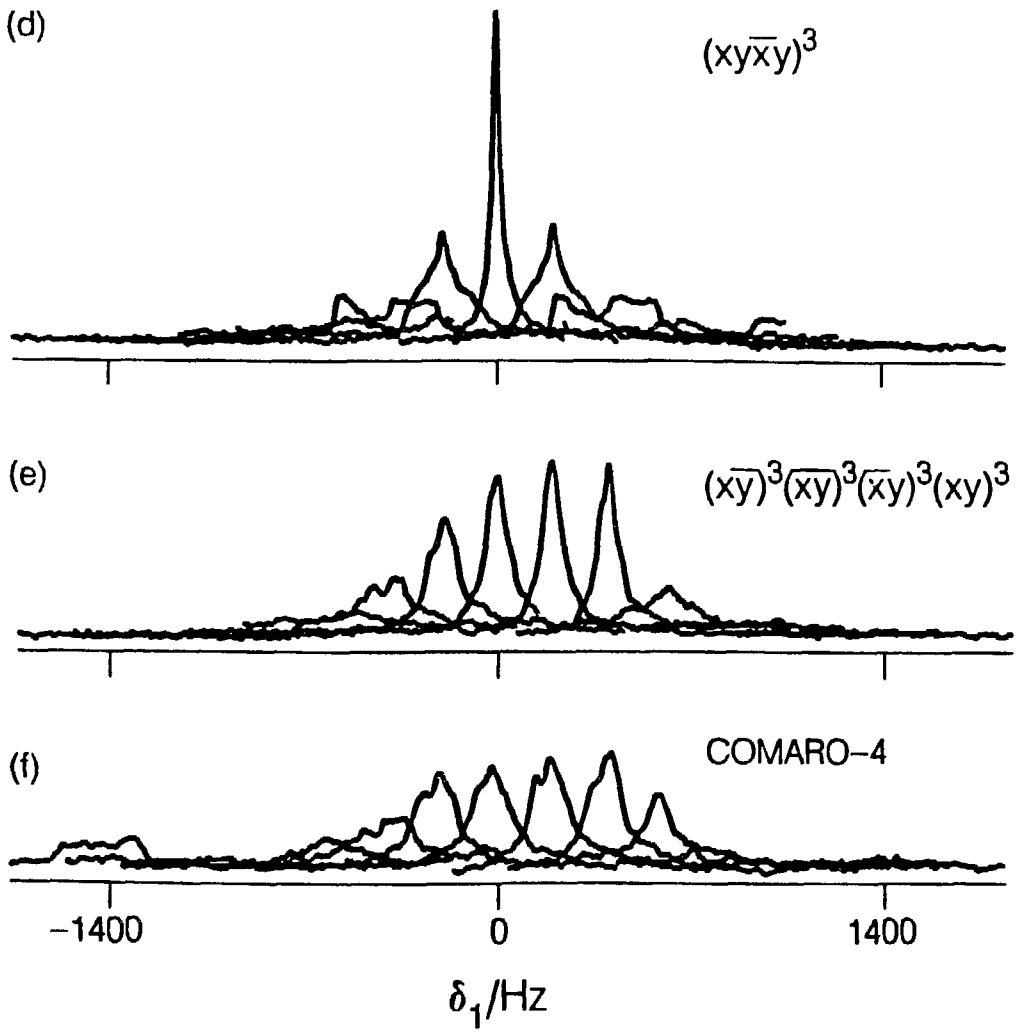

XBL 8711-5964

Figure 5.11 Carbon-13 resonance of methyl iodide showing the offset dependence of DIPSI-2, DIPSI-3,WALTZ-16, a 12 and a 24 pulse sequence, and COMARO. The decoupler offset has been stepped in 200 Hz increments over a ± 1400 Hz range about exact resonance. Sequences (a)-(c) give narrow resonances over their bandwidths, but WALTZ-16 decouples over the largest range. The variations in peak height are attributable to poor ω_2 homogeneity over the sample volume. Sequences (d)-(f) have very limited single-spin bandwidths, and are not suitable for decoupling in liquids

Hz of DIPSI-3. Nonetheless, DIPSI-3 gives more uniform and higher peak heights, an evidence of enhanced tolerance to B_2 inhomogeneity.

Single-spin bandwidths for schemes using 90^0 pulses with orthogonal channels are very small as Figs. 5.11(d)-(f) show. In Figs. 5.11(d) and (e) the seven-pulse composite 90^0 is plugged into the sequences $(x\ y\ \bar{x}\ y)^3$ and $(x\ \bar{y})^3(\bar{x}\ \bar{y})^3(\bar{x}\ y)^3(x\ y)^3$ (Eq.(4.50)). There is a very small improvement in bandwith of the 24-pulse sequence over that of the 12-pulse sequence, except at resonance. In Fig. 5.11(f), the performance of COMARO-4 is shown. The sequence does not even work at resonance. The only difference between COMARO-4 and the above 24-pulse sequence is the composite 90^0 pulses used. It follows that the composite pulse should be used carefully depending on the situation at hand. A similar discussion can be found in the literature in connection to multiple-quantum NMR.[18] Common to all these composite 90^0 pulses are very restricted bandwidths and intolerance to B_2 field inhomogeneity. Consequently, these sequences are not suitable for liquid decoupling experiments.

Now consider the case where there is a homonuclear coupling between two inequivalent protons, as in the case of most molecules of interest. In order to observe the fine structure due to homonuclear coupling the AM-500 spectrometer with a 5 mm probe was used. Once again, a sample consisting of methyl and ethyl iodide in acetone-d_6 is used. Fig. 5.12 shows the resonance peak of a methyl carbon-13 in ethyl iodide. The coupling constant J_{HH} between methyl protons and methylene protons is measured as 7 Hz. The magnet was once again shimmed until the linewidth resulting from coherent decoupling would gave 0.2 Hz.

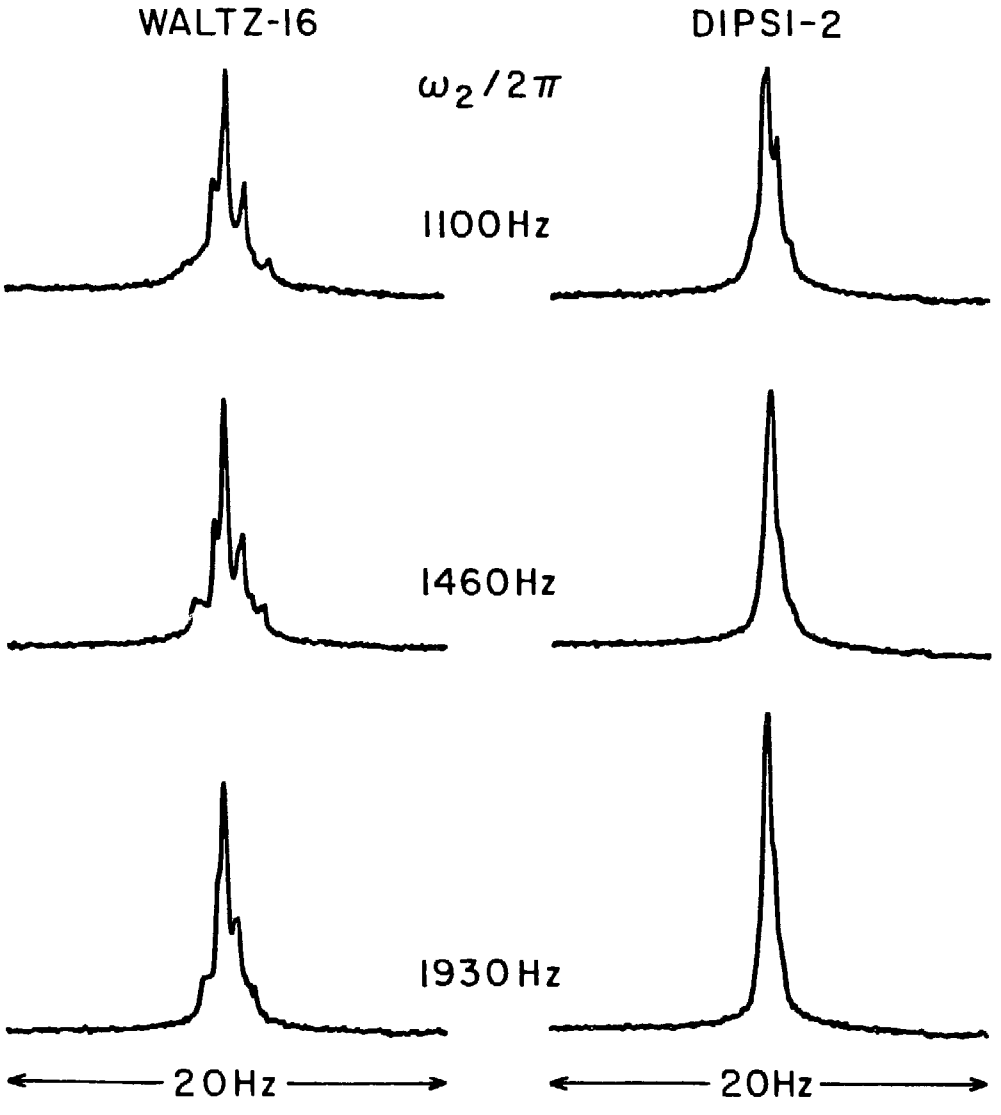

XBL 876-2668

Figure 5.12 Carbon-13 methyl resonance of ethyl iodide using three different values of ω_2. Due to the effect of scalar coupling between the protons, distorted lineshapes are obtained with WALTZ-16 (left-hand spectra). DIPSI-2 gives better results, as shown on the right.

No line broadening was added. Decoupler offset was set on resonance at the methyl protons, then the methylene protons are 690 Hz off resonance. Decoupler levels used were 1100, 1460, and 1930 Hz and sample was spun at 15 Hz, faster than the rate for the 10 mm tube. The number of scans is 64 for each spectrum.

WALTZ-16 at $\omega_2/2\pi$ = 1100 Hz gives a very broad multiplet. As B_2 field increases from 1100 Hz to 1460 Hz to 1930 Hz, a slight narrowing is achieved. However, even at the highest decoupler level there still exists distinct multiplet structure with a linewidth of 1.0 Hz. Furthermore, at all decoupler levels tested the "wing" at the base of each of the peak is seen to persist, but decreases as the B_2 field is increased. The wing is due to the "quartet effect"[19,20] of the C-13 quartet: The outer lines of the methyl quartet experience an effective decoupling three times as large as the inner lines, and they are three times more sensitive to the spatial inhomogeneity of the proton decoupling field B_2.

The right-hand series of spectra are the results of the DIPSI-2 sequence on the same sample with the same experimental settings. The result of DIPSI-2, with its similar cycling rate and complexity, is directly comparable to the result of WALTZ-16. At the decoupler level of 1100 Hz a slight trace of the wing is observed and splitting between the singlet state and the "triplet" state is seen. However, the performance is already better than that of WALTZ-16 at the highest decoupler level. As the B_2 level increased the lineshape approaches more closely the 3:1 pattern with the splitting unresolved, and at 1930 Hz the peak is essentially a singlet. Intensity enhancement of DIPSI-2 over WALTZ-16

trans – Cinnamic Acid Structure

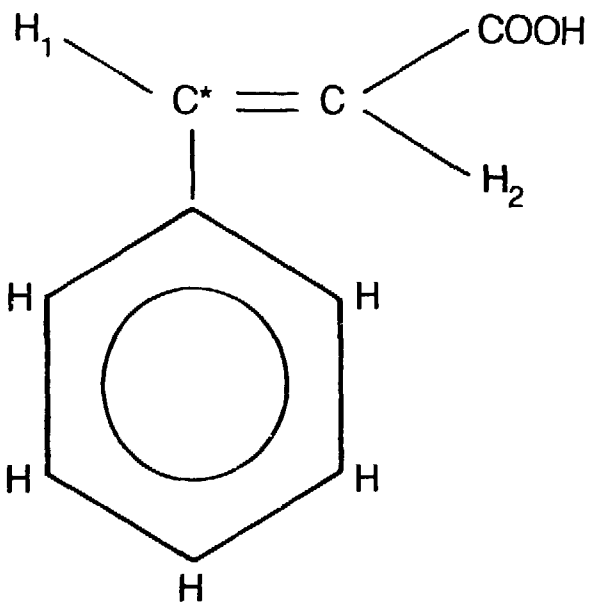

XBL 8711-5961

Fig. 5.13 The trans-cinnamic acid structure. The protons labeled 1 and 2 are a good approximation to an isolated pair of homonuclear-coupled spins, which are also coupled to the carbon-13 labeled with an asterisk.

is about 25 %. The linewidth of the peak obtained with DIPSI-2 at 1930 Hz is about 0.62 Hz as compared with 1 Hz linewidth obtained with WALTZ-16. One reason for the high intensity of the peak resulting from WALTZ-16, despite the breadth of the line may be inferred from Fig. 5.7. It can be seen that although the WALTZ-16 fails to make a scalar for the most part of the bandwidth, two scaling factors belonging to the "triplet" manifold stay quite close together and in fact closer than the overall spread of the three scaling factors for the DIPSI-2 sequence. Thus the two closely located scaling factors for the WALTZ-16 sequence accounts for the sharp center peak in Fig. 5.12. While DIPSI sequences manage to make the overall scalar better, the resultant scaling factors are separated slightly more than the two scaling factors for the WALTZ-16 sequence. In theory, therefore, the intensity of the spectrum for the DIPSI sequence can be enhanced by lengthening the sequence to C_xC_y, of which scaling factors lie much closer to each other as can be seen in Fig. 5.8. However, because sequences employing orthogonal channels are quite sensitive to instrumental imperfections, the possibility of improvement in performance of the lengthened sequence is questionable.

To compare the performances of the sequences in more complicated molecules, trans-cinnamic acid was chosen as the sample. The structure of the trans-cinnamic acid is shown in Fig. 5.13. In the Figure C^* denotes the C-13. Because of the small homonuclear coupling between methylene protons and ring protons, and the proton in the acid part of the molecule, the methylene protons can be considered to form a nearly isolated two-spin system. The coupling constant between the two

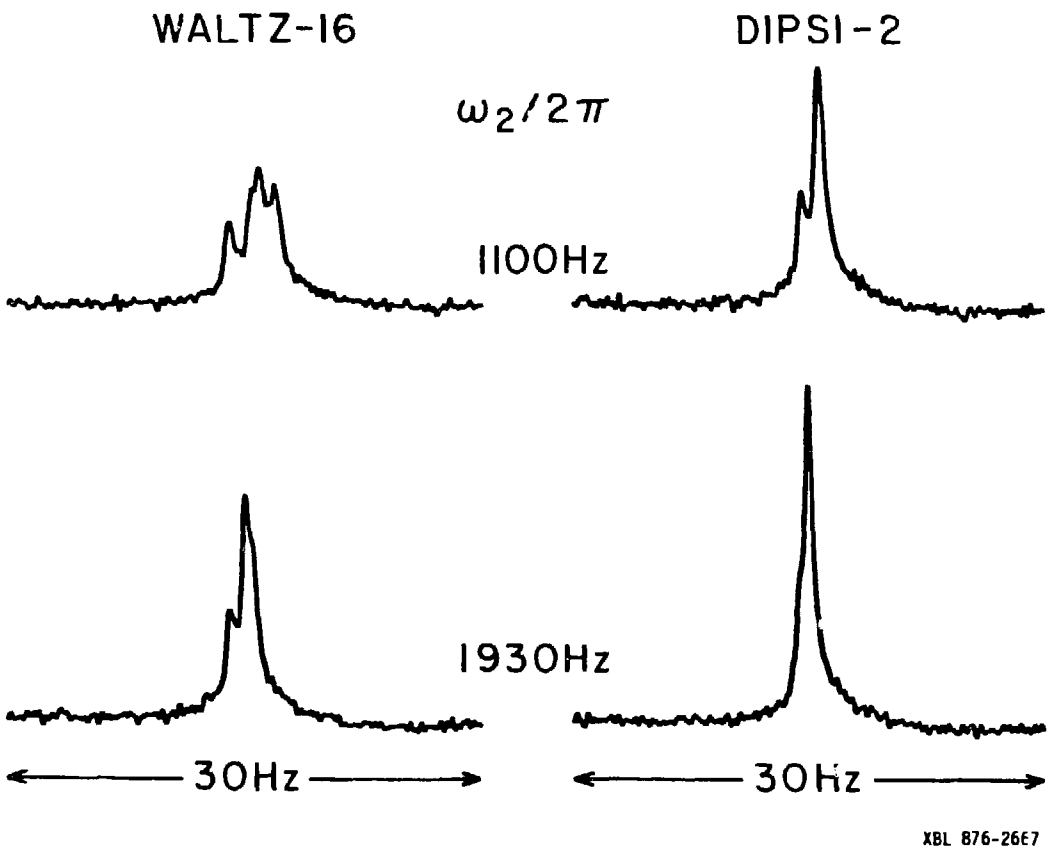

Figure 5.14 Low-field ethylene resonance of trans-cinnamic acid under conditions of broadband decoupling. WALTZ-16 gives broad multiplets, and at the lowest decoupler level all four lines are resolved. DIPSI-2 narrows the resonance considerably, resulting in better sensitivity and resolution.

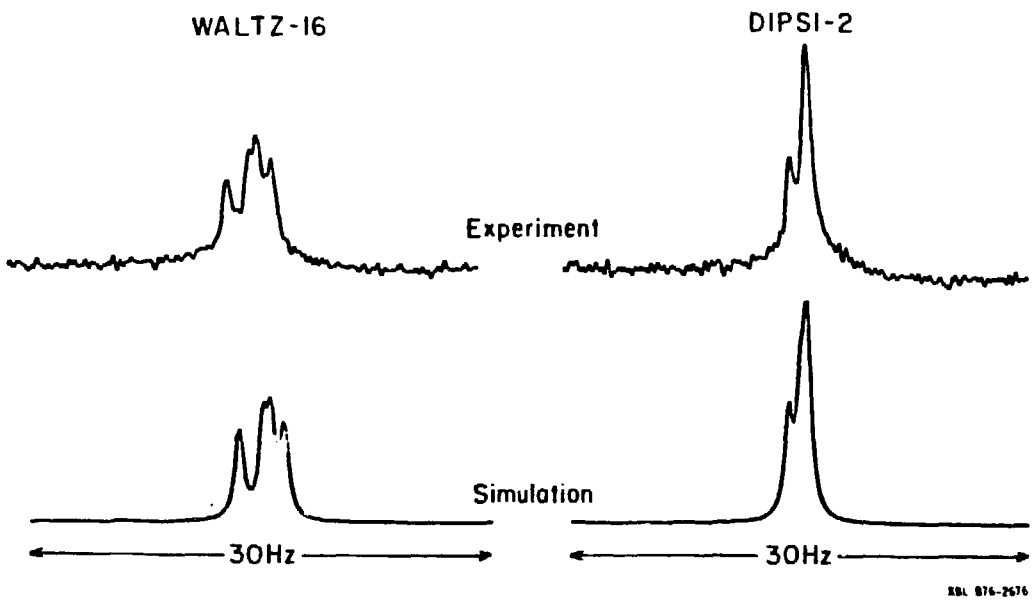

Figure 5.15 Comparison between simulation and experiment for trans-cinnamic acid using WALTZ-16 (left) and DIPSI-2 (right). The parameters used in the simulation are $\omega_2/2\pi$ = 1100 Hz, δ_1 = 0 Hz, δ_2 = -584 Hz, $^1J_{CH}$ = 150 Hz, $^2J_{CH}$ = 0 Hz and J_{HH} = 16 Hz. The simulations assume a completely homogeneous ω_2 field, and have been artificially line broadened to match the linewidths of the experimental spectra. No attempt has been made to fit the experimental spectra.

methylene protons is 16 Hz. The molecule has previously been used to see the effect of homonuclear interaction on the broadband heteronuclear decoupling experiment.[3] Decoupler offset was set at the resonance frequency of the proton (labeled as H_1) directly attached to C^*, and the resonance offset of the indirectly coupled proton (H_2) is -584 Hz. Fig. 5.14 compares the spectra resulting from the decoupling sequences DIPSI-2 and WALTZ-16 at the decoupler levels 1100 Hz and 1930 Hz. At 1100 Hz WALTZ-16 gives a spectrum showing four broad lines, while DIPSI-2 gives a much narrower linewidth and an intensity twice as big. Even at the higher decoupler level of 1930 Hz WALTZ-16 still does not give a 3:1 pattern comparable to those of the spectrum obtained with DIPSI-2 at the lowest decoupler level of 1100 Hz. By contrast, DIPSI-2 results in almost a singlet at 1930 Hz with an intensity 50 % higher than that of the corresponding spectrum resulting from WALTZ-16. Fig. 5.15 shows the good agreement between the simulated and the experimental spectra for WALTZ-16 and DIPSI-2 at 1100 Hz.

References

1. J. S. Waugh, J. Mag. Res. 50, 30 (1982).

2. D. Suter, K. V. Shenker, and A. Pines, J. Mag. Res. 73, 90 (1987).

3. A. J. Shaka, P. B. Barker, and R. Freeman, J. Mag. Res. 71, 520 (1987).

4. U. Haeberlen, High Resolution NMR in Solids, Selective Averaging, (Academic Press, New York, 1976).

5. For a review of various perturbation theories see, Perturbation Theory and Its Applications in Quantum Mechanics, C. H. Wilcox ed., (John Wiley & Sons, Inc., New York, 1966).

6.(a) B. M. Fung, D. S. L. Mui, I. R. Bonnell, and E. L. Enwall, J. Mag. Res. 58, 254 (1984). (b) D. S. Mui, B. M. Fung, I. R. Bonnell, and E. L. Enwall, J. Mag. Res. 64, 124 (1985).

7. J. S. Waugh, J. Mag. Res. 49, 517 (1982).

8. K. V. Shenker, D. Suter, and A. Pines, J. Mag. Res. 73, 99 (1987).

9. R. Tycko, Ph.D. thesis, University of California, Berkeley, (1984).

10. A. J. Shaka, and J. Keeler, Prog. in NMR Spect. 19, 47 (1987).

11.(a) A. J. Shaka and A.Pines, J. Mag. Res. 71, 495 (1987). (b) M. H. Levitt and R. Freeman, J. Mag. Res. 43, 502 (1981). (c) M. H. Levitt, R Freeman, and T. Frankiel, J. Mag. Res. 47, 328 (1982). (d) ibid, 50, 157 (1983). (e) J. W. M. Jacobs, J. W. M. Van Os, W. S. Veeman, J. Mag. Res. 51, 56 (1983). (f) A. J. Shaka, T. Frenkiel, and R. Freeman, J. Mag. Res. 52, 159 (1983). (g) R. Freeman, T. Frenkiel, and M. H. Levitt, J. Mag. Res. 50, 345 (1982). (h) A. J. Shaka, J. Keeler, T. Frenkiel, and R. Freeman, J. Mag. Res. 52, 335

(1983). (i) B. M. Fung, J. Mag. Res. 59, 275 (1984).

12. R. Tycko, H. M. Cho, E. Schneider, and A. Pines, J. Mag. Res. 61, 90 (1985).

13. A. J. Shaka, J. Keeler, and R. Freaman, J. Mag. Res. 53, 313 (1983).

14. F. Bloch, Phys. Rev. 93, 944 (1954).

15. F. Bloch, Physics Today 7, 30 (1954).

16. A. L. VanGeet, Anal. Chem. 40, 2227 (1968); ibid 42, 679 (1970); D. S. Raiford, C. L. Fisk, and E. D. Becker, Anal. Chem. 51, 2050 (1979).

17. R. R. Ernst, J. Chem. Phys. 45, 3845 (1966).

18. S. Wimperis and G. Bodenhausen, J. Mag. Res. 71, 355 (1987).

19. W. A. Anderson and R. Freeman, J. Chem. Phys. 37, 85 (1962).

20. R. Freeman, J. B. Grutzner, G. A. Morris, and D. L. Turner, J. Am. Chem. Soc. 100, 5637 (1978).

CHAPTER VI. The Modulation of the Spatial Coordinates of the Sample

VI.1. Introduction

As discussed in chapter I, the Hamiltonian for a system of nuclear spins is composed of coordinate and spin parts. If there were no external magneic field present, the Hamiltonian retains the full isotropic symmetry. In other words, the Hamiltonian becomes a scalar, and consequently there is no preferred orientation. The use of no magnetic field has been devised in the early days of NMR[1] and the recently introduced method of time-domain zero-field NMR[2] has been quite successful in structure determination in randomly distributed spins in solids. Without the external magnetic field however, valuable information is lost; namely the chemical shift cannot be recovered with the zero-field NMR technique. Thus the vast majority of NMR experiments are performed in high magnetic fields. Furthermore, the trend is to use higher magnetic fields to achieve better resolution.

In the presence of the high magnetic field only the terms which commute with the Zeeman term survive, and other terms are "truncated". Unfortunately, this makes the Hamiltonian assume cylindrical symmetry, and preferred orientation of nuclear interactions sets in. In liquids, the orientation dependence is averaged away naturally by molecular motions faster than the Larmor frequency. Nuclear spins in solids, in contrast, are locked in a rigid lattice and do not enjoy this benefit.

Hence the NMR spectra of powdered solids exhibit broad, and in many instances featureless, signatures reflecting the effects of the anisotropies of the spin interactions.

One way to overcome line broadening is the application of multiple pulses,[3] and this is one of the main goals of chapter III. If transformed into an appropriate frame, the spins acquire time dependence. Because of technological limitations on the amplitude and phases of pulses, it is futile to imitate nature and apply the pulses randomly. Thus most pulsed NMR techniques use carefully designed sequences of pulses, with the exception of stochastic excitation.[4] (Recently, Tycko et.al[5] introduced highly efficient iterative schemes, in which at high iterations the pulse sequences behave stochastically. However, this method is different than the random modulations such as "white noise".) Unfortunately, the chemical shift anisotropy cannot be removed with the multiple-pulse method without removing the isotropic chemical shift at the same time.

On the other hand, because of the duality of the spin Hamiltonian it is equally possible to achieve line narrowing by mechanical modulation on the spatial coordinates. The rotation of samples was introduced almost three decades ago[6-10] and has been used ever since. Provided that the rotation speed exceeds the coupling constant of the spin interaction under consideration, the rotation of the sample "truncates" the coordinate part of the Hamiltonian along the spinner axis much like the magnetic field truncates the spin part. In particular, if the spinner axis is tilted by the "magic" angle, $\theta_m = 54.7^0$, the truncated value of the (first order) anisotropy is equal to

zero. The magic angle spinning (MAS) method[11] has been the major method for obtaining isotropic chemical shifts. However, for abundant spins-1/2 or for nuclei with spin angular momenta greater than 1/2, the rotational speed has to exceed dipole or quadrupole coupling constants. Considering that currently the highest spinning speed rarely exceeds 20 kHz, the application of MAS to systems other than dilute spins-1/2 seems to be unfeasible.

A method to get around this problem is the use of multiple pulses to remove dipolar (or possibly quadrupolar) interactions while using MAS to remove the chemical shift anisotropy (CSA). The method was suggested by Haeberlen and Waugh[12] and experimentally implemented by Gerstein et.al.[13] Unfortunately, the application of multiple pulses scales the chemical shift range, and thus degrades the resolution. The use of higher magnetic fields may be a solution. However, this again is limited by the technically achievable spinning speed.

Recently, Maciel et. al.[14] showed how to recover the isotropic chemical shift without spinning the sample. Instead, the sample is discretely hopped by 120^0 around an axis tilted by the magic angle from the laboratory z axis along with appropriate sequences of pulses to initiate and terminate the evolution of the density operator. This obviates the necessity for rapid spinning, and thus constitutes a significant development in high resolution NMR of powdered solids. However, the application of the hopping technique is still confined to the case of dilute spins-1/2 such as ^{13}C. The reason is that for abundant spins-1/2 or for spins with angular momenta greater than 1/2, dipole or quadrupole interactions have to be considered. The hopping

technique may be generalized to treat these problems. However, the evolution under these interactions as well as the chemical shift, can no longer be regarded as rotations. Thus it is very difficult to express the resulting density matrix in terms of functions with closed form. In fact for spins $I \geq 3/2$ the basis operators, $(2I + 1)^2$ in number, have yet to be developed.

For these cases a solution may be once again the application of multiple pulses. But the scaling of the chemical shift range is unavoidable. Furthermore, because the resulting quantization axis would be different from z axis, the evolution of the density matrix under this effective Hamiltonian would be very complicated. Consequently, the design of schemes for removing CSA would be quite difficult. Another setback of this technique is that even for the removal of CSA four experiments are required for quadrature detection. The requirement stems from the inherent method of "storing" only half of the information about the evolution as a Zeeman order. In addition, the hopping time t_h must be $T_2 < t_h < T_1$, so that the unwanted information may dephase completely. Although the condition is easily met, half of the information is wasted (which is recovered only after doing three other experiments) and decay of the signal occurs because of the spin-lattice relaxation during t_h. This may be particularly serious for a system for which T_1 is not substantially longer than T_2. A superior approach then should be one which does not have the lower limit on t_h.

In this chapter, the magic-angle hopping technique will be generalized to be applicable to abundant spins-1/2 and, in principle, spins $I \geq 1$ as well as dilute spins-1/2. Basically, the extension

consists of the application of multiple pulses at appropriate times in addition to hopping of the sample. Also it will be shown that with this approach only one experiment is necessary for full quadrature detection. Furthermore, if more than one angle is allowed to be used, other anisotropies such as the second order quadrupole effects can also be removed.

VI.2. The Hamiltonian

As dicussed in Chapter I, in the laboratory frame (LAB) a general form of the internal spin Hamiltonian consisting of chemical shifts (CS), dipole (D), and quadrupole (Q) terms may be written as

$$\mathcal{H} = \sum_{\lambda}\sum_{\ell=0}^{2}\sum_{m=-\ell}^{\ell}(-1)^{m} R^{\lambda}_{\ell-m} T^{\lambda}_{\ell m} \qquad (\lambda = CS, D, Q) \tag{6.1}$$

where the sphrerical tensors $\overset{\leftrightarrow}{R}$ and $\overset{\leftrightarrow}{T}$ denote spatial and spin parts respectively. $T_{\ell m} = 0$ unless $\ell = 2$ for $\lambda = D, Q$. For $\lambda = CS$, the term corresponding to $\ell = 1$ (the antisymmetry part) does not contribute to the spectra to first order and thus will be ignored. Then Eq.(6.1) may be rewritten as

$$\begin{aligned}\mathcal{H} &= R^{CS}_{00} T^{CS}_{00} + \sum_{\lambda}\sum_{m=-2}^{2}(-1)^{m} R^{\lambda}_{2-m} T^{\lambda}_{2m} \\ &= R^{CS}_{00} T^{CS}_{00} + \mathcal{H}_{1}.\end{aligned} \tag{6.2}$$

Since $\mathcal{H}_1$ has a common structure for all λ, it suffices to consider a representative case and suppress the summation over λ. R_{2-m} in $\mathcal{H}_1$ can be expressed in terms of tensors in the principal axis system (PAS) as is given by Eq.(1.17). Thus

$$\mathcal{H}_1 = \sum_m (-1)^m \left(\sum_{m'} \mathcal{D}^{(2)}_{-m-m'}(\Omega') \rho_{2-m'} \right) T_{2m} . \tag{6.3}$$

Once again $\mathcal{D}^2_{mm'}$ denotes the Wigner rotation matrix connecting the LAB and PAS. Now consider a tilted space frame, related to the LAB by $\mathcal{D}^2_{mM}(\Omega)$. With the notation $\mathcal{D}^2_{ab}(\Omega) = \mathcal{D}_{ab}$ and $\mathcal{D}^2_{ab}(\Omega') = \mathcal{D}'_{ab}$, Eq.(6.3) in the tilted frame becomes

$$\mathcal{H}_1 = \omega_\lambda \sum_m (-1)^m T_{2m} \sum_M \mathcal{D}_{-m-M} \left\{ \sqrt{\frac{2}{3}} \mathcal{D}'_{-M0} + \frac{\eta}{3} \left(\mathcal{D}'_{-M2} + \mathcal{D}'_{-M-2} \right) \right\} . \tag{6.4}$$

In NMR, measurements are usually made in the rotating (spin) frame, which is defined by the transformation

$$R = \exp\left(i\omega_0 t \, I_z \right) . \tag{6.5}$$

Then from Eq.(1.12) the Hamiltonian becomes (henceforth the subscript "1" will be dropped)

$$\mathcal{H} = \sum_m (-1)^m R_{2-m} \sum_{m'} T_{2m'} \mathcal{D}^{(2)}_{mm'} \left(\psi, \theta, \phi(t) \right) . \tag{6.6}$$

Because of the rotational symmetry around the z axis ψ can be set to

zero. $\theta = 0$ because the axis of the rotation is along the z direction. Then

$$\mathcal{D}^{(2)}_{mm'}\left(0,0,\phi(t)\right) = \delta_{mm'} e^{im'\omega_0 t} , \tag{6.7}$$

where $\phi(t) = \omega_0 t$ is used. The Hamiltonian thus becomes

$$\mathcal{H}(t) = \omega_\lambda \sum_m (-1)^m T_{2m} \sum_M \mathcal{D}^{(2)}_{-m-M} \rho'_{2-M} e^{im\omega_0 t} . \tag{6.8}$$

where

$$\rho'_{2-M} = \sqrt{\frac{2}{3}}\, \mathcal{D}'_{-M0} + \frac{\eta}{3}\left(\mathcal{D}'_{-M2} + \mathcal{D}'_{-M-2}\right). \tag{6.9}$$

$\mathcal{H}(t)$ vanishes over a cycle $\omega_0 \tau = 2\pi$ unless $m = 0$. Thus

$$\bar{\mathcal{H}}^{(0)} = \omega_\lambda T_{20} \sum_M \mathcal{D}_{0-M} \rho'_{2-M} , \tag{6.10}$$

and this corresponds to the usual truncation.

VI.3. The Removal of the First Order Anisotropies

Magic angle experiments

It is well known that T_{20} in dipole and quadrupole Hamiltonians can be removed by either continuous coherent averaging with the

radiofrequency field tilted by the magic angle as in the Lee-Goldburg experiment[15] or the discrete isotropic average resulting from multiple-pulse sequences such as the WHH-4 sequence

$$T_{20}^{x} + T_{20}^{y} + T_{20}^{z} = 0, \tag{6.11}$$

where

$$T_{20}^{\alpha} = \frac{1}{\sqrt{6}}(3I_{\alpha}I_{\alpha}' - \vec{I}\cdot\vec{I}'). \quad \alpha = x, y, z \tag{6.12}$$

Thus three configurations such as x, y, and z are needed. In view of the analogy discussed in Chapter I, it is clear that the same continuous averaging around the magic angle and the three configurations can also be used to remove the spatial part of the spin Hamiltonian. Note that the configurations can be reached by 120^{0} rotations around the (111) axis. The removal of the spatial part will now be shown by detailed calculation. The principal equation to be used is Eq.(6.10), where the Wigner rotation matrix $\mathcal{D}_{0\text{-}M}$ is a function of two angles β and γ, namely $\Omega = (0, \beta, \gamma)$. β is the tilt angle of the symmetry axis from the LAB z axis, and γ is the azimuthal angle of the symmetry axis.

(i) Sample Spinning Experiments

These correspond to the continuous coherent averaging method. In this case Eq.(6.10) becomes

$$\mathcal{H}(t) = \omega_\lambda \, T_{20} \sum_M \mathcal{D}_{0-M} \, \rho'_{2-M} \, e^{-iM\omega_r t}, \tag{6.13}$$

of which average vanishes over the cycle $\omega_r \tau = 2\pi$ unless $M = 0$. Thus once again $\mathcal{H}$ is truncated along the direction of the spinner axis:

$$\mathcal{H} = \omega_\lambda \, T_{20} \, \mathcal{D}_{00} \, \rho'_{20}. \tag{6.14}$$

Note that

$$\mathcal{D}_{00}(\Omega) = \mathcal{P}_2(\cos\beta) = 1/2 \, (3\cos^2\beta - 1). \tag{6.15}$$

Thence $\mathcal{H} = 0$ if $\beta = \theta_m$ (the magic angle), and this is the origin of the magic angle spinning (MAS) experiments.

It is interesting to note that in principle there is an infinite number of angles β_k which make $\mathcal{P}_2(\cos\beta)$ vanish in the sense that

$$\sum_{k=1}^{N} \mathcal{P}_2(\cos \beta_k) = 0. \tag{6.16}$$

N is the number of degrees of freedom for choosing angles. For N = 1 there is only one angle which satisfies the above equation and this is the magic angle. For n = 2 there is an infinite number of sets of such angles. It will be shown in a later section that the increased number of degrees of freedom opens up possibilities of doing unusual experiments.

As discussed in the introduction to this chapter, it is difficult to achieve spinning speeds greater than the dipole (and of course the quadrupole) interactions. Thus, the MAS is mostly confined to dilute spins-1/2 such as ^{13}C, whose spectra is broadened predominantly by the CSA. Foe dipole coupled spins-1/2, the dipole interactions can be removed by the application of multiple pulses, while the CSA is removed by the MAS. This method is termed "CRAMPS" (the Combined Rotational And Multiple Pulse Spectroscopy)[13,16] CRAMPS is currently the most widely used method for extracting the isotropic chemical shifts of the abundant spins-1/2. However, the disadvantage of the method is, as pointed out earlier, that the the chemical shift range is scaled by the multiple pulses applied, degrading the resolution. This may be problematical for a system of spins with a wide range of closely spaced chemical shifts. The application of higher static magnetic field to separate these resonance lines are hampered by the limitation of the spinning speed available.

(ii) Sample Hopping Experiments

The spatial analog of the coherent averaging with discrete piecewise-constant configurations is the sample hopping experiment. The solid angles corresponding to the configurations x, y, and z are $\Omega_1 = (0, 0, 0)$, $\Omega_2 = (0, \pi/2, 0)$, and $\Omega_3 = (0, \pi/2, \pi/2)$. For simplicity the following notation will be used:

$$A(\Omega) = \sum_M D_{0-M}\left\{\sqrt{\frac{2}{3}}\ D'_{-M0} + \frac{\eta}{3}\left(D'_{-M2} + D'_{-M-2}\right)\right\} - \sum_M D_{0-M}\ \rho'_{2-M} \quad (6.17)$$

At those three solid angles $A(\Omega)$ becomes

$$A(\Omega_1) = \rho'_{20}$$

$$A(\Omega_2) = -\frac{1}{2}\rho'_{20} + \sqrt{\frac{3}{8}}\left(\rho'_{22} + \rho'_{2-2}\right)$$

$$A(\Omega_3) = -\frac{1}{2}\rho'_{20} - \sqrt{\frac{3}{8}}\left(\rho'_{22} + \rho'_{2-2}\right) \quad (6.18)$$

It follows that

$$\sum_{k=1}^{3} A(\Omega_k) = 0, \quad (6.19)$$

showing that indeed the three configurations remove all (first order) anisotropies. It can easily be proved that if the sample is not spun, the first order anisotropies cannot be removed with angles fewer than three. Thus the minimum number of degrees of freedom for this case is three.

Implementation

A question arises immediately: How can one implement Eq.(6.19) experimentally? Of course, Eq.(6.19) cannot be satisfied in the sense of time-averaging, because the time scale for manipulation of the

spatial coordinates is much bigger than that of the spin coordinates. For dilute spins-1/2 the experimental implementation of Eq.(6.19) can be done with the hopping technique developed by Maciel et. al.[14] : Consider the Hamiltonian for spins-1/2 in powdered solids consisting of the Zeeman($\mathcal{H}_z$) and the chemical shift($\mathcal{H}_{cs}$) terms. For simplicity only a representative crystallite will be considered. However, the result holds for a system with an arbitrary number of crystallites as well.

The Hamiltonian in the rotating spin, tilted space frame may be written as

$$\mathcal{H} = \omega_0 \sigma_{iso} I_z + \omega_0 \sum_M D_{0-M}(\Omega)\ \rho_{2-M}(\Omega') I_z \tag{6.20}$$

where the index M runs from -2 to 2, and σ_{iso} is the isotropic shielding tensor.

First position the sample axis at Ω_1 and apply a $\pi/2$ pulse along the (-y) direction. Then the initial density operator is allowed to evolve under the Hamiltonian corresponding to the angle for the duration of $\tau/3$. The density operator at $\tau = \tau/3$ is thus

$$\begin{aligned} \rho(\tfrac{\tau}{3}) &= \exp\left(-i\tfrac{\tau}{3}\Phi_1 I_z\right)\ I_x\ \exp\left(i\tfrac{\tau}{3}\Phi_1 I_z\right) \\ &= I_x \cos\tfrac{\tau}{3}\Phi_1 + I_y \sin\tfrac{\tau}{3}\Phi_1, \end{aligned} \tag{6.21}$$

where

$$\Phi_1 = \omega_0 \sigma_{iso} + \omega_0 \sum_M D_{0-M}(\Omega_1)\ \rho_{2-M}(\Omega'). \tag{6.22}$$

The x component is stored by applying a second $\pi/2$ pulse along the y axis and the sample axis is hopped to the next angle Ω_2. A $\pi/2$ pulse along (-y) allows the magnetization to evolve, and after another period $\tau/3$ the density operator becomes

$$\rho(t) = \exp\left(-i\frac{\tau}{3}\Phi_2 I_z\right)\ I_x \cos\Phi_1\ \frac{\tau}{3}\ \exp\left(i\frac{\tau}{3}\Phi_2 I_z\right). \tag{6.23}$$

The procedure is continued until the angle dependence of the magnetization becomes

$$f_1 = \exp\left(-i\frac{\tau}{3}\phi_3\right)\ \cos\frac{\tau}{3}\phi_2\ \cos\frac{\tau}{3}\phi_1. \tag{6.24}$$

Three other experiments to store various components result

$$\begin{aligned} f_2 &= -i\exp\left(-i\tfrac{\tau}{3}\phi_3\right)\ \cos\tfrac{\tau}{3}\phi_2\ \sin\tfrac{\tau}{3}\phi_1 \\ f_3 &= -i\exp\left(-i\tfrac{\tau}{3}\phi_3\right)\ \sin\tfrac{\tau}{3}\phi_2\ \cos\tfrac{\tau}{3}\phi_1 \\ f_4 &= -\exp\left(-i\tfrac{\tau}{3}\phi_3\right)\ \sin\tfrac{\tau}{3}\phi_2\ \sin\tfrac{\tau}{3}\phi_1. \end{aligned} \tag{6.25}$$

It follows that

$$\sum_{k=1}^{4} f_k = \exp\left(-i\frac{\tau}{3}(\Phi_1 + \Phi_2 + \Phi_3)\right)$$

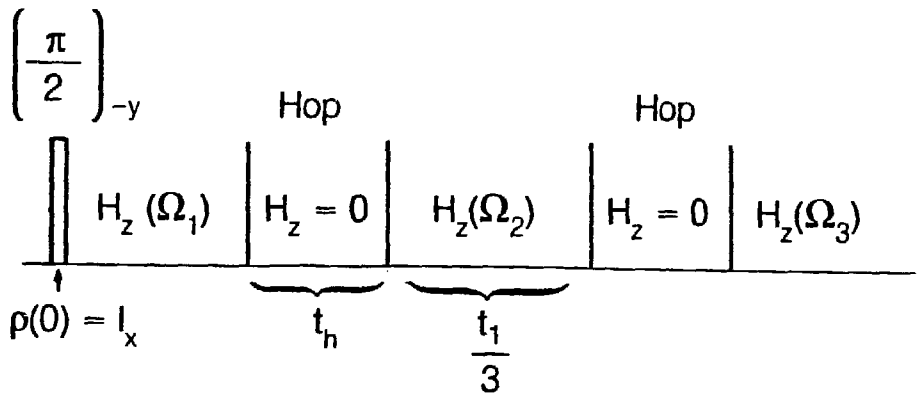

XBL 8711-5970

Fig. 6.1(a) Schematic diagram of the experiment for removal of the first order anisotropies. The initial density operator created by a 90^0 pulse along -y axis evolves under $\mathcal{H}_z(\Omega_k)$. See text for the definition of the Hamiltonian. The Hamiltonian is made to vanish during t_h, the individual hopping period. Overall evolution time is t_1.

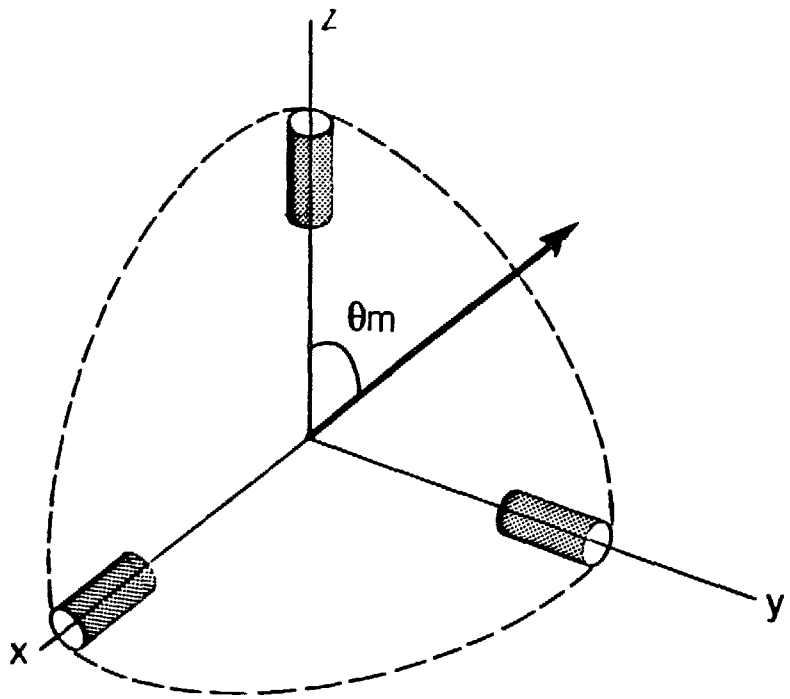

XBL 8711-5953

Fig. 6.1(b) The three orientations of the sample Ω_k to be used for the experiment given in Fig. 6.1(a). The sample is hopped about an axis tilted by the magic angle, θ_m with respect to the z axis.

Here

$$\Phi_1 + \Phi_2 + \Phi_3 = 3\omega_0\sigma_{iso} \tag{6.26}$$

Thus the isotropic chemical shift is recovered. However, a disadvantage of the method is that four experiments are required for quadrature detection. A superior method is to recover the isotropic chemical shift in one experiment. The key is not to discard half of the information while storing the remainder. To achieve this, consider the experiment shown in Fig.6.1.

The evolution operator for the scheme at time $t = t_1 + 2t_h$ is

$$U(t) = \exp\left[-i\mathcal{H}_z(\Omega_3)\frac{t_1}{3}\right] \exp\left[-i\mathcal{H}_z(\Omega_2)\frac{t_1}{3}\right] \exp\left[-i\mathcal{H}_z(\Omega_1)\frac{t_1}{3}\right]$$

$$= \exp\left[-i\left\{\mathcal{H}_z(\Omega_1) + \mathcal{H}_z(\Omega_2) + \mathcal{H}_z(\Omega_3)\right\}\frac{t_1}{3}\right]. \tag{6.28}$$

where $\mathcal{H}_z(\Omega_k)$ denotes the high field truncated Hamiltonian with the sample oriented along Ω_k. The second equality in Eq.(6.28) follows from the fact that

$$\left[\mathcal{H}_z(\Omega_i)\ ,\ \mathcal{H}_z(\Omega_j)\right] = 0, \qquad i,j = 1,2,3 \tag{6.29}$$

From Eqs.(6.2), (6.20) and (6.28) it follows that

$$U(t) = \exp\left(-it_1 R_{00}^{CS}\ T_{00}^{CS}\right)$$

$$= \exp\left(-it_1\omega_0\textstyle\sum_k \sigma_{iso,k}\ I_{kz}\right) \qquad (6.30)$$

where $\sigma_{iso,k}$ is the isotropic shilding tensor for the kth spin. Consequently the spectrum should show sharp lines at their respective chemical shift values.

The procedure also holds when there are dipole and/or quadrupole interactions present as well as the chemical shift term in the Hamiltonian. If the hopping procedure of Maciel et. al. is followed, it is extremely difficult to express the density matrix evolved under the Hamiltonian. Furthermore, for spins $I \geq 3/2$, it is not even known whether one can write down the density operator at all, let alone decipher the information and design schemes to remove unwanted terms. A straightforward method analogous to CRAMPS is to apply multiple pulses to remove the dipole (and quadrupole interactions), while the hopping technique is used to remove the CSA. However, once again the chemical shift range would be scaled and the resulting quantization axis would be different from I_z, which makes the design of the schemes very difficult. Thus the present method may be the most versatile one. The crucial point is to make $\mathcal{H}_z = 0$ during the hopping periods, to which the next section is devoted.

VI.4. The Design of Dead Time for Evolution

The general approach adopted here to make $U(t_h) = 1$ during hopping

periods is the Average Hamiltonian Theory (AHT). Of course other approaches such as iterative schemes can be incorporated.

First consider a Hamiltonian containing only the chemical shift term. As usual, the density operator starts evolution by a $\pi/2$ pulse along the -y direction. Instead of terminating the evolution by another $\pi/2$ pulse, apply 2π pulses continuously while the sample is hopped. Then the density operator at $t = \tau/3 + t_h$ becomes

$$\rho(\tfrac{\tau}{3} + t_h) = \mathcal{T}\exp\left[-i\int_0^{t_h} dt' \left\{\Phi(\tfrac{\tau}{3} + t')I_z + \omega_1 I_y\right\}\right] \exp\left(-i\tfrac{\tau}{3}\Phi_1 I_z\right)\ I_x$$

$$\times\ \exp\left(i\tfrac{\tau}{3}\Phi_1 I_z\right)\ \mathcal{T}^{-1}\exp\left[i\int_0^{t_h} dt' \left\{\Phi(\tfrac{\tau}{3} + t')I_z + \omega_1 I_y\right\}\right]$$

$$= \exp\left(-it_h\omega_1 I_y\right)\ \mathcal{T}\exp\left[-i\int_0^{t_h} dt \int_0^{t_h} dt' \left\{\Phi(\tfrac{\tau}{3} + t')\ \tilde{I}_z(t)\right\}\right]\ U_1 I_x$$

$$\times\ U_1^{\dagger}\ \mathcal{T}^{-1}\exp\left[i\int_0^{t_h} dt \int_0^{t_h} dt' \left\{\Phi(\tfrac{\tau}{3} + t')\ \tilde{I}_z(t)\right\}\right]\exp\left(it_h\omega_1 I_y\right) \qquad (6.31)$$

Here $\mathcal{T}$ is the time-ordering operator,

$$U_1 = \exp\left(-i\Phi_1 \tau I_z/3\right), \qquad (6.32)$$

$$\Phi(t) = \omega_0\sigma_{iso} + \omega_0 \sum_M \mathcal{D}_{0,-M}\left(\Omega(t)\right)\ \rho_{2,-M}(\Omega'), \qquad (6.33)$$

with $\beta(0) = \beta_1$, and $\beta(t_h) = \beta_2$. Finally,

$$\tilde{I}_z(t) = \exp\left(it\omega_1 I_y\right)\ I_z\ \exp\left(-it\omega_1 I_y\right). \qquad (6.34)$$

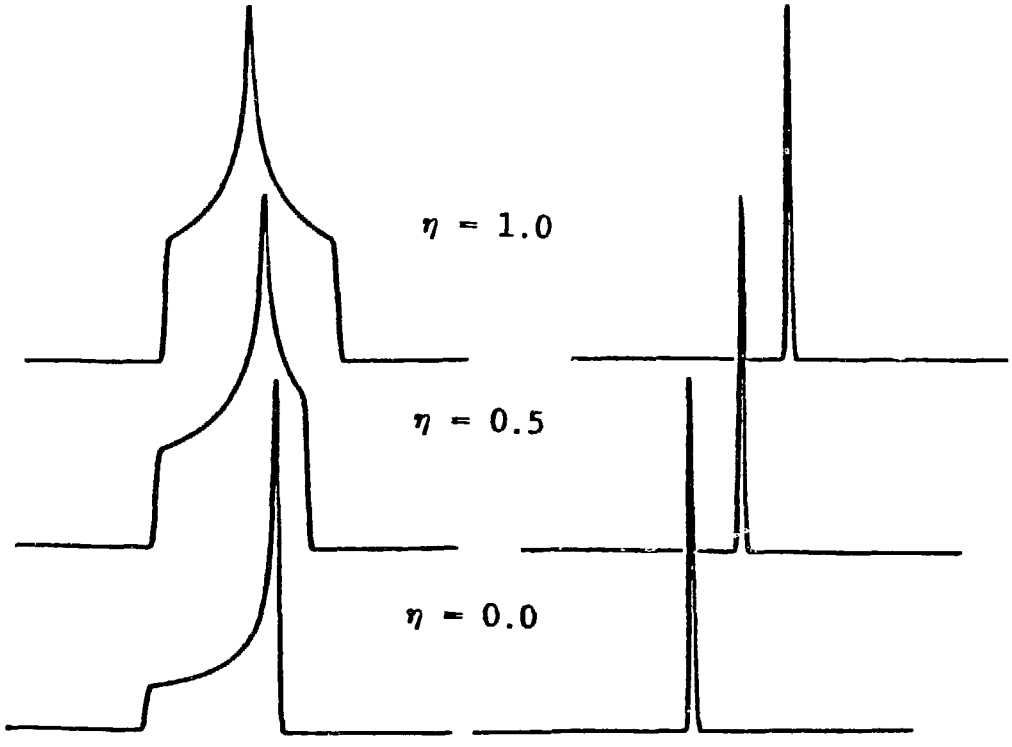

Fig. 6.2 Simulated spectra of a powder sample of dilute spins-1/2 with asymmetry parameters η = 1.0, 0.5, and 0.0. The three spectra on the left are for the static sample, while those on the right are spectra predicted to result from the experiment.

Supposing that $\omega_1 >> |\Phi|$, one may approximate the time-ordered integration of the "switched" operator $\tilde{I}_z(t)$ in Eq.(6.31) by the zeroth order average over the duration

$$\bar{I}_z^{(0)} = \frac{1}{t_h}\int_0^{t_h} \tilde{I}_z(t)\, dt, \tag{6.35}$$

which vanishes if $\omega_1 t_h = 2m\pi$, $m = 1,2,\cdots$. Furthermore, because the 2π pulse imparts cyclicity to the switched Hamiltonian, all odd order correction terms vanish. Similarly, the Hamiltonian is made zero with the 2π pulses during the second hopping period. Hence, to this degree of approximation, at $t = \tau + t_h$ the density operator becomes

$$\begin{aligned}\rho(t) &= \exp\Big(-i\frac{\tau}{3}\sum_{k=1}^{3}\phi_k I_z\Big)\, I_x \exp\Big(i\frac{\tau}{3}\sum_{k=1}^{3}\phi_k I_z\Big) \\ &= \exp\big(-i\tau\omega_0\sigma_{iso}I_z\big)\, I_x \exp\big(i\tau\omega_0\sigma_{iso}I_z\big)\end{aligned} \tag{6.36}$$

Therefore, once again the isotropic chemical shift is recovered. However, it is achieved in one experiment. The continuous irradiation of 2π pulses may be somewhat demanding. A better way may be to apply π pulses at appropriate times to create a spin-echo while the sample is hopped.

Fig.6.2 shows the simulated spectra of a powdered sample of dilute spins-1/2 with η values 0, 0.5, and 1.0. Fig.6.2(a) is for a static sample and displays full powder pattern. Fig.6.2(b) shows a sharp single line which is predicted to result from the experiment proposed in Fig.6.1.

For a dipolar or a quadrupolar system it is easy to create an

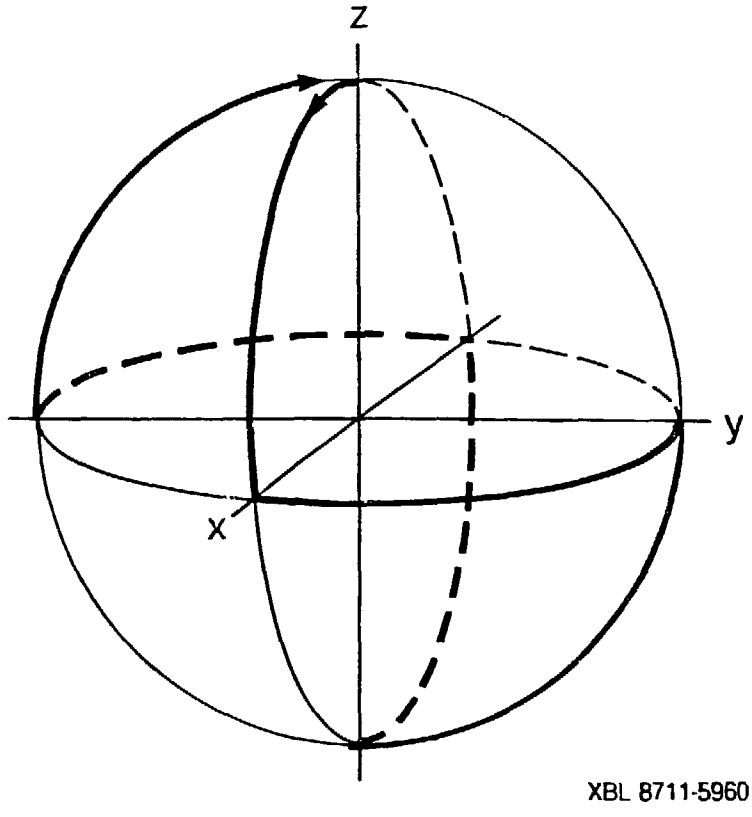

Fig. 6.3 Trajectory of I_z for the sequence $(x\ y)^8$. Note that the trajectory traverses all six points, where the three coordinate axes intersect the unit sphere.

echo by applying $(\pi/2)_x(\pi/2)_y$ pulse sequence.[17] However, if the Hamiltonian contains the chemical shift term in addition to dipole and quadrupole terms, there are no time-reversal sequences for creating the echo. Consequently, sequences to get rid of all these terms must be designed. For a general discussion of methods to average various terms the reader is referred to Chapter III. As discussed earlier, it requires three configurations to remove the T_{20} terms in the dipole (and quadrupole) Hamiltonian to zeroth order. In addition, two configurations are are required to remove I_z terms (T_{00}^{CS} and T_{20}^{CS}). Since these two averaging processes are independent of each other, at least six configurations (or six pulses) are required.

Two examples of such sequences are $(x\ y)^3$ and $(\bar{y}\ x\ 2x\ \bar{x}\ y)$, where x, y, $\bar{x}$, and $\bar{y}$ are 90° pulses with four quadrature phases. The trajectory of $\tilde{I}_z(t)$ resulting from the sequence $(x\ y)^8$ is shown in Fig.6.3. It is well known that for symmetric cycles all odd order terms vanish.[18] As shown in Appendix 5, such a sequence can be constructed by concatenating an inverse sequence with an original sequence. Examples are given in Figure 6.4.

VI.5. The Second-Order Quadrupole Effect

VI.5.1. The problem[19-21]

For a powder sample of spins $I \geq 1$ the biggest broadening is due to the anisotropic quadrupole effects. The first order quadrupole effect was treated in the last few sections. It will be shown in this

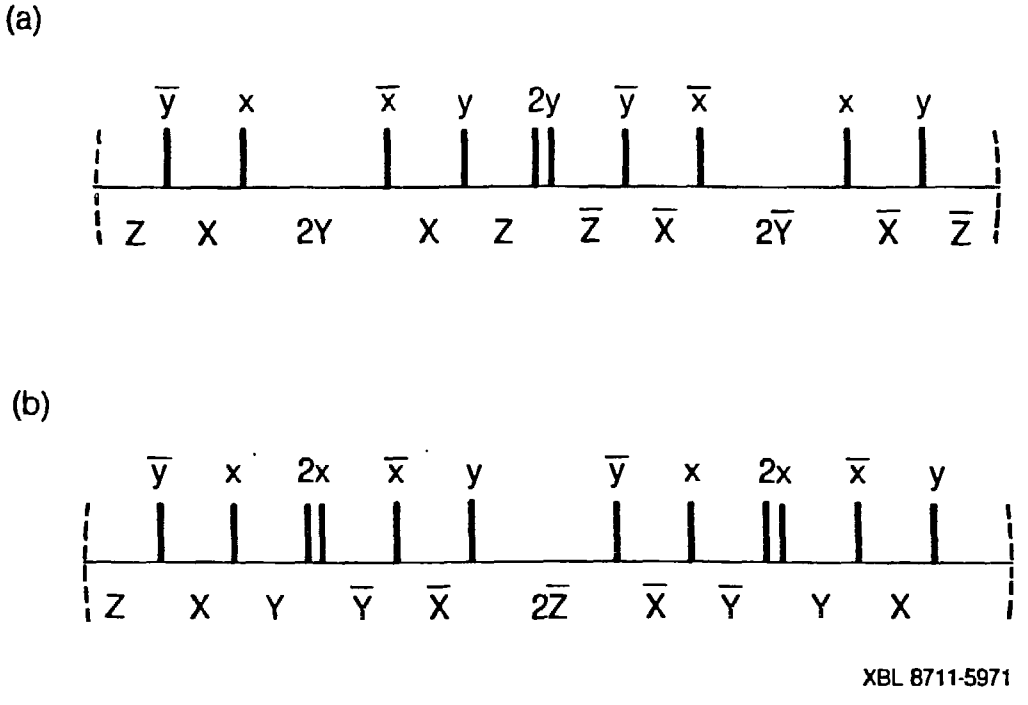

Fig. 6.4 Two sequences which produce symmetric evolution operators, and thus make all odd order correction terms in the Magnus expansion vanish.

section that the geometrical arguments associated with the magic angle are no longer tenable for the higher order anisotropies. Nonetheless, there are some interesting symmetries for these higher order anisotropies, which will be exploited to design experiments for the removal of the anisotropy associated with the second order quadrupole.

The second order quadrupole effect is most prominent for nuclei with half-integer spins. Especially, for these spins the first order effect does not manifest itself in the central transition $m = -1/2 \leftrightarrow m = 1/2$ of the spectrum. Figure 6.5 shows this situation schematically.

To see this mathematically, consider the signal resulting from the secular quadrupolar Hamiltonian $\bar{\mathcal{H}}_Q^{(0)}$ qiven by Eq.(6.10) with $\omega_\lambda = \omega_Q$:

$$S_x(t) = \mathrm{Tr}\left\{ I_x I_x(t)\right\}. \tag{6.37}$$

where

$$I_x(t) = \exp\left\{-it\bar{\mathcal{H}}_Q^{(0)}\right\}\ I_x\ \exp\left\{it\bar{\mathcal{H}}_Q^{(0)}\right\}. \tag{6.38}$$

Now consider only the subspace connected by the transition between $m = -1/2$ and $m = 1/2$, which is relevant to the discussion. Then

$$S_{\pm 1/2} = \sum_{\pm} \langle \pm 1/2 |\ I_x\ I_x(t)\ | \pm 1/2 \rangle$$

$$= \sum_{\pm} \sum_{m_1 m_2 m_3} \langle \pm\tfrac{1}{2} |\ I_x\ | m_1 \rangle\langle m_1 |\ \exp\left\{-it\bar{\mathcal{H}}_Q^{(0)}\right\} | m_2 \rangle\langle m_2 |\ I_x\ | m_3 \rangle$$

$$\times \langle m_3 |\ \exp\left\{it\bar{\mathcal{H}}_Q^{(0)}\right\}\ | \pm\tfrac{1}{2} \rangle$$

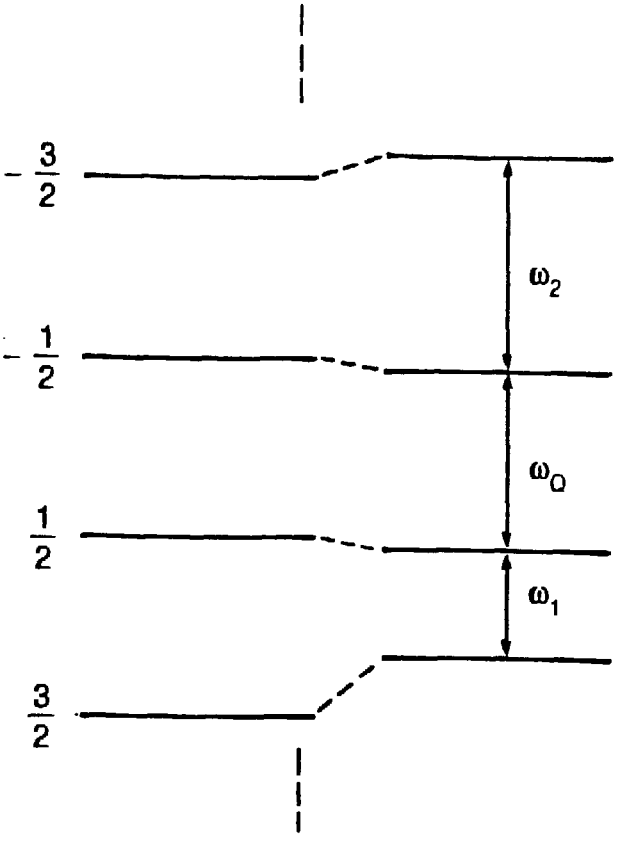

Fig. 6.5 Central portion of the energy levels of a nucleus with a half-integer spin. The Zeeman energy levels are perturbed by the first order quadrupole interaction. However, the energy level difference between m = 1/2 and m = -1/2 remains unchanged.

$$- \sum_{\pm} \langle \pm\tfrac{1}{2}| \, I_x \, |\mp\tfrac{1}{2}\rangle\langle \mp\tfrac{1}{2}| \, \exp\left(-it\bar{\mathcal{H}}_Q^{(0)}\right) \, |\mp\tfrac{1}{2}\rangle$$

$$\times \langle \mp\tfrac{1}{2}| \, I_x \, |\pm\tfrac{1}{2}\rangle\langle \pm\tfrac{1}{2}| \, \exp\left(it\bar{\mathcal{H}}_Q^{(0)}\right) \, |\pm\tfrac{1}{2}\rangle$$

$$- \sum_{\pm} |\langle \pm\tfrac{1}{2}| \, I_x \, |\mp\tfrac{1}{2}\rangle| \, \exp\left\{-it\left(\mathcal{E}_{Q\pm}^{(0)} - \mathcal{E}_{Q\pm}^{(0)}\right)\right\}. \qquad (6.39)$$

Since

$$\langle 1/2| \, T_{20} \, |1/2\rangle = \langle -1/2| \, T_{20} \, |-1/2\rangle, \qquad (6.40)$$

$$\mathcal{E}_{Q\,+}^{(0)} - \mathcal{E}_{Q\,-}^{(0)} = 0. \qquad (6.41)$$

Thus the broadening in the central transition is due to the second order quadrupole interaction.

VI.5.2. Mathematical Formulation for the Removal of the Second Order Effect

In a tilted space, rotating spin frame the first order correction term is given by

$$\bar{\mathcal{H}}^{(1)} = -\frac{i}{2\tau} \sum_{\lambda,\lambda',\ell,\ell',m,m'} \omega_\lambda \, \omega_{\lambda'} (-1)^{m+m'} \, V_{\ell -m}^{\lambda} \, V_{\ell' -m'}^{\lambda'}$$

$$\times \left[T_{\ell m}^{\lambda} \, , \, T_{\ell' m'}^{\lambda'} \right] \int_0^\tau dt_1 \int_0^\tau dt_2 \, e^{im\omega_0 t1} \, e^{im'\omega_0 t2}, \qquad (6.42)$$

where

$$V^{\lambda}_{\ell\text{-}m} = \sum_{M} D_{\text{-}m\text{-}M}\, \rho'_{2\text{-}M}. \tag{6.43}$$

Among the various cross terms only the terms $\lambda = \lambda' = Q$ and $\ell = \ell' = 2$ are responsible for the second order quadrupole effect. After some algebra it can be shown that the part of the Hamiltonian which gives rise to the second order quadrupole effect reduces to

$$\bar{\mathcal{H}}_Q^{(1)} = -\frac{\omega_Q^2}{2\omega_0} \sum_{m\neq 0} \frac{1}{m} (-1)^m \Big\{ 2\, V_{2\text{-}m}\, V_{20} \left[T_{2m}, T_{20} \right] - V_{2\text{-}m}\, V_{2m} \left[T_{2m}, T_{2\text{-}m} \right] \Big\}, \tag{6.44}$$

where the label Q is suppressed for simplicity except for ω_Q in the expression.

Table 6.1 lists commutation relatioships among various operators $T_{\ell m}$. In the basis of the Zeeman interaction only $\left[T_{2m}, T_{2\text{-}m} \right]$ (m = 1,2) are nonzero, and thus these are the terms which contribute to the first order energy shifts to the energy levels determined by the Zeeman and $\bar{\mathcal{H}}_Q^{(0)}$ term. Therefore, these are ultimately responsible for the second order quadrupole effects.

It is easy to show that

$$\langle -1/2 | \left[T_{2m}, T_{2\text{-}m} \right] | -1/2 \rangle - \langle 1/2 | \left[T_{2m}, T_{2\text{-}m} \right] | 1/2 \rangle = 16 \qquad m = 1,2. \tag{6.45}$$

Thus the second order <u>frequency</u> shift is given by

Table 6.1 Commutation Relations for Various Spin Operators Expressed in Terms of Spherical Tensors

$$\left[T_{2\pm1}, T_{20} \right] = -\frac{3}{2\sqrt{6}} \left(I_z^2 I_\pm + I_z I_\pm I_z + I_\pm I_z^2 \right)$$

$$\left[T_{2\pm2}, T_{20} \right] = \pm \frac{3}{2\sqrt{6}} \left(I_\pm^2 I_z + 2\, I_\pm I_z I_\pm + I_z I_\pm^2 \right)$$

$$\left[T_{2+1}, T_{2-1} \right] = \left(17 I_z - 4 I_z^3 \right)$$

$$\left[T_{2\pm1}, T_{2\pm2} \right] = - I_\pm^3$$

$$\left[T_{2+2}, T_{2-2} \right] = -\frac{1}{2} \left(4\, I_z^3 - 33\, I_z \right)$$

Here

$$I_\pm = I_x \pm i\, I_y .$$

$$\omega_Q^{(2)} = \mathcal{E}_{-1/2}^{(2)} - \mathcal{E}_{1/2}^{(2)} = \frac{8\omega_Q^2}{\omega_0} \sum_{m\neq 0} \frac{1}{m}(-1)^m V_{2-m} V_{2m}. \qquad (6.46)$$

Eq.(6.46) is the principal expression to be utilized for the design of the schemes for the removal of the second order quadrupole effects.

Spinning Experiments

Now consider the case in which the sample is spun around a tilted axis. With the definition of V_{2M} given by Eq.(6.43) and the following property of the Wigner rotation matrix

$$D_{-m-M} = (-1)^{M-m} D_{mM}^* \qquad (6.47)$$

the second order shift reduces after some lengthy calculations to

$$\omega_Q^{(2)} = \frac{16\omega_Q^2}{3\omega_0} \sum_{M=-2}^{2} \left| D'_{M0} + \sqrt{\frac{2}{3}} \left(D'_{M2} + D'_{M-2} \right) \right|^2$$

$$\left\{ |D_{1M}|^2 + |D_{1-M}|^2 - \frac{1}{2} \left(|D_{2M}|^2 + |D_{2-M}|^2 \right) \right\}. \qquad (6.48)$$

More explicit expression of Eq.(6.48) is prohibitively complicated. The geometry of the scheme for the removal of $\omega_Q^{(2)}$ can be found as follows:

The line broadening is due to the distribution of the orientations $\Omega'(0,\beta',\gamma')$ of the spins in the powder sample. The orientation dependence can be expanded in terms of independent basis functions of

β' and γ'. Thus

$$\omega_Q^{(2)} = \sum_k a_k(\Omega) F_k(\Omega'). \tag{6.49}$$

Explicit calculation of Eq.(6.49) shows that

$$\omega_Q^{(2)} = \sum_{m,n=0,1,2} C_{mn}(\Omega) \cos(2m\beta') \cos(2n\gamma'). \tag{6.50}$$

Here m = n = 0 correponds to the orientation-independent terms, which give rise to the isotropic shift. The isotropic shift can be calculated to give

$$\omega_{Q,iso}^{(2)} = \frac{\omega_Q^2}{\omega_0}\left\{\left(\sqrt{\frac{3}{2}}\right)^2\left\{\frac{11f_1 + 12f_2 + 9f_3}{32}\right\} + \left(\frac{\eta}{2}\right)^2\left\{\frac{9f_1 + 20f_2 + 35f_3}{64}\right\}\right\}, \tag{6.51}$$

where

$$\begin{aligned} f_1 &= 3\, s^2c^2 - \frac{3}{8}\, s^4 \\ f_2 &= \frac{-1}{16}\left(9\, c^4 + 6\, c^2 - 7\right) \\ f_3 &= \frac{1}{4}\left(9\, c^4 - 6\, c^2 + 1\right) \end{aligned} \tag{6.52}$$

with

$$\begin{pmatrix} s \\ c \end{pmatrix} = \begin{pmatrix} \sin\beta \\ \cos\beta \end{pmatrix}, \tag{6.53}$$

β being the tilt angle of the spinner axis from the LAB z axis. It is interesting that the sum of the coefficients of f_k in each parenthesis is equal to 1.

The coefficients C_{mn} in Eq.(6.50) are determined by the orientation of the spinner axis. The removal of the second order quadrupole effect thus reduces to making

$$C_{mn} = 0 \qquad (m,n = 0,1,2), \tag{6.54}$$

except the coefficient of the isotropic shift C_{00}. C_{mn} can also be expanded in terms of f_k, and it can be shown that Eq.(6.54) is achieved when

$$f_1 = f_2 = f_3. \tag{6.55}$$

Note that

$$f_1 - f_2 \sim f_1 - f_3 \sim A\,\mathcal{P}_4 + B\,\mathcal{P}_2, \tag{6.56}$$

where

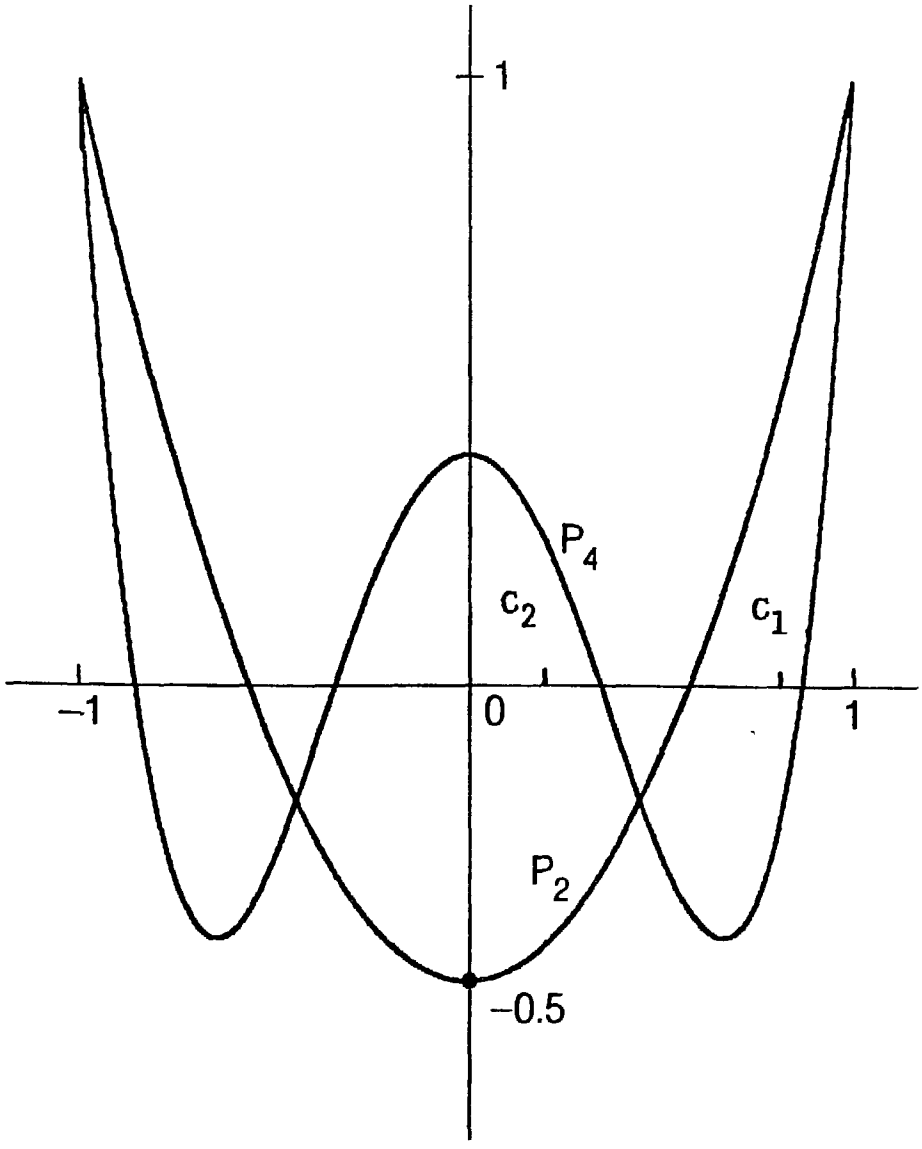

XBL 8711-5959

Fig. 6.6 The second and fourth order Legendre polynomials. $c_k = \cos\beta_k$ (k = 1,2) where β_1 and β_2 are angles which make the polynomials vanish simultaneously.

$$\mathcal{P}_4(\cos\beta) = \frac{1}{8}\left(35\cos^4\beta - 30\cos^2\beta + 3\right) \tag{6.57}$$

is the fourth order Legendre polynomial and once again

$$\mathcal{P}_2(\cos\beta) = \frac{1}{2}\left(3\cos^2\beta - 1\right) . \tag{6.58}$$

The second and fourth order Legendre polynomials are shown in Fig.6.6. Thus it may be conjectured that the removal of an nth order anisotropy by mechanical sample spinning is associated with a function g_n having the form

$$g_n = \sum_{m=1}^{n} b_{nm}\,\mathcal{P}_{2m}(\cos\beta). \tag{6.59}$$

However, the rigorous proof of Eq.(6.59) for $n \geq 3$ requires more work and is of no further interest here.

In view of Eq.(6.56), the angles which satisfy Eq.(6.55) must be the roots of the simultaneous equations

$$\sum_{k}^{N} \mathcal{P}_2(\cos\beta_k) = 0 \tag{6.60}$$

and

$$\sum_{k}^{N} \mathcal{P}_4(\cos\beta_k) = 0. \tag{6.61}$$

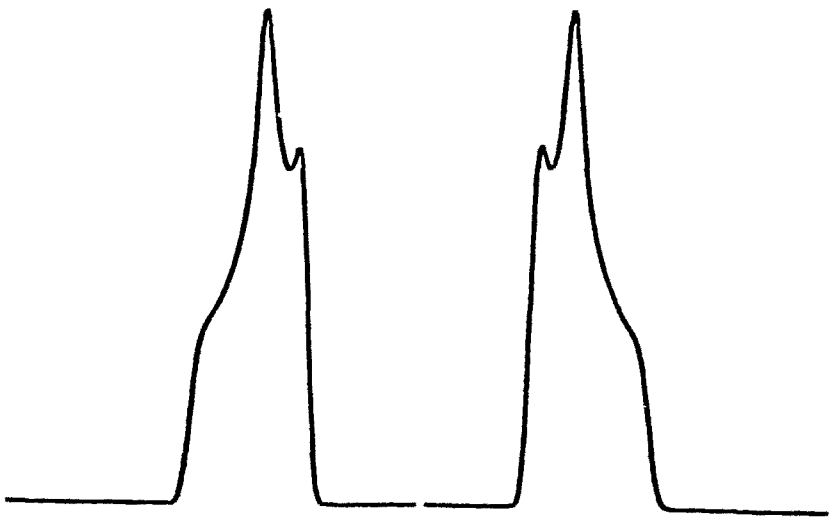

Fig. 6.7 Simulated spectra for a powder sample which is spun around an axis tilted from the z axis by β_1 and β_2 respectively. The line broadening is due to the CSA and the second order quadrupole interaction.

In this case the minimum number of degrees of freedom, N, is two. Unlike the case of the first order anisotropies, there is only one set of two angles which satisfy Eqs.(6.60) and (6.61).

Recently the variable-angle sample spinning (VASS) method has been introduced[22-27] to deal with the line broadening due to the CSA and the second order quadrupole effect. The VASS studies show that there is no "magic" angle which satisfies Eqs.(6.60) and (6.61) simultaneously, although there are angles at which the overall anisotropies are minimum. The optimal angles sould be different for different samples. Another interesting feature observed in the VASS studies is that at certain two angles the resulting powder patterns are exactly opposite to each other. This behavior is shown in Fig.6.7. These angles are the roots $\beta_1 = 37.377365^0$ and $\beta_2 = 79.187691^0$ of the above simultaneous equations. It follows that the two angles also remove the first order anisotropies, which are proportional to $P_2(\cos\beta)$.

VI.5.3. Implementation

In principle Eqs.(6.60) and (6.61) may be achieved by hopping the sample between β_1 and β_2 as shown schematically in Fig.6.8(a). Because many nuclei of interest such as ^{27}Al (I= 5/2) have the quadrupole coupling constants of $O(10^6)$ Hz, it is impractical to apply multiple-pulse sequences to make the Hamiltonian vanish during hopping periods. Another possibility is shown in Fig.6.8(b). Instead of hopping, the sample axis is rapidly rotated about an axis orthogonal to the sample

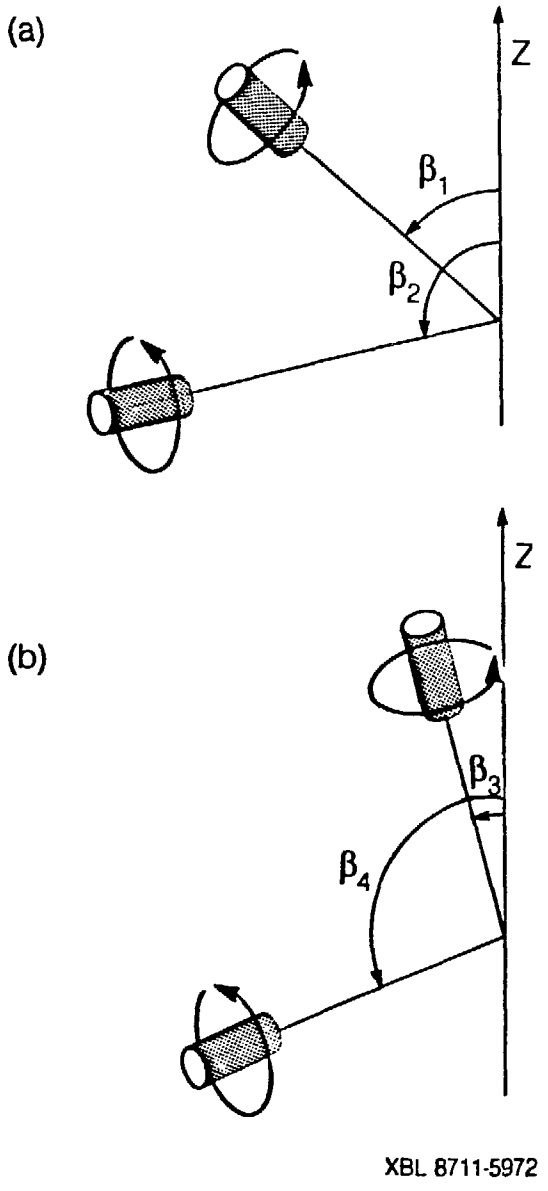

Fig. 6.8 Two experiments for the removal of the CSA and the second order quadrupole interaction. In (a), the spinner axis is hopped between two angles β_1 and β_2. In (b), the spinner is quickly rotated from β_3 to β_4.

spinning axis. In this case the angles (denoted as β_3 and β_4) must be found from the integral equations

$$\int_{\beta_3}^{\beta_4} \mathcal{P}_2(\cos\beta)\, d\beta = 0 \tag{6.62}$$

and

$$\int_{\beta_3}^{\beta_4} \mathcal{P}_4(\cos\beta)\, d\beta = 0 \tag{6.63}$$

rather than the discrete summation Eqs.(6.60) and (6.61). They are: $\beta_3 = 19^0$ and $\beta_4 = 99^0$. The summation or the integration is possible because the portions of the Hamiltonian responsible for the first order anisotropies and the second order quadrupole effect commute with themselves at all times during the experimental methods proposed above. The rotation of the sample axis requires time of $O(10^{-2})$ seconds with current technology. Consequently, many sidebands may clutter the spectrum. However, in principle, these side bands can be suppressed with the techniques developed for the MAS experiments or the extensions thereof.[28-37]

VI.6 Remarks

A technique used throughout this Dissertation is the AHT. The connection between the zeroth order term in the AHT and the first order

perturbation theory has been discussed by Haeberlen.[38] It was shown in Chapter II that the first order correction term in the AHT gives a result identical to the first order correction term in the Taylor series expansion of the exact theory of the interaction of a spin-1/2 with the quantized-electromagnetic theory. It can be shown that the second-order quadrupole effects as calculated in this chapter by using the first-order correction term in the AHT results in an expression identical to the second-order perturbation theory. An advantage of the AHT over perturbation theory is the explicit appearance of the operators in the expressions, allowing a quick decision on which operator terms are important for the situation under consideration.

The increased number of degrees of freedom in selecting angles will undoubtly shed light on the design of schemes for the removal of various anisotropies. Although the large magnitude of the quadrupole coupling constants prevents the modulation of the spin degrees of freedom by the application of pulses, in general the complementary modulation of spin and spatial coordinates will be the most versatile tool for the high-resolution NMR spectroscopy. In fact, a combined approach of multiple pulses and mechanical motion has been proposed[39] for achieving one of the ultimate goals of NMR —— reducing the Hamiltonian to a scalar.

References

1(a). F. Reif and E. M. Purcell, Phys. Rev. 91, 631 (1953).

1(b). T. P. Das and E. L. Hahn, Solid State Physics (Suppl.) 1 (1958).

1(c). A. Abragam and W. G. Proctor, Phys. Rev. 109, 1441 (1958).

1(d). M. Goldman, Spin Temperature and Nuclear Magnetic Resonance in Solids, (Clarendon, Oxford, 1970).

2(a). D. P. Weitekamp, A. Bielecki, D. Zax, K. Zilm and A. Pines, Phys. Rev. Lett. 50, 1807 (1983).

2(b). For a recent account of the developments in this field see, A. M. Thayer and A. Pines, Acc. Chem. Res. 20, 47 (1987).

3. See, for example, M. Mehring, Principles of High Resolution NMR in Solids, (Springer-Verlag, Berlin, 1983).

4(a). R. R. Ernst, J. Mag. Res. 3, 10 (1970).

4(b). R. Kaiser, J. Mag. Res. 3, 28 (1970)

4(c). B. Blümich, Prog. in NMR Spect. 19, 331 (1987).

5(a). R. Tycko, Ph.D. thesis, University of California, Berkeley (1984).

5(b). R. Tycko, A. Pines, and J. Guckenheimer, J. Chem. Phys. 83, 2775 (1985).

6. E. R. Andrew, A. Bradbury, and R. G. Eades, Arch. Sci. (Geneva) 11, 223 (1958).

7. E. R. Andrew, A. Bradbury, and R. G. Eades, Nature 182, 1659 (1958).

8. E. R. Andrew, Arch. Sci. (Geneva) 12, 103 (1959).

9. I. J. Lowe, Phys. Rev. Lett. 2, 285 (1959).

10. E. R. Andrew, A. Bradbury, and R. G. Eades, Nature 183, 1802 (1959).

11(a). E. R. Andrew, Prog. in NMR Spect. 8,1 (1971).

11(b). R. G. Griffin, in Proceedings of the 100th Fermi School on Physics (B. Maraviglia, Ed.), in press.

12. U. Haeberlen and J. S. Waugh, Phys. Rev. 175, 453 (1968).

13. B. C. Gerstein, in Magnetic Resonance in Colloid and Interface Science, Eds. J. P. Fraissard and H. A. Resing, 175, D. Reidel Pub. Co. (1980), and references therein.

14(a). A. Bax, N. M. Szeverenyi, and G. E. Maciel, J. Mag. Reso., 52, 147, (1983).

14(b). N. M. Szeverenyi, A. Bax, and G. E. Maciel, J. Mag. Res., 61 440 (1985).

14(c). G. E. Maciel, N. M. Szeverenyi, and M. Sardashti, J. Mag. Res., 64, 365 (1987).

15. M. Lee and W. I. Goldburg, Phys. Rev. 140A, 1261 (1965).

16(a). B. C. Gerstein, C. Chow, R. G. Pembelton and R. C. Wilson, J. Phys. Chem., 81, 565 (1977).

16(b). B. C. Gerstein, R. G. Pembelton, R. C. Wilson and L. M. Ryan, J. Chem. Phys., 66, 361 (1977).

16(c). L. M. Ryan, R. E. Taylor, A. J. Paff and B. C. Gerstein, J. Chem. Phys., 72, 508 (1980).

16(d). R. E. Taylor, R. G. Pembelton, L. M. Ryan and B. C. Gerstein, J. Chem. Phys., 71, 4541 (1979).

17. J. G. Powles and P. Mansfield, Phys. Lett. 2, 58 (1962).

18(a). C. H. Wang and J. D. Ramshaw, Phys. Rev.B6, 3253 (1972).

18(b). C. H. Wang, J. Chem. Phys. 59, 225 (1973).

19. A. Abragam, The Principles of Nuclear Magnetism (Oxford U. Press, London), 1961.

20(a). E. Kundla, A. Samson and E. Lippmaa, Chem. Phys. Lett., 83, 229 (1981).

20(b). A. Samson, E. Kundla and E. Lippmaa, J. Mag. Res., 49, 350 (1982).

21. D. Muller, W. Gessner, H. -J. Behrens and G. Scheler, Chem. Phys. Lett. 79, 59 (1981).

22. E. Oldfield, S. Schramm, M. D. Meadows, K. A. Smith, R. A. Kinsey and J. L. Ackerman, J. Am. Chem. Soc. 104, 919 (1982).

23. E. Oldfield, R. A. Kinsey, B. Montey, T. Ray and K. A. Smith, J. Chem. Soc., Chem. Commun., 254 (1982).

24. S. Schram and E. Oldfield, J. Chem. Soc., Chem. Commun., 980 (1982).

25. S. Ganapathy, S. Schramm, and E. Oldfield, J. Chem. Phys., 77, 4360 (1982).

26(a). S. J. Opella and M. H. Frey, J. Am. Chem. Soc. 101, 5854 (1979).

26(b). T. Terao, H. Miura and A. Saika, J. Chem. Phys.75, 1573 (1981).

26(c). T. Terao, H. Miura and A. Saika, J. Am. Chem. Soc. 104, 5228 (1982).

26(d). T. Terao, H. Miura and A. Saika, J. Mag. Res. 49, 365 (1982).

26(e). K. W. Zilm and D. M. Grant, J. Mag. Res. 48, 524 (1982).

27. F. Lefebvre, J.-P. Amoureux, C. Fenandez, and E. G. Derouane, J. Chem. Phys., 86, 6070 (1987).

28(a). M. M. Maricq and J. S. Waugh, J. Chem. Phys. 70, 3300 (1979).

28(b). M. M. Maricq and J. S. Waugh, Chem. Phys. Lett. 47, 327 (1977).

29. J. S. Waugh, M. M. Maricq and R. Cantor, J. Mag. Res. 29, 183 (1976).

30. M. M. Maricq and J. S. Waugh, Chem. Phys. Lett. 47, 327 (1977).

31. W. T. Dixon, J. Mag. Res. 44, 220 (1981).

32. W. T. Dixon, J. Chem. Phys. 77, 1800 (1982).

33. W. T. Dixon, J. Schaefer, M. D. Sefcik, E. O. Stejeskal and R. A. McKay, J. Mag. Res. 49, 341 (1982).

34. M. A. Hemminga, P. A. deJager, K. P. Datema and J. Berg, J. Mag. Res. 50, 508 (1982).

35. M. A. Hemminga and P. A. deJager, J. Mag. Res. 57, 339 (1983).

36. N. Zumbulyadis, J. Mag. Res. 49, 329 (1982).

37. W. P. Aue, D. J. Ruben and R. G. Griffin, J. Mag. Res. 46, 354 (1982).

38. U. Haeberlen, High Resolution NMR in Solids: Selective Averaging (Academic, New York), 1976.

39. R. Tycko, J. Mag. Res. 75, 193 (1987).

Appendix 1

To prove that a second rank tensor may be regarded as a direct product of two vectors, first note the following transformation properties of a second rank tensor and a vector:

$$T'_{mn} = \sum_{k\ell} C_{mk} C_{n\ell} T_{k\ell} \tag{A1.1}$$

$$V'_{\alpha} = \sum_{m} a_{\alpha m} V_{m}. \tag{A1.2}$$

Let

$$T_{\alpha\beta} = p_{\alpha} q_{\beta}, \tag{A1.3}$$

where p_{α} and q_{β} are components of vectors $\vec{p}$ and $\vec{q}$ respectively. Then

$$\begin{aligned} p'_{\alpha} q'_{\beta} &= \left(\sum_{m} a_{\alpha m} p_{m}\right)\left(\sum_{n} a_{\beta n} q_{n}\right) \\ &= \sum_{mn} a_{\alpha m} a_{\beta n} T_{mn} \\ &= T'_{\alpha\beta}. \qquad \text{(Q.E.D.)} \end{aligned} \tag{A1.4}$$

Appendix 2

Consider the total Hamiltonian consisting of an internal($\mathcal{H}_v$) and a time-dependent external($\mathcal{H}_1$) parts:

$$\mathcal{H} = \mathcal{H}_1(t) + \mathcal{H}_v. \tag{A2.1}$$

The evolution operator for the Hamiltonian satisfies

$$dU/dt = -i\,\mathcal{H}U. \tag{A2.2}$$

Now suppose U can be separated into two parts:

$$U = U_1 U_v, \tag{A2.3}$$

with U_1 satisfying

$$dU_1/dt = -i\,\mathcal{H}_1 U_1. \tag{A2.4}$$

Then Eq.(A2.2) becomes

$$\begin{aligned} dU/dt &= (dU_1/dt)U_v + U_1(dU_v/dt) \\ &= -i\,\mathcal{H}_1 U + U_1(dU_v/dt) \\ &= -i(\mathcal{H}_1 + \mathcal{H}_v)U. \end{aligned} \tag{A2.5}$$

It follows that

$$dU_v/dt = -i\,U_1^{\dagger}\,\mathcal{H}_v\,U_1. \tag{A2.6}$$

Therefore

$$U_v = \mathcal{T} \exp\left(-i\int_0^t dt' \; U_1^\dagger \, \mathcal{H}_v \, U_1\right). \qquad \text{(A2.7)}$$

Appendix 3

List of 24 pulse sequences which removes all linear and bilinear cross terms. The definition of phases is: 0 ≡ x, 1 ≡ y, 2 ≡ $\bar{x}$, and 3 ≡ $\bar{y}$.

032123210323210301032101
030103232123210323032101
032101210323210323032101
012101230323030121232101
012101232303230121232101
012103010123230121232101
012301030123230121232101
012303010323230121232101
012101230301212321232101
030103010323212321232101
030103010301030103010301
012101210121030103010301
032123212321230103010301
012321232123230103010301
012123212301012103010301
012321232301012103010301
012323010121012103010301
032303012123212303010301
030121232123212303010301
032303012321232303010301
032303012323010123010301
012123212301210123010301
012321232301210123010301
012303230121232123010301
030123030121230101210301
012323012321230101210301
012303230123230101210301
012323032123230101210301
030121232123012101230301
030123230123212301012301
030123032301232301012301
012303230123230121012301

012101012101012101012101
030103010301012101012101
030301030301012101012101
012101210121012101012101
030103030103012101012101
032303230323012101012101
032323032323012101012101
030323032303212101012101
032303232303212101012101
012321232123212101012101
030323230323212101012101
012303230323032101012101
012323032323032101012101
012123212321232101012101
032121030321010301012101
012103010303010301012101
012123032303230301012101
012123230323230301012101
030101230301212301012101
012103230323032301012101
012123032323032301012101
030103010301210121012101
030103030103210121012101
032303230323210121012101
030323032101030121012101
032303232101030121012101
032321010301030121012101
032321030103030121012101
030323032103010321012101
032303232103010321012101
032321010303010321012101
030323032301030321012101
032303232301030321012101
030323230321030321012101
012321210303230321012101
032123210303230321012101
012103032303230321012101
012103230323230321012101
012101232123212321012101
032321032303210103012101
012321210323210103012101
032123210323210103012101
032321230323210103012101
032321232101030103012101
032121030321030103012101
032121032303210303012101
032121230323210303012101
012101230323032303012101
012123032303012123012101
012123230323012123012101
012301012323012123012101
012123030121232123012101
012101212321232123012101
012101230323230323012101
012123030123212323012101
012103232123210303212101
012103212103032303212101
012103212103232101032101
032321030323010301032101
032321032303210301032101

030321232123210323210101
030323212323210323210101
032101032323210323210101
030323032323030323210101
032303012121230323210101
030121232121230323210101
030123212321230323210101
030321232321230323210101
030123232123230323210101
030123232301012323210101
012323012121012323210101
012103030123212323210101
030101032323212323210101
030101030101030101030101
012101012101030101030101
030103010301030101030101
030301030301030101030101
012101210121030101030101
012121012121030101030101
030103030103030101030101
030323030323030101030101
032303230323030101030101
032323032323030101030101
012101212101230101030101
032121232121230101030101
012321212321230101030101
032123212321230101030101
032321232321230101030101
030323032303230101030101
032303232303230101030101
012123212123230101030101
012321232123230101030101
032123232123230101030101
030323230323230101030101
012323212323230101030101
032303030101012101030101
012121232101012101030101
012123212301012101030101
012321232301012101030101
032123232301012101030101
012323010121012101030101
030101210121012101030101
030121012121012101030101
012323012101212101030101
030123212123212101030101
030321232123212101030101
030323212323212101030101
030323032323032101030101
032303012121232101030101
030121232121232101030101
030123212321232101030101
030321232321232101030101
012121230301010301030101
012101012103010301030101
030103010303010301030101
012101210123010301030101
012121012123010301030101
012101012301030301030101
030103230303230301030101
030123032303230301030101

```
030101032101012101010101
012103212123012101010101
030101030301010301010101
012101012301010301010101
030123030323010301010101
010301230303210301010101
030103230303210301010101
030123032303210301010101
030123230323210301010101
030301012323210301010101
030123232101030301010101
030303212123030301010101
030303212101010121010101
030101030121010121010101
012101212121010121010101
030103010321010121010101
030301030321010121010101
030101032101210121010101
012103212123210121010101
012101232121230121010101
012103212321230121010101
012103232123230121010101
012121010323230121010101
012103232301012121010101
030101032121012121010101
030321212103212121010101
030101010303212121010101
012121230303212121010101
030303232323212121010101
030303210303032121010101
030101010301010103010101
012121230301010103010101
030303232321010103010101
030101030103010103010101
012101012103010103010101
030103010303010103010101
012101012301010103010101
312121012123010103010101
030101030301030103010101
012101012301030103010101
030123030323030103010101
030103230303230103010101
030123032303230103010101
030123230323230103010101
030301012323230103010101
030323030301212103010101
032303230301212103010101
032323032301212103010101
030301010121212103010101
032323230321212103010101
030121212321212103010101
030123212323212103010101
030321232323212103010101
030321210303032103010101
030103032303032103010101
030103230323032103010101
030123032323032103010101
```

```
032303012321232103010101
030121232321232103010101
030103232303232103010101
032303032123232103010101
032323230101010303010101
030121212101010303010101
030103232321010303010101
030101030303010303010101
012101012303010303010101
012123030301230303010101
012101010121230303010101
032323212121230303010101
032321010103230303010101
030101012323230303010101
012121232323230303010101
030123030301212303010101
012121230121212303010101
032303012323212303010101
030121232323212303010101
030121232323212303010101
030121210303032303010101
032321010123032303010101
032303012121030323010101
030121232121030323010101
030123212321030323010101
030321232321030323010101
030123232123030323010101
030121210303230323010101
032321010123230323010101
030303230101012323010101
030323032101012323010101
032303232101012323010101
032321010301012323010101
032321030103012323010101
032323010303012323010101
032321030301032323010101
030121210323032323010101
030303212121232323010101
032323230303232323010101
030121212303232323010101
012101010121010101210101
032323212121010101210101
032321010103010101210101
030101012323010101210101
012121232323010101210101
030101030101210101210101
012101012101210101210101
030103010301210101210101
030301030301210101210101
012101210121210101210101
030103030103210101210101
032303032303210101210101
030323030323210101210101
032303032303210101210101
032323032323210101210101
030303230101030101210101
030323032101030101210101
032303232101030101210101
032321010301030101210101
032321030103030101210101
```

032121012121032121210101
030103010103032121210101
030301030103032121210101
012103212121030321210101
032323212103030321210101
032321030323030321210101
032321032303230321210101
012321210323230321210101
032123210323230321210101
032321230323230321210101
012103032323230321210101
012103030121212321210101
030101032321212321210101
012323010103212321210101
030101210103212321210101
030121012103212321210101
032101212103212321210101
030121210123212321210101
032321212323212321210101
032321032323032321210101
030121210321232321210101
032101010321010103210101
032321032323210103210101
030323032103030103210101
032303232103030103210101
030123232103230303210101
032303012121032303210101
030121232121032303210101
030123212321032303210101
030321232321032303210101
030123232123032303210101
030121210303232303210101
032321010123232303210101
012321210303012123210101
032123210303012123210101
032321230303012123210101
012103032303012123210101
012103230323012123210101
012123032323012123210101
032321010101212123210101
012103232303212123210101
030101032123212123210101
012103030121232123210101
030101032321232123210101
012323010103232123210101
030101210103232123210101
030121012103232123210101
032101212103232123210101
030121210123232123210101
012123212301010323210101
012321232301010323210101
032123232301010323210101
012323010121010323210101
030101210121010323210101
030121012121010323210101
012323012101210323210101
030101212101210323210101
012323210121210323210101
030321212321210323210101
030123212123210323210101

032323010303030101210101
030303212101012101210101
030101030121012101210101
012101012121012101210101
030103010321012101210101
030301030321012101210101
030101032101212101210101
012103212123212101210101
012103212123212101210101
012101232121232101210101
012103212321232101210101
012103232123232101210101
012121010323232101210101
030303210301010301210101
030303230103010301210101
030323032103010301210101
032303232103010301210101
032321010303010301210101
030303230301030301210101
030323032301030301210101
032303232301030301210101
012321232121030301210101
032123232121030301210101
030323230321030301210101
012323212321030301210101
012121010103030301210101
030303012123030301210101
012103030323030301210101
012321210303230301210101
032123210303230301210101
032321230303230301210101
012103032303230301210101
012103230323230301210101
012123032323230301210101
012123030121212301210101
012101212321212301210101
012101232123212301210101
012103212323212301210101
032321032303032301210101
012321210323032301210101
032123210323032301210101
032321230323032301210101
012103032323032301210101
012101232321232301210101
032121232103232301210101
012321212303232301210101
032123212303232301210101
032321232303232301210101
032323010123232301210101
012103030301010121210101
030303210121010121210101
012101232323010121210101
030303212101210121210101
030101030121210121210101
030103010321210121210101
030301030321210121210101
032101012101032121210101
030301010301032121210101
030121010121032121210101
032101210121032121210101

```
030301012323012123030101
030301030101212123030101
012323230301212123030101
030123232303212123030101
012323012123212123030101
030101212123212123030101
030123030121232123030101
012323012321232123030101
030101212321232123030101
012303230123232123030101
012101030101230323030101
012101030103012303230101
012301030301230323030101
012103030103230323030101
030101230323230323030101
030123030123212323030101
012323012323212323030101
030101212323212323030101
012103030123032323030101
012301010123010101230101
030123030123230101230101
012323012323230101230101
030123030301012101230101
032303012323012101230101
012321232301212101230101
032303012323012101230101
032321010123030121230101
012103232301232121230101
012321210303012321230101
032321230303012321230101
012103032303012321230101
012103232303012321230101
012123032323012321230101
012103232303212321230101
030103212321210303230101
030103212321210303230101
030103232123210303230101
030121010323210303230101
032101210323210303230101
032121012323210303230101
030103212103032303230101
012101012323032303230101
012101030101232303230101
012103010301232303230101
012301030301232303230101
012103030103232303230101
032121030321010123230101
012101030103010123230101
012103010303010123230101
012101030301030123230101
012123030323030123230101
012123032303230123230101
012123230323230123230101
012301012323230123230101
012103230323032123230101
012123032323032123230101
012103232303232123230101
030103212103230323230101
012101012323230323230101
```

```
030123230323230301030101
030301012323230301030101
032303230301212301030101
032323032301212301030101
030301010121212301030101
030121212321212301030101
032303012123212301030101
030123321232321230301030101
030103230323032301030101
030123032323032301030101
032303012321232301030101
030121232321232301030101
030103232303232301030101
032303032123232301030101
030123030301010121030101
012121230121010121030101
032303012323010121030101
030121232323010121030101
032303030101210121030101
012121232101210121030101
012321232301210121030101
032123232301210121030101
012323010121210121030101
012303232303012121030101
012123232301232121030101
012323032121232121030101
030101232121232121030101
030103212321232121030101
030321232121030321030101
030323212321030321030101
032101032321030321030101
030321210303230321030101
030103032303230321030101
030123030121232321030101
012323012321212321030101
030101212321212321030101
012303230123212321030101
012323032123212321030101
030101232123212321030101
030103212323212321030101
030321210323032321030101
030103032323032321030101
012303032301232321030101
030321210323032321030101
012121230301030103030101
012101012103030103030101
012101210123030103030101
012121012123030103030101
012301010301012303030101
012121010121012303030101
012301030103012303030101
012303010303012303030101
012101210101212303030101
012121012101212303030101
030123032303012123030101
030123230323012123030101
```

Appendix 4. Some useful commutation rules.

$$[\ I_1 \cdot I_2\ ,\ \alpha_k^2\ ] = \pm\, i\, \beta\gamma^-\quad (+ \text{ sign for } k = 1,\ - \text{ sign for } k = 2)$$

$$[\ I_1 \cdot I_2\ ,\ \beta\gamma^-\ ] = \alpha^-/2i$$

$$[\ I_1 \cdot I_2\ ,\ \alpha^+\ ] = 0$$

$$[\ I_1 \cdot I_2\ ,\ \alpha\beta^+\ ] = 0$$

$$[\ I_1 \cdot I_2\ ,\ \alpha_1\alpha_2\ ] = 0$$

where

α,β,γ = x,y,z and cyclic permutations.

$\alpha^{\pm} = \alpha_1 \pm \alpha_2$

$\beta\gamma^{\pm} = \beta_1\gamma_2 \pm \gamma_1\beta_2$.

With the above commutation rules it is easy to show that

$$\exp\left(-iJtI_1 \cdot I_2\right)\ \alpha^-\ \exp\left(itJI_1 \cdot I_2\right)$$
$$= \alpha^-\ \cos Jt + 2\beta\gamma^-\ \sin Jt.$$

Appendix 5

In this Appendix it will be shown that any sequence of pulses of the type $(P_1 \cdots P_n)(P_1 \cdots P_n)^{-1}$ makes the switched Hamiltonian cyclic, if

$$\left[\mathcal{H} \ , \ I_z\right] = 0. \tag{A5.1}$$

(pf.) Consider the following evolution operator with n piecewise-constant Hamiltonians

$$\begin{aligned} U &= \exp\left(-i\tau(-\omega_1 I_{\phi_1} + \mathcal{H})\right) \cdots \exp\left(-i\tau(-\omega_1 I_{\phi_n} + \mathcal{H})\right) \\ &= \mathcal{T}^{-1} \prod_{k=1}^{n} \exp\left(-i\tau(-\omega_1 I_{\phi_k} + \mathcal{H})\right), \quad \phi = \pm x, \pm y. \end{aligned} \tag{A5.2}$$

where $\mathcal{T}$ is the time-ordering opertor. Eq.(A.2) can be rewritten as

$$\begin{aligned} U &= e^{i\pi I_z} \mathcal{T}^{-1} \prod_k \exp\left(-i\tau(\omega_1 I_{\phi_k} + \mathcal{H})\right) e^{-i\pi I_z} \\ &= \left\{e^{i\pi I_z} \mathcal{T} \prod_k \exp\left(i\tau(\omega_1 I_{\phi_k} + \mathcal{H})\right) e^{-i\pi I_z}\right\}^{\dagger} \\ &= \left\{ \mathcal{T} \prod_k \exp\left(i\tau(-\omega_1 I_{\phi_k} + \mathcal{H})\right)\right\}^{\dagger} \\ &= \left\{ \mathcal{T} \prod_k \exp\left(-i\tau(\omega_1 I_{\phi_k} - \mathcal{H})\right)\right\}^{\dagger}. \end{aligned} \tag{A5.3}$$

Now separate the rf part from the internal Hamiltonian:

$$U_k = \exp\left(-i\tau(\omega_1 I_{\phi_k} + \mathcal{H})\right)$$

$$= \exp\left(-i\tau\omega_1 I_{\phi_k}\right) \mathcal{T}\exp\left(-i\int_0^\tau dt\ \tilde{\mathcal{H}}_k(t)\right)$$

$$= P_k V_k. \tag{A5.4}$$

In general, the exact form of V_k cannot be calculated, but it may be expressed in terms of $(2I + 1)^2$ basis operators O_m.

$$V_k = \exp\left(-i\tau\textstyle\sum_m a_m O_m\right). \tag{A5.5}$$

It follows that

$$\exp\left(-i\tau(\omega_1 I_{\phi_k} - \mathcal{H})\right) = P_k \exp\left(i\tau\textstyle\sum_m a_{mk} O_m\right)$$

$$= P_k V_k^\dagger. \tag{A5.6}$$

Thus Eq.(A5.3) may be rewritten as[k]

$$U = \left(\mathcal{T}\textstyle\prod_k P_k V_k^\dagger\right)^\dagger$$

$$= \left(\mathcal{T}\textstyle\prod_{k,m} P_m \tilde{V}_k^\dagger\right)^\dagger$$

$$= \mathcal{T}^{-1} \textstyle\prod_{k,m} \tilde{V}_k P_m^\dagger, \tag{A5.7}$$

where

$$\tilde{V}_j = \left(P_{j-1} \cdots P_1\right)^\dagger V_j \left(P_{j-1} \cdots P_1\right), \quad j \geq 2 \tag{A5.8}$$

and

$$\tilde{V}_1 = V_1. \tag{A5.9}$$

Therefore, for a sequence of the type $(P_1 \ldots P_n)(P_1 \ldots P_n)^{-1}$, the total evolution operator becomes

$$\begin{aligned} U_{tot} &= \left(\mathcal{T}^{-1}\prod_{k,m} \tilde{V}_k P_m^{\dagger}\right)\left(\mathcal{T}\prod_{k',m'} P_{m'} \tilde{V}_{k'}\right) \\ &= \tilde{V}_1 \ldots \tilde{V}_n \tilde{V}_n \ldots \tilde{V}_1. \quad \text{(Q.E.D.)} \end{aligned} \tag{A5.10}$$